International Journal of Biological Macromolecules 206 (2022) 115–147

Contents lists available at ScienceDirect

International Journal of Biological Macromolecules

journal homepage: www.elsevier.com/locate/ijbiomac

Review

Fluorescent-based nanosensors for selective detection of a wide range of biological macromolecules: A comprehensive review

Saman Sargazi [a], Iqra Fatima [b], Maria Hassan Kiani [b], Vahideh Mohammadzadeh [c], Rabia Arshad [d], Muhammad Bilal [e], Abbas Rahdar [f,*], Ana M. Díez-Pascual [g,*], Razieh Behzadmehr [h]

[a] Cellular and Molecular Research Center, Research Institute of Cellular and Molecular Sciences in Infectious Diseases, Zahedan University of Medical Sciences, 98167-43463 Zahedan, Iran
[b] Department of Pharmacy, Quaid-i-Azam University, Islamabad 45320, Pakistan
[c] Department of Pharmaceutical Nanotechnology, School of Pharmacy, Mashhad University of Medical Science, Mashhad 1313199137, Iran
[d] Faculty of Pharmacy, University of Lahore, Lahore 45320, Pakistan
[e] School of Life Science and Food Engineering, Huaiyin Institute of Technology, Huaian 223003, China
[f] Department of Physics, University of Zabol, Zabol, P. O. Box. 98613-35856, Iran
[g] Universidad de Alcalá, Facultad de Ciencias, Departamento de Química Analítica, Química Física e Ingeniería Química, Ctra. Madrid-Barcelona, Km. 33.6, 28805 Alcalá de Henares, Madrid, Spain
[h] Department of Radiology, Zabol University of Medical Sciences, Zabol, Iran

ARTICLE INFO

Keywords:
Electrochemical
Optical detection
Nanosensors
Fluorescence probes
Carbon dots
Quantum dots

ABSTRACT

Thanks to their unique attributes, such as good sensitivity, selectivity, high surface-to-volume ratio, and versatile optical and electronic properties, fluorescent-based bioprobes have been used to create highly sensitive nanobiosensors to detect various biological and chemical agents. These sensors are superior to other analytical instrumentation techniques like gas chromatography, high-performance liquid chromatography, and capillary electrophoresis for being biodegradable, eco-friendly, and more economical, operational, and cost-effective. Moreover, several reports have also highlighted their application in the early detection of biomarkers associated with drug-induced organ damage such as liver, kidney, or lungs. In the present work, we comprehensively overviewed the electrochemical sensors that employ nanomaterials (nanoparticles/colloids or quantum dots, carbon dots, or nanoscaled metal-organic frameworks, etc.) to detect a variety of biological macromolecules based on fluorescent emission spectra. In addition, the most important mechanisms and methods to sense amino acids, protein, peptides, enzymes, carbohydrates, neurotransmitters, nucleic acids, vitamins, ions, metals, and electrolytes, blood gases, drugs (i.e., anti-inflammatory agents and antibiotics), toxins, alkaloids, antioxidants, cancer biomarkers, urinary metabolites (i.e., urea, uric acid, and creatinine), and pathogenic microorganisms were outlined and compared in terms of their selectivity and sensitivity. Altogether, the small dimensions and capability of these nanosensors for sensitive, label-free, real-time sensing of chemical, biological, and pharmaceutical agents could be used in array-based screening and *in-vitro* or *in-vivo* diagnostics. Although fluorescent nanoprobes are widely applied in determining biological macromolecules, unfortunately, they present many challenges and limitations. Efforts must be made to minimize such limitations in utilizing such nanobiosensors with an emphasis on their commercial developments. We believe that the current review can foster the wider incorporation of nanomedicine and will be of particular interest to researchers working on fluorescence technology, material chemistry, coordination polymers, and related research areas.

1. Introduction

Biological and chemical agents are composed of proteins and chemical structures for receiving and transducing signals for biological system integration [1]. Measuring some of these analytes in serum [including proteins, acute phase proteins, neurotransmitters, serum

* Corresponding authors.
E-mail addresses: a.rahdar@uoz.ac.ir (A. Rahdar), am.diez@uah.es (A.M. Díez-Pascual).

https://doi.org/10.1016/j.ijbiomac.2022.02.137
Received 16 December 2021; Received in revised form 1 February 2022; Accepted 23 February 2022
Available online 26 February 2022

enzymes, carbohydrates, lipids, hormones, circulating nucleic acids, vitamins, ions, electrolytes, and blood gases], urine, and other clinical samples appear to be necessary for disease detection, monitoring, and management [2–12]. These biological, chemical and pharmaceutical agents can bind to receptors and induce biological- and tissue-based responses that develop into the modification of the cell's electrical activity [13,14].

Biosensors work via surface-dependent mechanisms. Hence, the larger the surface area and higher the electron transfer proficiency and biocompatibility, the better the sensing ability and utility [15,16]. Piezoelectric or thermal transducers are pivotal components in sensing concentrations and physical properties of all types of agents into analog voltage signals followed by conversion into digital signals [17]. As promising tools, biosensors help detect several biological agents and are currently gaining momentum by the low instrumentation cost, reasonable sensitivity, high accuracy, and easy operation. [18]. The most common sensing techniques involved are optical- and electrochemical-sensing. Optical sensing is based on the use of spectrophotometer and electrodes like pH, and conduction ions are electrochemical sensing [19]. The major shortcoming of these conventional approaches is the requirement of specific biosensor devices, leading to costly and non-specified sensing [20].

Nanomedicine has helped formulate innovative methods for targeted delivery of drugs and developing ultra-sensitive nanosensors for accurate detection of various biological agents [21–36]. Nanomaterials (NMs) have provided an extended range of powerful sorbents for separation strategies of purification, bio-sensing, and bio-imaging of biological analytes [37–39]. Nanosensors are promising analytical tools for understanding biological features providing advanced sensing properties [40].

Fluorescence analysis using fluorescent nanosensors can be used for qualitative and quantitative analysis of biological, pharmaceutical, and chemical agents [41]. Fluorescence-based nanosensors are superior to various other analytical instrumentation techniques like gas chromatography, high-performance liquid chromatography, and capillary electrophoresis for being more economical, operational, and sensitive [42]. Fluorescent probes are based on organic molecules, fluorescent dyes, fluorescent molecules, florescent nanocarriers, and rare earth metals [43]. Some most practicing florescent nanosensors include quantum dots (QDs) and carbon dots (CDs) [44]. Lately, a new type of glowing carbon NMs, CDs, have been developed and gained much attention due to their distinctive properties, such as strong chemical inertia, stable lighting, and low toxicity and biocompatibility. These features make CDs a great candidate for developing new and sensitive sensors. Fluorescent CDs with responsive ion properties that can selectively respond to specific ions are highly regarded among intelligent sensors due to the critical role of ions in life and health processes [45–47]. These nanosensors are biodegradable, eco-friendly, and act theranostically against various infectious diseases and cancers [48,49].

Because of their simplicity, high sensitivity, and rapid response, trace amounts of analytes can be detected by fluorescent methods, which are exploited for biomedical imaging and bioanalysis. There are a lot of fluorescent NMs that have been introduced recently, but CDs are the most unique and robust method having low cytotoxicity, attractive photostability, easy functionalization, and ideal biocompatibility [50]. Nobel-metal nanocarriers are mild, possess controlled fluorescence, biocompatibility, and targeted theranostic activity against various carcinomas [51]. Similarly, nanoscaled metal-organic frameworks (MOFs) are diverse in their functionality, possess controlled fluorescence biocompatibility, and are widely used for cancer imaging, biosensing, and therapy [52]. Moreover, triplet annihilation-based florescent probes help detect potassium levels in the body [53], while lysine sensing via florescent graphene QDs is efficient in detecting tumor markers [54]. CDs-based florescent nanosensors help determine the quality and assessment of food nutrients [55]. Florescent nanosensors have also been found to detect physicochemical properties and multi-functionalization aspects of DNA [56]. A well-distinguished approach is also to determine exhalation kinetics for volatile cancer biomarkers by florescent nano-probes [42]. Finally, fluorescent nanosensors are involved in detecting the pesticide/herbicide residues, human proteins, and contents of pollutants in pharmaceutical-related samples [57].

The rapid development of nanosensors revolutionized tissue monitoring, pharmaceutical detection, and *in-vivo* sensing [58–60]. Previous studies have reviewed recent advancements in NMs fabricated paper-based [61], DNA-functionalized graphene oxide [62], aggregation-induced emission (AIE)-based [63], luminescent MOF [64], as well as innovative "turn-on" [65] fluorescent-based sensors for analysis of environmental, biological, clinical, and food samples. However, the majority of these studies have reviewed different strategies to design novel fluorescent sensors to sense heavy metals, ions, and nutrients [66–69]. To the best of our knowledge, this is the first comprehensive review casting light on the recent trends in nanotechnology-based approaches towards monitoring various biological, chemical, or pharmaceutical agents exploiting selective fluorescent-based probes and providing the broadest panorama of the state-of-the-art in this field. We also discuss some technical barriers that may limit their commercialization and practical application in the clinic.

2. Fluorescent nanosensors for the detection of different analytes

The fluorescence imaging method has gained increasing attention to detect numerous biomolecules in real-time and in-situ because of its high sensitivity, selectivity, fast feedback, and excellent spatiotemporal resolution. Recently, many different fluorescent probes have been manufactured for imaging and bioassay by using different fluorophores. Resorufin is a robust fluorophore with long emission and excitation wavelength, high fluorescence quantum yield, and distinct capability in both colorimetric and fluorescent analysis. The rapidly growing development in analytical chemistry contributes to medical and biological identification by giving fast analytical procedures to recognize numerous biomolecules (biomarkers) [70–73]. Fluorescence bioanalysis and imaging process using novel personalized probes have been extensively accepted in biomedicine, preclinical and diagnostics areas, and other life sciences because of its high sensitivity, outstanding selectivity, high resolution, simplicity, and ability non-invasive and real-time recognition [74–78]. Thanks to these features, fluorescent-based sensors have provided significant advantages over conventional methods to detect a variety of biological macromolecules. Table 1 summarizes the literature review of different fluorescent-based nanobiosensors concerning their biological, chemical, and pharmaceutical utilizations.

2.1. Amino acids, proteins, and peptides

Some detection techniques, i.e., fluorescence resonance energy transfer (FRET) and enzyme-linked immunosorbent assay (ELISA), have been formerly established to sense serum proteins [88,89]. Meanwhile, chromatography was introduced as the gold standard method to detect amino acids (AAs) in biological samples [90,91]. Recently, the FRET-related protease recognition method using hybrid biological nanomaterial (NM) sensors has been developed to sense protein and its derivatives. These FRET sensors are highly sensitive and have a unique detection scheme [92]. For instance, Zhou and coworkers have investigated fluorescent nanosensors to detect cysteine in skeletal muscles associated with paracetamol-induced pro-sarcopenic effects [93].

Graphene oxide (GO) has unique benefits such as pragmatic surface modification, high water solubility, and large surface that can be utilized to design innovative nanosensors to detect proteins or peptides, mainly due to outstanding quenching efficiency [94,95]. In one study, GO was prepared by the oxidation process of graphene and combined with fluorescence-labeled biomolecules to detect a specific protease. GO, and fluorescent-labeled peptides are conjugated to form unique bacteria and

Table 1
The biological, chemical, and pharmaceutical applications of various fluorescent-based nanosensors.

Nanosensors	Examples	Characteristics/advantages	Applications	Analytes	*In-vitro*/*in-vivo* studies	Ref
Electrochemical	GQDs and CQDs	Robustness, selectivity, and sensitivity, lower toxicity, higher solubility, strong chemical inertness, high specific surface areas	Biological imaging, drug/gene delivery, antibacterial, and antioxidant activity	Dopamine, tyrosine, epinephrine, norepinephrine, serotonin and acetylcholine	Mitochondria isolation, CQD loading, *in-vitro* imaging, the NIR fluorescent CQD development, daylight 680, loading CQD-Dy680 into the mitochondria (Mito-CQD-Dy680) for *in-vivo* imaging	[79]
Optical or electrochemical antifouling sensors	Semiconducting QDs, metallic nanoparticles, mesoporous particles, and metal oxide particles	Highly selective, capable of operating in complex sample matrix (serum)	Chemical, physical and biological applications	Proteins, nucleic acids, cells, neuronal transmitters	PEG-based SAMs, zwitterions, SAMs on gold (*in-vitro*), antifouling in vivo nanovectors for the development of *in-vivo* nanosensors	[80]
Optical/electrochemical sensors	NMs	Food safety	Real-time and non-invasive optical bioimaging	Food-borne pathogens and toxins	NM-assisted *in-vitro* detection methods for pathogens and toxins, *in-vivo* quantification of target pathogens or toxins and their behaviors inside the living body	[81]
Luminescent/optical polymer dot oxygen transducer	Glucose-oxidase-functionalized polymer dots	Specific and sensitive, large dynamic range, strong luminescence signal	Transdermal detection, responsive to blood glucose	Small molecules, glucose detection	Glucose detection in cell and tissue environments, in vivo detection and quantitative determination of a variety of small molecules	[82]
Biosensors	Nano-carbons	Fast, efficient, sensitive, specific and real-time detection, real-life clinical applications	Targeting, therapeutic, and diagnostic functions	Detection of bacteria	Towards novel routes in clinical diagnosis	[83]
Biosensors	Chitosan, collagen, graphene, carbon nanotubes, metallic nanoparticles, quantum dots, and various polymer composites	High sensitivity, specificity, portability, cost-effectiveness, possibilities for miniaturization, mass production, high efficacy, biocompatibility, and biofouling	Biomedical research, drug discovery, the environment, pharmaceutical, nutraceutical and process industries, cancer, and bio-imaging	Biomaterials and enzymes	Point-of-care diagnostic testing and/or *in-vivo* and *in-vitro* diagnostics	[84]
Nano-biosensors	AuNPs and QDs	Diagnosis at the single cell and molecule level can be incorporated in the current molecular diagnostics such as biochips	Molecular diagnostics and enable point-of-care diagnosis as well as the development of personalized medicine,	Biomarker research, cancer diagnosis, and detection of infectious microorganisms	Have the potential to be incorporated in clinical laboratory diagnosis	[85]
Electrochemical and optical sensors	MIP-based sensors	Robustness, high affinity, specificity, and low-cost production	Medical and forensic diagnostics, cell imaging	Biomolecules, drugs of abuse, explosives, natural antibodies	*in-vitro* diagnostics and *in-vivo* applications	[86]
Optical	DF-HSI	Versatility, high-throughput quantitative molecular analyses	Targeted drug delivery during chemotherapies, photodynamic therapy, and immunotherapy, spectroscopic and microscopic imaging, cancer diagnosis and treatment, microbiology, surgical procedures	Microorganisms, single-cell, and proteins	To understand the cellular uptake and transport of these materials in cells, tissues, and environment	[87]

protease nanosensors. To achieve this conjugated sensor, GO was used to adsorb fluoropeptides and quench their fluorescence. These fluoropeptides were sliced in the presence of a particular protease to retrieve the fluorescent signals. A linear relationship was found between protease concentration and fluorescence signals. Bacteriophages that were synthesized to hold a gene for tobacco etch virus (TEV) protease were used to spot the bacteria. Phages are specific viruses that contaminate the host bacteria, replicate within them, and lyse them. After lysis, the TEV protease was unconfined into the sample and caused peptide cleavage. The combination of peptide-GO with engineered phages to analyze the bacteria was the first study of its kind ever [96].

Alzheimer's disease (AD) is considered the leading cause of dementia in the elderly [97]. AD is explained with various pathogenesis reasons, but the leading cause is still unknown. An LSPR (Localized Surface Plasmon Resonance) linked optical nanosensor was developed by triangular silver nanoparticles (TSNPs) for the discovery of amyloid-β peptide, which is known as the initial stage in the pathogenesis of AD. A label-free LSPR nanobiosensor was constructed to detect DNA and tumor necrosis factors (TNFs) using silica nanoparticles (NPs). These NPs were capped with gold (Au) on a glass substrate treated with peptides. The absorbance strength increased after hybridization with DNA, and it was an indication of the increase in the biomolecular layer. The limit of detection (LOD) was 0.677 pmol/L for the examined DNA. The designed LSPR was used to discover whole cells, receptors, and proteins with high sensitivity [58].

Today, a lot of analytical and instrumental methods such as Fourier transform infrared spectroscopy (FTIR), high-performance liquid chromatography (HPLC) [98], mass spectrometry, as well as capillary

electrophoresis [99] are applied to detect AAs. Despite their acceptable selectivity and accuracy, many disadvantages (complicated operation, high cost, and time-consuming process) make them a less reliable choice [100,101]. Fluorescence-based detection methods are more straightforward, realistic, and sensitive; that is why they are preferred nowadays [102,103]. Among the fluorescence-based detection methods, the most important has been given to the fluorescent quenching (turn-off) mechanism [104,105]. However, the turn-on fluorescent probes show greater signal to noise in dim background [106–108], which might be why they have more practical applications. The pioneer one is the aggregation-induced emission (AIE) method projected by Lou et al. in 2001. DMBFDPS molecule was proposed as an aldehyde-functionalized AIE fluorescent probe. The AIE properties could be displayed with greater emission after the reaction of DMBFDPS with cysteine (Cys) [109].

Zhang et al. presented the tetraphenylethene (TPE) into the supramolecular coordinatelectrolyte cages. Cysteine (Cys), a thiol-bearing amino acid, and glutathione were both detected when AIE properties were adjusted, and cages displayed outstanding turn-on fluorescence [110]. In recent times, Liu's group proposed that the quenching properties of the starting materials could be altered to gain AIE properties with extremely near-infrared (nIR) turn-on emission after simple methylation of the 2-(2,6-bis(4-(diphenylamino)stryryl-4H-pyranylidene)malononitrile (TPA-DCM) [111,112].

There is another method to analyze the AAs called the "on-off-on" model. The quenching groups are initially proposed into the high-emission fluorescent probes to turn off the emission [113]. For this purpose, the analytes are introduced, demolishing the collaboration between the quenching groups and probes. At this stage, the high fluorescence emission of the starting probes is recovered (off-to-on). For example, carboxyl-functionalized polymer dots were reported by Shamsipur et al. The Cu2+-histidine (His) "off-on" fluorescent biosensors can use Cu2+ to cause the quenching of its fluorescence. This can be selectively improved by adding the His amino acid. Despite having a lot of advantages and wide current use, there are some disadvantages. For example, they contain heavy metal ions, which are harmful to human bodies and many steps (needed for functional groups incorporation while synthesis) are related to these two methods hindering their practical applications [114].

Recently, new fluorescent sensors, known as heteroatom-doped carbon dots, have been designed to use as striking nanosensors with wide applications [115]. Similarly, gold nanoparticles (AuNPs) can also be used as fluorescence quenchers. FRET or IFE related to AuNPs/CDs pair has been extensively used in many bioanalytical fields, nucleic acid detection, and immunoassay due to the broad absorption spectrum and high extinction coefficient of AuNPs. Exploiting the pyrolysis method, a study reported using *N*-acetyl-L-cysteine and citric acid as starting materials to manufacture high quantum yield N, S co-doped carbon dots (N, S-CDs). NS-CDs were used as fluorophores, and AuNPs were taken as fluorescence absorbers to construct a robust nanosensor for the sensitive sensing of trypsin and protamine. The fluorescence of N, S-CDs could be effectively quenched by IFE (inner filter effect) that would take place between N, S-CDs, and AuNPs. The adsorbed N, S-CDs are detached from AuNPs' surface and reinstate the fluorescence of N, S-CDs. Trypsin acts explicitly on peptide bonds having arginine and lysine carboxyl groups and can hydrolyze protamine. Consequently, the AuNPs were disaggregated, and the fluorescence of N, S-CDs was further quenched. The fluorescence intensity of N, S-CDs depended on the concentration of trypsin and protamine. The applicability and validity of the proposed sensor were established after a chain of experiments. Hence, an extremely sensitive and rapid "off-on-off" fluorescent nanosensor was established to sense protamine and trypsin in biological samples [116].

Juan Hu et al. fabricated a Cy5/biotin-modified peptide containing one serine hydroxyl group to sense O-linked *N*-acetylglucosamine transferase (OGT) and an exclusive protease location neighboring the glycosylation site for proteinase breakdown. There was also a general non-radioactive UDP-GlcNAc acting as a peptide (substrate) and a sugar donor. The glycosylation reaction is catalyzed in the presence of OGT, and a glycosylated peptide acting like a protease-protective peptide is formed. A QD-peptide-Cy5 nanostructure was formulated when the glycosylated Cy5/biotin modified peptides accumulated on the surface of streptavidin-coated QDs. Then, it causes an efficient FRET from QD to Cy5 and results in the emission of Cy5 that is enumerated by total internal reflection fluorescence (TIRF)-linked single-molecule sensing. There are many other applications of this single-QD-based nanosensor, such as investigating OGT inhibitors and enzyme kinetic analysis as well as quantitative assessment of OGT activity [117]. In the past, trypsin detection was not easy because of conventional sensing techniques such as colorimetry, electrochemistry, quartz microbalance sensor, surface-enhanced Raman spectroscopy (SERS). For example, AgNPs were fabricated by a reduction process and intended as SERS substrates for the recognition of methimazole. The shape and structure of the NMs were characterized by using UV–Vis spectroscopy, Raman spectroscopy, transmission electron microscope (TEM), and Fourier transformed infrared spectroscopy. Methimazole was adsorbed on the surface of AgNPs substrates, detected by density functional theory (DFT) and SERS measurements. SERS calculations indicated that a chemical association is developed between methimazole and NPs. An increase in the bands was used to create a linear correlation between SERS signal intensity and the amount of methimazole [118]. An efficacious procedure was designed to clarify and quantitative measurement of 2-Thiouracil by using SERS with AgNP's substrates planted on graphene nanosheets (Ag/G). TEM images indicated that graphene was used to endorse the equal distribution of silver nanoparticles. Nevertheless, Ag/G is a highly robust SERS substrate for the identification of 2-Thiouracil at ultra-low concentration. This process can be modified in future to use to sense different drugs [119]. Procaine was detected in aqueous media by surface-enhanced Raman scattering spectroscopic process by using gold nanoparticles substrates. Gold nanoparticles were manufactured by a reduction procedure and were characterized by Raman and infrared systems. Procaine showed SERS spectra which were considered at different concentration ranges, and the spectroscopic shifts along with Raman peaks have been detected and allocated. The potential association modes between procaine molecules and gold atoms were determined by Density Function Theory (DFT). The increase in the intensity of Raman peaks was used to design a consistent quantitative measurement technique for procaine detection in aqueous media [120]. Graphene treated with Polyamidoamine dendrimer and functionalized with silver nanoparticles (G-D-Ag) was manufactured and calibrated as a substrate to detect methimazole (MTZ) by using surface-enhanced Raman scattering (SERS). AgNPs were developed on the dendrimer by using a reducing agent known as sodium borohydride. The achieved G-D-Ag was characterized by the use of scanning electron microscope (SEM), Fourier-transformed infrared (FT-IR), Raman spectroscopy, UV–Vis spectroscopy, and high-resolution transmission electron microscopy (TEM). G-D-Ag formation was confirmed by the SEM images. SERS detected the steadfast and robust performance of MTZ on the G-D-Ag as a substrate that showed a chemical association between MTZ and G-D-Ag. The MTZ normal spectra bands such as 1538, 1463, 1342, 1278, 1156, 1092, 1016, 600, 525, and 410 cm^{-1} were increased because of the SERS effect. The associations between the SERS signal intensities and logarithmical scale of MTZ were developed successfully and the lowest recognition limit noted was 1.43×10^{-12} M. The primary Raman bands were assigned by density functional theory (DFT) [121] and fluorescence-based techniques [122,123].

Fluorescent-based techniques are most widely used because of their simple instrumentation, real-time detection, high sensitivity, and easy operation. The fluorescence turn-on techniques are of specific importance, thanks to their enhanced sensitivity, less false fluorescence, and high specificity. Nowadays, many different turn-on strategy-linked assays have been testified to sense trypsin. For example, Chen et al. [124] stated a trypsin-specific turn-on fluorescence-based method. There are a

series of steps involved, such as Cu2+ driven fluorescence quenching of gold nanoclusters (AuNCs) occurring in the first step. Secondly, to release the amino acid fragments after the breakdown of bovine serum albumin by trypsin. In the third step, the amino acids show more affinity towards Cu2+ than to the AuNCs, and it converts the fluorescence from off to on-state. Wang et al. described a unique technique of immobilizing fluorophore-categorized peptides with arginine and a terminal cysteine onto the AuNPs' surface to sense the trypsin. Fluorophores from AuNPs are released after the addition of trypsin which causes the C-terminus of arginine to be hydrolyzed. This results in a strong fluorescence signal recovery. Wu and the group used cytochrome C (Cyt C) while working on direct manufacturing of Mn-doped ZnS QDs, got some QDs that had the property of protease sensing. These methods have several disadvantages, such as using traditional fluorescent dyes, fluorescent labeling, the relatively high toxicity of QDs, high material cost, etc.

CDs have gained much attention compared to organic dyes because they are relatively simple to fabricate, have lower toxicity, high photostability, reasonable water solubility, and are low-cost in terms of raw materials. CDs are considered perfect fluorescent probes in FRET-related biosensors. Similarly, the quenching efficiency of AuNPs usually overlaps with the emission of CDs; and that is why the AuNPs are considered fluorescence quenchers. When the emission spectra of a donor overlap with the absorption spectra of the acceptor, then the phenomenon of FRET occurs. AuNPs/C-dots based FRET has been broadly used to accurately sense various small molecules, nucleic acids, and ions [125,126].

Aptamer-linked sensors have shown an outstanding detection capability towards proteins, metal ions, and other biomolecules. In a study, Shreya Ghosh et al. designed an optical turn-off nanosensor containing AuNPs on a 3′ terminus and a deoxyribonucleic acid aptamer linked to a QD on the 5′ terminus. The C-reactive protein (CRP) was detected by this sensor following the principle of fluorescence resonance energy. The photoluminescence intensity decreases when the concentration of the target in the sensor increases; therefore, improving quenching efficiency. This sensor is extremely sensitive to C-reactive proteins and has a detection limit of 1.77 picomoles. This sensor effectively detects the clinical samples showing almost 10% quenching (at a concentration of 10 picomolar). Future studies on this sensor will include an *in-vivo* examination of the sensor to be used for inflammatory disease control [127].

Another technique for detecting proteins is to utilize a natural binding partner of a specific protein as a detection site on the single-walled carbon nanotubes (SWCNTs). For example, in this process, an aptamer or a DNA detection order, or an antibody can be used to achieve the novel protein-protein or protein-DNA interactions for sensing applications. Nanotubes treated with chitosan polymer adapted with nitrilotriacetic acid (NTA) were described by Ahn et al. for label-free detection. For further modification, chitosan was used because of the availability of functional groups. The NTA chelated Ni2+ and aided as a vicinity quencher moderating the SWCNT fluorescence intensity as a purpose of distance. The NTA-Ni2+ group bind to hexahistidine treated capture protein, serving as a natural linkage location for the target protein. For instance, human immunoglobulin G (IgG) was detected by a His-tagged protein A linked to the NTA-Ni2+. After linkage of target protein, there is a variation in fluorescence intensity allowing the reviewing of protein glycoprofiles, protein quantification, and protein-protein interactions [128].

Satishkumar et al. used fluorescent SWCNT sensors to detect avidin by conjugation redox-active dyes linked to a detection unit called biotin to the SWCNT surface. After adsorption onto the SWCNTs, the biotinylated dyes were quenched so that linkage of avidin resulted in their adsorption from the nanotubes, and the fluorescence was recovered. In this connection, the fluorescence quenching mechanism is governed by the oxidative charge-transfer reactions having small redox-active organic dye molecules. After attaching precise receptor groups, the dye-ligand complex linked to SWCNT can show very high versatility for various bioanalytes. Additional experiments indicated that by using DNA-SWCNTs linked to an anti-uPA antibody, sensing of prostate cancer biomarker urokinase plasminogen activator (uPA) was easily possible [129], and the detection of single repressor-activator protein 1 (RAP1) proteins released from specific *Escherichia coli* cells by SWCNT treated with RAP1 aptamer [130]. Lee et al. described platelet-derived growth factor and optical detection of insulin by using two specific aptamers by two unique mechanisms known as separation of the aptamer from SWCNTs' surface, resulting in protein binding and direct protein linkage to the aptamer-SWCNT complex. Both of these processes cause a decrease in fluorescence intensity [131].

Live cell imaging with the effective spatiotemporal resolution has become increasingly simple after discovering exceptionally equipped sensitive automated software and fluorescence microscopy [132]. Periplasmic binding protein (PBP) aids as a ligand detecting domain in developing FRET-sensor. Wang and Zhang designed a signal-on single nanosensor based on QD-linked FRET for cyclic-AMP-dependent protein kinase (PKA) assay. In the presence of PKA, the serine hydroxyl group can link a biotinylated γ-phosphate when PKA is catalyzed, resulting in the formation of biotinylated Cy5-labeled peptide substrate. The streptavidin-coated 605 nm emission QD (605QD) can bring together a lot of biotinylated Cy5-labeled peptides by unique streptavidin-biotin linkage to get the 605QD-substrate-y5 nanostructure, this resulted in the manifestation of FRET from the QD to Cy5 and finally, the emission of Cy5. This assay results in a signal-on recognition of PKA with a LOD of 9.3×10^{-6} U/μL, which is 10 folds more robust than the TiO_2-coated magnetic microsphere-linked fluorescent method. This nanosensor was also used to detect PKA activators and inhibitors; on the other hand, this nanosensor was overextended to recognize some other protein kinases after embracing particular substrate peptides.

Fluorescence is a spectroscopic procedure with modest equipment such as ultra-violet (UV) and high sensitivity, such as HPLC [133]. A fluorescence technique was introduced for detecting forkhead box P3 (FOXP3) via quantifying messenger ribonucleic acid (mRNA) quantity. The immune system has dynamic parts called regulatory T cells or suppressor T cells that usually function to dank down the overexcited immune response. Nowadays, the identification of Tregs is related to surface markers such as forkhead P3 (FOXP3) transcription factor and CD25, CD4, CD127 markers. DNA-templated AgNPs hybridized with mRNA of FOXP3 is comprised of a minimum of one G-rich order to form a ternary system. Tregs were isolated by this intracellular detection sensor [134].

Members of the periplasmic-binding protein superfamily (PBPs) are more likely to develop FRET sensors because many metabolites can bind to them. FRET-based nanosensors are fabricated by inserting the ligand-binding domain between donor and acceptor fluorophores. Large conformational changes occur to PBPs when the substrate is linked to its active site between their N and C lobes. FRET efficiency is the change in distance between the FRET pair when the conformational changes cause the ligand-binding domain to be changed. The genetically encoded FRET-based nanobiosensors were fabricated, filtered, and successfully characterized in this study. These nanosensors were used to non-invasively detect thiamine levels in human cells, yeast, and bacteria [135].

Choi et al. [136] reported a fluorescence quenching-related technique to detect the β-site amyloid precursor protein cleaving enzyme 1 (BACE1) in live HEK 293 cells. β-Secretase (BACE1) is used in the formation of amyloid-β (Aβ) peptides. Aβ peptides are used to detect, control, and therapy AD. CdSe/ZnS QDs and AuNPs form a binary complex together that was utilized for the particular identification of BACE1. The QDs were linked to the BACE1 substrate to produce a covalent bond with the Ni-nitrilotriacetate (Ni-NTA) treated AuNPs. The selective breakdown of bonds between QDs and His in the presence of BACE1 helped the recovery of quenched fluorescence relative to the BACE1 concentration. The sensor showed a LOD of 0.15 μM. This sensor can be used for the clinical recognition of BACE1 because of its high

stability, sensitivity, and efficiency.

In opposition to the probe described by Choi and group, Thirumalraj et al. [137] described a turn-on fluorescence process to identify L-cysteine molecules released from MKN-45 gastric cancer cells and Colo-205 colorectal cells. The rGO's surface was treated with AuNPs stabilized with gelatin to form a quenched fluorescent rGO/Au nanocomplex. In the presence of L-cysteine molecules, the probe's fluorescence was recovered. This probe has the benefits of high sensitivity, versatility, specificity, and ease of use, which shows that the rGO/Au nanoprobes can detect many diseases related to L-cysteine, such as PD, AD, and acquired immune deficiency syndrome (AIDS) [138]. Finally, Chen and coworkers have demonstrated near-infra-red fluorescent sensors to detect kidney-specific peptides to assess kidney function. The sensor was used for long-term monitoring of kidney function as well as urine analysis [139].

SWCNTs fluoresce in the nIR part of the spectrum, where proteins and some other biological macromolecules are somewhat transparent, without blinking or photobleaching [140]. In this connection, Hendler-Neumark et al. prepared a label-free protein sensor array with florescent SWCNTs utilizing SWCNTs functionalized with synthetic heteropolymers or natural recognition moieties. For this purpose, the SWCNT suspension was placed on a glass functionalized with nitrilotriacetic acid (NTA)-Ni2+ to attach the tagged capture proteins and determine possible interactions between the target and capture proteins. After adding the target protein, the distance between the SWNT surface and the Ni2+ quencher is altered. [141].

In 2020, Wang and coworkers developed a red emissive fluorescent nanoprobe YZ-A4, based on xanthene dyes, for rapidly detecting L-selenocysteine (Sec), the 21th amino acid naturally existing in all kingdoms of life. The florescence of YZ-A4 is quenched because of the presence of 2,4-dinitrobenzene sulfonate ester group that truncates the intramolecular charge transfer (ICT). As shown in Fig. 1, When the sensor reacts with Sec, the ICT effect of the produced YZ-A3 is restored. The designed nanobiosensor demonstrated fast reaction time, excellent selectivity and ultrasensitivity, and desirable optical properties. The quantitative detection range for sensing Sec was from 0 to 32 μM, with a LOD of 11.2 nM, which is very low [142].

2.2. Neurotransmitters

As a neurotransmitter of the catecholamine family, dopamine (DA) has essential roles in the brain. Alterations in DA levels can cause disorders such as movement disorders. Therefore, accurate and rapid determination of this neurotransmitter is crucial for diagnosing various diseases [143,144].

Mass spectrometry imaging (MSI) indicates unique advantages in detecting molecular information and imaging the dispersal of neurotransmitters in in-situ vesicles [145]. Electrochemistry has exceptionally high resolution and quantifiable ability, making it an essential tool for studying neurotransmitter storage and release. Yun et al. indicated the effect of cationic G3, G4, and G5 PAMAM Poly (amidoamine) dendrimers on the fibrillation of α-synuclein. G5 PAMAM was the most beneficial one with an 8-fold decrease in the TFT fluorescence process and comparable effect on α-synuclein fibrillation. The PAMAM G4 dendrimer showed an enhanced fluorescence in tyrosine residue and suppressed the fibrillation of Ambient Sensing Node (ASN). On the other hand, no inhibition or decrease was observed with PAMAM G3.5 dendrimers. During incubation, the absence of a positive signal in the range of 195–206 nm with G4 PAMAM dendrimers shows inhibition of protein aggregation [146]. Nowadays, many different classes of neurochemical sensors have been merged in the field of fluorescence detection. Optical electronics is a new field inspired by carbon NMs, and they have fabulous profiles and physiochemical properties. SWCNTs enclosed in synthetic biomimetic polymers have been exploited to detect DA within the nIR spectrum are using corona phase molecular detection, a facilitated linkage connecting SWCNT corona and DA using a pinned polymer [147].

Chen et al. described a GO-based photoinduced charge transmission and label-free nIR fluorescent biosensor for DA. The recognition phenomenon of dopamine depends on the substantial quenching of nIR GO with a left move to bound DA. QDs are fluorescent nanocrystals fabricated from semiconductor ingredients that show novel luminescent properties. QDs show 20-fold higher brightness than the conventional fluorescent reporters and organic dyes and demonstrated size-based emission features. Recently, a nanobiosensor for *in-vivo* examination linked to nitrogen-doped grapheme QDs (NGQDs) and CoCOOH nanosheets was described [148].

To overcome the toxicity challenges of QDs, neurochemical methods are introduced, which are simple, nontoxic, and highly desired. Conjugated polymer nanoparticles (CPNPs) have enhanced photo-stability, and they are more biocompatible than QDs. A CPNP was fabricated for fluorescence detection of DA in the ventricles of zebrafish larvae brains. After the linkage of (phenylboronic acid) PBA on the surface of DA, a photoinduced charge transfer takes place between the CPNP emission core and the DA. Fluorescence quenching of the CPNPs occurs after charge transfer. As a result, the fluorescence intensity diminishes as the DA concentration increases (i.e., turn-off response). Optical reporters such as fluorescent false neurotransmitters (FFNs) are bundled together with mark analytes into the vesicles. Upon their co-release into the synaptic cleft following an action potential, FFNs make the imaging of neurotransmitters. FFNs are robust enough for single vesicle recognition, but FFNs cannot directly sense neurotransmitters and give less information related to extracellular dynamics [149–151].

Morell and coworkers fabricated L-cysteine capped Mn-doped ZnS QDs related sensing technique to identify DA in the nanomolar range [152]. The sensor showed an orange emission band at approximately

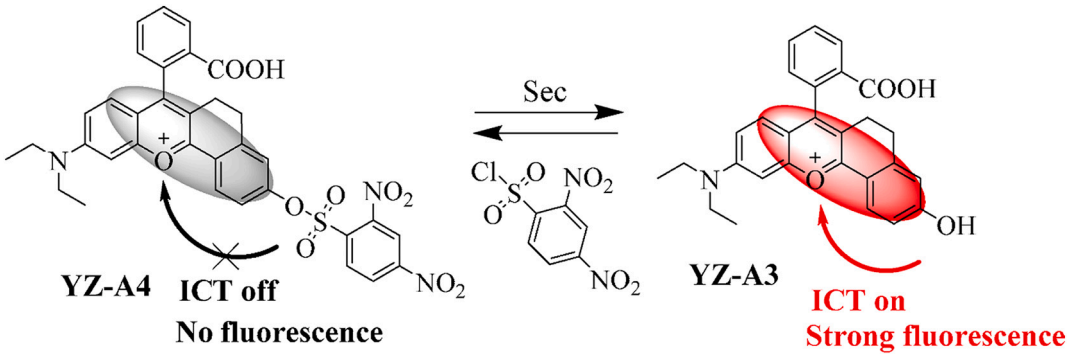

Fig. 1. The detection process of selenocysteine using a red emissive fluorescent turn-on nanobiosensor. (For interpretation of the references to color in this figure legend, the reader is referred to the web version of this article.)
Reprinted from ref. [142].

598 nm. It was quenched when DA was added in an alkaline medium; in the case of urine samples, the lowest concentration of the target molecule was approximately 7.80 nM. A QDs based sensor known as CdTe QD linked FRET-based fluorescent tool was designed to identify 8 nM concentration of DA in a linear range of 1–300 nM [153]. In the same way, Chen and coworkers have described an anodic ruthenium (II) tris(2,2′-bipyridyl-4,4′-dicarboxylato), and cathodic graphene-CdTe QDs with tris(2-aminoethyl)amine (TAEA-Ru) linked detection platform for DA detection at the minimum concentration of 2.9 fM in a diluted serum sample [154].

Shalini et al. have designed a honey-based PEG6000 treated carbon NPs-linked fluorescent detection tool for EP in urine samples with a LOD of 7.59 × 10–10 M in the linear range of 9.9 nM–0.107 μM. In extension to this technique, Hu et al. have designed MIP sensors related to CdTe/CdS/ZnS/SiO_2 and QDs CdTe@SiO_2 to identify EP and NE. This novel QDs related detection system excites at the wavelength of 365 nm. It radiated green and scarlet fluorescent signals simultaneously, and there is no intersection with a LOD of 9 nM and 12 nM for norepinephrine (NE), epinephrine (EP), correspondingly. In the same way, a free fluorescent sensor based on GQDs was fabricated to recognize EP in human serum samples [155].

To simultaneously detect NE, EP, and DA, Hettie et al. have fabricated a turn-on fluorescence-based molecular sensor named Neuro-Sensor 521. For this matter, they utilized *p*-methoxyphenyl elements linked to fluorescent stuff attached to NE and not to EP because there were secondary amines present on EP, which hindered the binding affinity of EP [156]. After that, Dunn et al. described a fluorescent tracer of NE known as fluorescent false neurotransmitter 270 (FFN270) to detect synaptic neurotransmission in live cells. The FFN270 imaging linked optogenetic motivation to study heterogenous NE release in the noradrenergic synapse in an *in-vivo* process that was studied additionally by amphetamine management [157,158]. Lin and coworkers have manufactured a series of genetically encoded single-wavelength fluorescent G protein-coupled receptors (GPCRs) Activation-Based NE/EPi (GRABNE) instruments for sensing NE and studying it's dynamic [158]. This was the first report on utilizing all mathematical models to fabricate a highly sensitive sensor for NE detection [159].

Gupta et al. identified DA in neuronal cells (PC12) using high quantum yield CDs. The formulated sulfur doped-CDs indicated bright fluorescence that was used to recognize DA at the amounts up to 2 × 10^4 nM with LOD of about 50 nM [138]. A most advanced procedure of artificial engineered clonal HEK293 cells, Cell-based Neurotransmitter Fluorescent Engineered Reporters (CNiFERs), was described to detect acetylcholine (Ach), DA, and NE in genetically altered FRET exploiting GPCR-linked reaction. Brown et al. have fabricated a fluorescent sensor known as cyclotriveratrylene probe used in an aqueous medium to sense Ach because of precise electrostatic interaction that increases fluorescence by wrapping alongside water and devastating the II system. This process continued, and an SPR-related fiber optic sensor based on Ta_2O_5: PPy: rGO conjugated ACh was fabricated to detect the ACh with a sensitivity of 4.382 nM/μM and a LOD of 76 nM. After that, the researchers manufactured chitosan and rGO matrix condensed AChE trapped Ta_2O_5 nanoflowers sensing tool for ACh recognition having LOD of 73 nM in the linear range of 0–8 μM. Additionally, Soleymani et al. developed a fluorescent biosensor based on AuNPs with a linear detection range of 1 × 10^{-6} to 1 × 10^{-5} M [134].

Shi et al. developed a new fluorescent detection system based on ficin-H_2O_2-tyramine to detect dopamine in cerebrospinal fluid (CSF). Ficin oxidizes non-fluorescent tyramine to fluorescent dithyramine. The fluorescent signal of dithyramine, due to the oxidation of non-fluorescent tyramine catalyzed by ficin in the presence of H_2O_2, is significantly reduced by the addition of DA due to DA competing with OH radicals with tyramine and is a new method for measuring DA. With a LOD of 46 nM. This test was performed in CSF to diagnose DA with acceptable results [160].

Govindaraju et al. used red-fluorescent emission of bovine serum albumin (BSA) and protein conjugated fluorescent AuNCs (BSA-Au NCs) to sense DA in CSF selectively. The particle size of BSA-Au NCs ranged from 4 to 6 nm, with ~8% of QY and strong fluorescence, and desirable stability. These NPs were analyzed by lighting spectroscopy (PL), X-ray photoelectron spectroscopy (XPS), X-ray diffraction (XRD) and high-resolution transmission microscopy (HRTEM), UV–vis spectroscopy. The findings demonstrated that BSA-Au NCs bind strongly to DA. This provides a diagnostic limit of 0.622 nm and, therefore, can sense DA in biological samples, for example, CSF, selectively in an ultra-sensitive manner [161].

In another study, Chen and associates have explored infrared-based graphene oxide nanosensor to detect DA through fluorescence quenching [162](Fig. 2).

Gasotransmitter hydrogen sulfide (H2S) was fabricated by enzymatic reaction in the body, and it has a lot of metabolic and biological signaling and applications. The atypical concentration of H2S is linked with many diseases; hence, the designing of unique bioanalytical procedures for fast and proficient recognition of H2S in biological systems is of great significance. The (Ru@FITC-MSN) is a nanosensor manufactured by halting luminescent ruthenium (II) (Ru (II)) composite into a fluorescein isothiocyanate (FITC) conjugated aqueous-dispersible MSNs. It indicates double emission bands at 600 nm (Ru-composite) and 520 nm (FITC). In the presence of Cu+, the red luminescence of the developed Ru@FITC-MSN was quenched. The Ru@FITC-MSN indicated rapid response to H2S along with high selectivity. It showed a linear ratiometric luminescence shift in FITC and Ru (II) passages with the H2S level of 0.5–4 μM [164].

2.3. Enzymes

Nanomaterial scaffolds have been used as reactors for enzyme-based catalysis. These constituents help the management and increase the rate of catalyzed reactions governed by the NPs. Compared to the traditional homogenous analyses in solution, the enzyme-linked nanoreactors can limit the catalysis of enzymes. A nanoscale 'enzymogel' reactor for cellulase-catalyzed hydrolysis that is made up of a polymer shell and an inorganic core has been described. In cells, detecting enzyme-linked self-assembly from the fabricated chemical originators helped detect inhibitors for those enzymes. Larger biomolecules such as microRNA can be identified in live cells with the help of self-assembled NPs. The *in-vivo* examples are peptide-treated AuNPs and self-assembled magnetic nanogrenades that were used to recognize intratumoral pH and trypsin activity, respectively [165].

Wang and associates used a QD-based nanosensor to precisely sense the human 8-oxoguanine-DNA glycosylase 1 (Hogg1). This nanosensor can recognize Hogg1 up to the concentration range of 1.8 × 10^{-6} U/μL, which is equivalent to that of Exo III-assisted isothermal magnification-based fluorescent assay. It can be used for accurate measurement of parameters related to enzyme kinetics, as well as detecting the hOGG1 action in crude cell extracts and transmission of hOGG1 inhibitors as well [166]. It can be used for precise measurement of enzyme kinetic parameters, for the detection of hOGG1 action in crude A549 cell extracts with an accuracy of 5 cells, and transmission of hOGG1 inhibitors as well [166]. Zhang and colleagues, in another study, have investigated

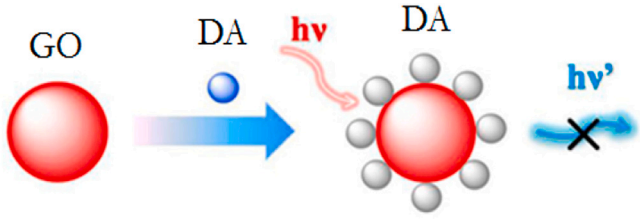

Fig. 2. Schematic presentation for detection of DA using graphene oxide (GO) NPs through fluorescent quenching [163].

glutamic acid conjugated fluorescent sensors to detect γ glutamyl transpeptidase to predict drug-induced liver injury [167].

Chen and coworkers have explored the use of fluorescent sensors to accurately detect enzymes and biomarkers for drug-induced liver injury [168]. Similarly, Ma and associates have investigated fluorescent-based polymer dots to recognize alkaline phosphatase with high selectivity and sensitivity [169]. Wang and Zhang designed a signal-on single nanosensor based on QD-linked FRET for cyclic-AMP-dependent protein kinase (PKA) assay. When PKA is present, the serine hydroxyl group can link a biotinylated γ-phosphate when PKA is catalyzed, resulting in the formation of biotinylated Cy5-labeled peptide substrate. The streptavidin-coated 605 nm emission QD (605QD) can bring together a lot of biotinylated Cy5-labeled peptides by unique streptavidin-biotin linkage to get the 605QD-substrate-y5 nanostructure, this resulted in the manifestation of FRET from the QD to Cy5 and finally, the emission of Cy5. This experiment results in a signal-on detection of PKA with a LOD of 9.3×10^{-6} U/μL, which is 10 folds greater than the TiO_2-coated magnetic microsphere-linked fluorescent technique. This nanosensor was also used to detect PKA activators and inhibitors; on the other hand, this nanosensor was overextended to sense some other protein kinases after embracing particular substrate peptides. Nowadays, many outstanding review articles have been published to design the fluorescence probes to identify biothiols such as glutathione (GSH), homocysteine (Hcy), cysteine (Cys), etc. [72,170]. Many fluorescence probes for the identification of biothiols have been marketed by Invitrogen and Thermo Fisher Scientific [171]. Liu et al. designed a chlorinated coumarin-hemicyanine molecular probe 10, having three possible reaction spots for Cys detection [172]. When Cys is present in the sample, Cl-exchange first took place at spot 1, then the intra-molecular readjustment and cyclization flow reactions happened at site 2. This method is considerably different from the Hcy-activated substitution-relocation reactions (at spot 1) and GSH-activated substitution (at site 1)-cyclization (at location 3) reactions. in In PBS, a specific coumarin emission at 420 nm was attained (Kex = 360 nm) after reacting 10 with Cys, (1 mM CTAB, pH 7.4, 10 mM) and the emission intensity was increased steadily by enhancing the amounts of Cys. Li et al. deliberated probe 11 as well for particular recognition of Cys grounded on Cl-exchange and aldehyde-cyclization of the coumarin fluorophore [173]. In a study, Wang et al. fabricated a fluorescein-linked probe 39 by pairing the hydroxyl group of fluorescein to the 2,4-dinitrobenzenesulfonyl agent to detect Cys at pH 11 in 10 mM in milk [174]. The probe indicated zero fluorescence, but an "off-on" phenomenon was attained when the Cys-activated cessation reaction took place. Hao et al. established a colorimetric and NIR fluorescence probe 43 established on the Cu2+-dislocation technique to detect Cys accurately [180]. Yue et al. designed a ratiometric fluorescence reaction probe 81 for specific recognition of Cys with the help of adapted coumarin as fluorophore [75,175].

2.4. Monosaccharides

Chemiluminescence [176,177], Rayleigh scattering spectroscopy [178], electrochemical methods [179–181], fluorescence [182], electrochemiluminescence (ECL) and spectrophotometry [183,184] etc., are the analytical tools that are primarily used to detect biological analytes including carbohydrates. Most of these methods are related to single signal capturing. For example, Chang and coworkers developed a fluorometric analysis technique for sensing glucose and H_2O_2 based on TRE-M-L [185]. Wang et al. applied MoS_2 for fluorescent quantification of H_2O_2 and glucose [186]. A team of researchers manufactured the ratiometric and colorimetric fluorescence double signal detection array to quantify H_2O_2 and glucose. The detection technique projected an efficient, suitable and label-free ratiometric fluorescent and colorimetric detection system for glucose and H_2O_2. At the first step, the glucose oxidase enzyme catalyzes the glucose to form H_2O_2. Secondly, the hydroxyl radical (—OH) is formed by a Fenton reaction between H_2O_2 and Fe2+ in an acidic medium. At last, the OH quenches the red fluorescence of C-dots, which are promising fluorescent probes with stable chemical properties, desirable safety profile, and high fluorescence intensity. At the same time, the OH will oxidize non-fluorescent VB1 to form blue-emitting oxVB1. On the other hand, a smartphone-related platform was described for on-site detection of glucose. The colorimetric and fluorescent images were taken by a smartphone when a considerable amount of glucose was added. The images were subjected to detection and computation with R, G, and B values by an APP to analyze glucose amounts [187].

Shinki t al. [188] developed the anthracene monoboronic acid sensor 7 specifically detecting D-fructose while D-glucose was detected by anthracene diboronic acid sensor 8. Sensor 7 was linked with carbohydrates to make 7a (Fig. 3). The photoinduced electron transfer (PET) technique from the tertiary amino group to anthracene fluorophore was delayed when the N—B bond of 7a was enhanced.

Recently, Sun et al. [188] described an internal translation process endorsed by three features. Firstly, the receptors and their complexes with fructose are solvent-linked without B—N association. Secondly, the nanosensors were tested not to be aggregated. Thirdly, they found no fluorescence reaction in pure methanol when fructose was bounded, and —$B(OH)_2$ was transformed to the —$B(OMe)_2$ groups.

In the same way, anthracene was implied as a fluorescent moiety of the sensor, but it showed a reversed selectivity because of many boronic acid groups. Eggert et al. [188] designed a sensor related to the above research that demonstrated greater selectivity for D-glucose than either fructose or mannose. Nevertheless, the diboronic acid sensors study was extended by other groups. Diboronic acid has a better selectivity than carbohydrates structured by the molecular design of its development, i.e., having two boronic acids. After that, Mulla and the group manufactured a sensor 10 having a redox-active tetrathiafulvalene (TTF) unit and two boronic acid groups for selective detection of carbohydrates. Recently, Wang and coworkers described a sandwich boronate affinity sorbent assay (SBASA) to sense glucose. Anthracene group was incorporated into sensor 11, which is a fluorescent monomer. This sensor was effectively utilized for glucose detection in human serum samples [188].

Takeuchi et al. used anthracene boronic acid sensor 12 described by Shinkai et al. to formulate injectable-sized fluorescent beads by polymerization. The fluorescent beads were implanted into mice's skin for nonstop glucose monitoring. They noticed that the fluorescent intensity efficaciously traced the fluctuation in blood glucose amounts from 0 mg/dL to 1000 mg/dL. Afterward, Takeuchi et al. have done some more research by refining the polymerization process. Hydrogel fibers were designed, which could remain inside of the mice for up to 140 days. After implantation, the amount of fluorescence was controlled and quantified. Moreover, they have better applicability and are easy to remove from the body [188]. Glucowatch is the non-invasive biosensor related to electric current to draw glucose in a transdermal pad to quantify glucose. The basic drawback of Glucowatch is the need for nonstop calibration tests by finger pricking [189].

CD-related chemiluminescence (CL) has been reported in different chemical reactions. For example, Lin [190] and the group developed the

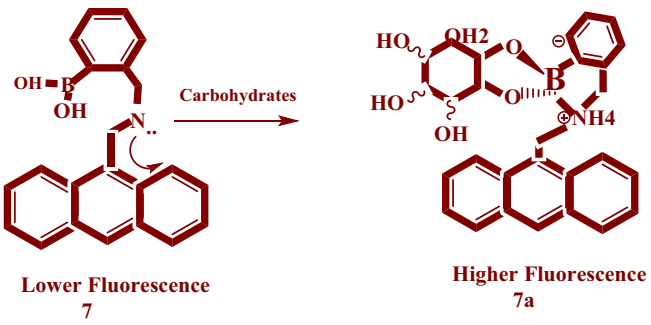

Fig. 3. Sensor 7 was linked with carbohydrates to make 7a [188].

CL of CDs in $NaNO_2$-H_2O_2 solution, while Dong et al. [190] reported the CL of CDs in alkali solution. In recent years, the CL emitted by CL emitter, H_2O_2, and peroxalate fuel has been utilized to detect glucose and H_2O_2 *in-vitro* and *in-vivo* [191–196].

In the study, Billingsley [197] and colleagues based on ion-selective optodes designed fluorescent nanosensors capable of detecting small molecules. By placing the sensor components in a hydrophobic core, these nanosensors could monitor dynamic changes in the model analyte concentration of glucose. The results showed that changes in blood glucose levels measured by nanosensors *in-vivo* were similar to measurements made using a glucometer. In addition to showing a reversible response to dynamic changes in glucose concentration, these nanosensors have a dynamic range that includes physiological glucose levels [197]. The ability of the nanosensor system to monitor glucose dynamics *in-vivo* can be used in the treatment of diabetes as well as in research such as monitoring the effects of cell function or new therapies for the disease.

A glucose nanosensor was developed with a glucose/galactose-binding protein into *Escherichia coli* with two different types of green fluorescent proteins to carefully monitor glucose and its dynamics in individual cells. After substrate binding, the FLIPglu-170n sensor showed a decrease in the fluorescence resonance energy transfer between the connected chromophores with the 170 nm glucose binding affinity, following a concentration-dependent manner. Measurement of fluorescence resonance energy transfer with other carbohydrates showed a wide selectivity, specifically for monosaccharides. Therefore, nanosensors were used to determine the level of cytosolic glucose in living cells. The data showed that the cytosolic concentration could be several times larger depending on the external source. Due to the high affinity of hexokinase and the maximum transfer to the maximum ratio of 10 phosphorylation, the amount of external glucose in physiological blood sugar levels was not limited. Interestingly, cytosolic levels respond rapidly to external source modulation. Thus, FLIPglu-600 may serve as a beneficial tool that helps to understand better the mechanisms of glucose sensation and metabolic conditions related to glucose homeostasis in other living organisms [198].

Semiconductor nanocrystals covered with sugars (glycol-QDs) have been used as probes for *in-vivo* imaging and labeling. Glyco-QDs were firstly used *in-vitro* as bio-labels and were described by Fang and co-workers [199]. Man-encapsulated CdSe/ZnS core and shell QDs or *N*-acetylglucosamine (GlcNAc)- showed optical properties used in confocal microscope imaging to dye live sperms of pigs, mice, and sea-urchin. Due to the difference in the dispersal of the Man receptors and GlcNAc on the surface of sperm, the mannose-QDs spread over the entire body of sperm while the GlcNAc-QDs showed more concentration at the sperm heads. Recently, Seeberger tested PEGylated-QDs coated with galactose, mannose, and galactose products to get robust nanotools for *in-vivo* targeting of the liver. PEG has a hydrophilic nature in linkage with sugars, enhances the water solubility of QDs, and decreases the inherent cytotoxicity of the colloidal core of QDs. QD covered with D-mannose and D-galactosamine were isolated precisely in the liver after IV injection. Galactosamine-QDs highly increased the concentration of transaminases in serum, indicating a particular biological function in the liver.

With progression of cancer, the transition from oxidative phosphorylation to glycolytic anaerobic metabolism markedly increases [200]. In a study by Nascimento et al., nanopipettes were designed to assess glucose levels in individual cells to confirm that cancer cells could show higher intracellular glucose levels. The nanopipettes were covalently activated as glucose nanosensors by immobilizing glucose oxidase (GOx). The interaction of glucose with GOx leads to the catalytic oxidation of β-D-glucose to D-gluconic acid, which measured the change. The nanopipettes were covalently activated as glucose nanosensors by immobilizing GOx. The interaction of glucose with GOx leads to the catalytic oxidation of β-D-glucose to D-gluconic acid, which measured the change. Unicellular glucose levels were assessed in human breast cancer cells (MDA-MB-231 and MCF7) and in fibroblasts using the developed nanosensors. They showed that cancer cells showed a reproducible and reliable increase in glucose levels in comparison with non-cancerous cells. As a result, nanotube-based glucose sensors provided a way to correlate changes in glucose levels with changes in proliferation or progression of the malignant cells. The platform could be used in the future as a diagnostic tool to differentiate malignant cells from normal human cells in heterogeneous tissue biopsies and to monitor the progression of cancer in situ [200].

AuNPs that have reasonable dyes or semiconductor nanocrystals are used in optical imaging. Park [201] and group injected AuNPs capped with hyaluronic acid and labeled with nIR fluorescence dye (Hylite 647) for *in-vivo* imaging of human ovarian carcinoma (OVCAR-3) and arthritic inflammation in mice. When AuNPs reach the target areas, the fluorescence quenching by energy transmission between the gold surface and the dye is deactivated (Fig. 4) In this case, the interaction between reactive oxygen species (ROS) and increased hyaluronidase destroys the hyaluronic acid units. *In-vivo* fluorescence imaging of disease states was recognized selectively after the dye release.

Recently, fluorescent organic silicon nanodots (OSiBNs) have inherent properties such as strong stability, low toxicity, strong fluorescence, and advanced photostability. It has good biodegradability and promising biocompatibility [203,204]. They have got much consideration from analytical scientists, especially in biomedical areas, because they substitute general fluorophores, e.g., metal NPs and organic fluorescent dyes [205]. Extensive fluorescence released by sub-5 nm OSiNDs basically resulted from the direct-to-direct band hole changeovers related to quantum-size detection and surface properties, which impart OSiNDs a vast outlook for the formation of photovoltaic cells and bioimaging properties [206]. Here, a robust fluorescent and colorimetric double-mode technique related to fluorescent OSiNDs that were applied for the ultrasensitive detection of glucose and H_2O_2 with approximately 100% quantum yield. The water-dispersible OSiNDs were fabricated by a simple one-pot hydrothermal path using PPD as a chromogenic substrate. The inner filter effect (IFE) procedure of the projected technique resulted in the unique spectral overlap between absorption of PPDox fluorescence emission of OSiNDs. It was examined and confirmed by 2,5-diamino-NN′-bis-(*p*-aminophenyl)-1,4-benzoquinone di-imine (PPDox) PPDox calculating the difference of fluorescence lifetimes of OSiNDs before and after relating to 2,5-diamino-NN′-bis-(*p*-aminophenyl)-1,4-benzoquinone di-imine (PPDox) PPDox. The described technique was additionally used to detect serum glucose [207].

2.5. Nucleic acids

FRET-based nanosensors can be used to detect heat change, ionic content, and changes in pH. Nanosensors can be broadly used for natural applications such as nucleic acid (DNA and RNA) examination, cancer therapy, etc. Nucleic acid detection is used in clinical and forensic studies such as DNA and protein linkages to examine the alterations and conformational changes in the configuration and tissue engineering as well [208,209].

In a study, the researcher presented a new carrier, i.e., peptide nucleic acid (PNA) treated core-shell Fe_3O_4-AuNPs linked to a nanopore detection tool to isolate and link to miRNA goal in complex samples specifically. Core-shell Fe_3O_4-AuNPs were fabricated because of their novel magnetism segregation and biochemical characteristics. PNA modified core-shell Fe_3O_4-Au NPs can be parted and recognized from complex samples using a magnet without centrifugation. Before and after binding with miRNA, the PNA treated Fe_3O_4-Au NPs indicate a difference in the zeta potential can circumvent the boundless PNA modified Fe_3O_4-Au NPs from entering nanopore that decreases the interfering from coexisting carriers. Besides, the new tools having large sizes can enhance signal-to-noise because a high amount of current obstruction resulted from their large excluded volume. Precise quantitative analysis can be achieved by modifying the concentration ratio

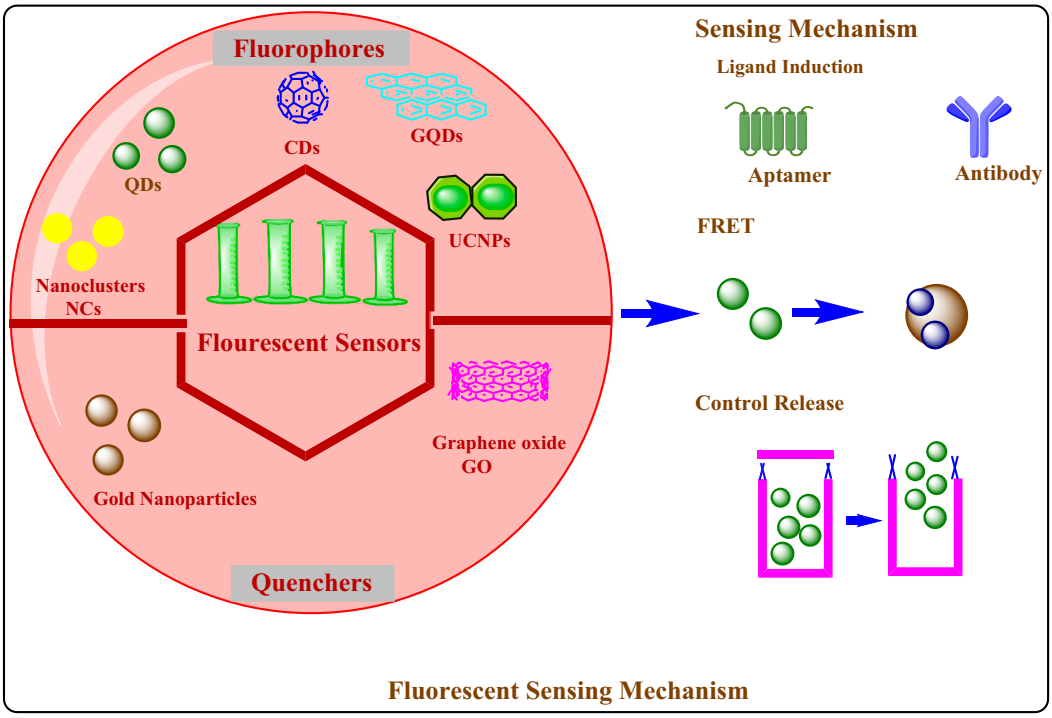

Fig. 4. Fluorescence approaches for comprehending the fluorescent mechanism by different NMs as fluorophores and quenchers. Reprinted from ref. [202].

between Fe_3O_4 and PNA as one AuNP binds with only one PNA. This technique can detect nucleic acids and other small molecules with excellent specificity [210].

Generally, fluorescent-based nucleic acid detection was accomplished using signal-on (signal generation) and signal-off (signal quenching) after hybridizing complementary nucleic acid with its target miRNA. Fluorescent proteins, organic dyes, and inorganic nanostructures such as QDs or AuNPs have been applied as fluorescent reporters. GO-linked quenchers were highly specific for mir-16, mir-21, and mir-26a [211].

Cui et al. also used GO to identify miRNAs in the compound biological specimens by cyclic enzymatic magnification technique by which GO secured DNA-probes labeled with a dye were implied to get the target miRNA that will be liberated after hybridization by DNA probes on GO surface. After desorption, the probes are converted into fluorescent probes, and the DNAase I enzyme catalyzes the DNA leaving the miRNA integral. These miRNAs are used for many other probes on GO to start the next cleavage cycle. The whole process continues until all the DNA probes labeled with dye are used completely. Scientists got to measure the expression points of miRNA quantitatively inside living cells with the help of peptide nucleic acid-treated GO (PNAGO) by using a similar principle. In this work, dye-labeled PNA probes were used to detect relapsed quenching after hybridization of target miRNA [211].

Another technique to enhance sensitivity is to use QDs because of their good compatibility and stability with nucleic acids and a satisfying association between the emission wavelength and the size of QDs [212]. Zhang et al. developed a two-phase exponential amplification reaction (EXPAR) and single quantum-dot based nanosensor to recognize miRNA in aM sensitivity. In the first step, the target miRNA is amplified, while in the second step, miRNAs are transformed to the reporter oligonucleotides. Doyle et al. fabricated a unique and robust fluorescent-linked tool commercialized by FireFly Bioworkers an Abcam company. The equipment depends on optical liquid stamping (OLS), which indicates stamping microparticle tools onto photosensitive liquids. Three-dimensional hydrogel particles were developed and encoded with novel 'barcodes', which can be used to sense target miRNAs with an attomole sensitivity in a multiplexed manner [212].

Zhang et al., in recent research, fabricated a fiber displacement amplification and rolling circle amplification (RCA)-related fluorescent technique to detect let-7d having LOD of 1.5×10^{-13} M [211]. Usually, nanomaterial related to miRNA recognition depends on their excellent electrochemical and optical measures such as highly-efficient delivery capability and fluorescence quenching ability. QDs and AgNPs were applied to detect miRNA with their projecting fluorescence emission properties. They designed the QDs linked miRNA detection methods using exponential amplification reaction (EXPAR) and primer formation-treated RCA [213].

Liu et al. used DSN-assisted (duplex specific nuclease) recycle magnification to attain silver nanocluster (AgNC)-related fluorescence detection of miRNA [214]. Zhang et al. fabricated a strand-displacement amplification (SDA) as a unique beacon and hairpin DNA-templated AgNCs probes for miRNA detection. Many 2-D nanostructures like AuNPs, WS_2, GO and MoS_2 have an outstanding fluorescence quenching capability and high-efficacy-targeted delivery. Many fluorescent probes were linked to the NP's surface and got quenched. Nevertheless, the fluorescence emission was reestablished through cooperation with target miRNA to detect it sensitively. Nucleic acid amplification procedures are combined with NMs to enhance miRNA identification sensitivity [214].

Ju et al. first fabricated polyethylenimine-grafted graphene nanoribbon (PEI-GNR) as a nanostructure for imaging miRNA in a single cell. GNR has a large surface area, whereas the PEI has a high charge density that certified the cargo of locked nucleic acid-modified molecular beacon (LNA-m-MB) probes on PEI-g-GNR with efficiently transporting LNA-m-mb into the cells. In-situ sensing of miRNA in the single-cell was obtained due to the extraordinary specificity and affinity of LNA for target miRNAs. The team also described a unique multifunctional SnO_2 (mf-SnO_2) for miRNA detection, cell imaging, and effective delivery. The SnO_2 NPs were treated with folic acid to gain cell-specific delivery and target the tumor cells. Fluorescence SnO_2NPs permitted the imaging of the distribution and intracellular response of the mf-SnO_2 nanoprobe. A molecular beacon gene probe was linked by a pH-specific disulfide bond

to detect the target miRNA. The mf-SnO_2 NPs were subjected to guard the conjugated oligonucleotides against nuclease digestion and SSB linkage while delivering its cargo to the cell. The miRNA-21 expressing Hela cells were used as ideal models for successfully in-situ sensing of the intracellular miRNA via mf-SnO_2 nanostructures [215,216].

Lately, miRNA detection by new straight procedures has been presented, like NPs arrays that have appeared as precious molecular detection methods using fluorescence quenching nanostructures in a classy way. Currently, in addition to the routine fluorescence-related equipment, a lot of evolving fluorometric detection tools have been presented which can recognize miRNAs with high specificity and efficiency, for instance, single-molecule level detection by total internal reflection (TIRFM), fluorescence energy transfer or FRET, time-resolved fluorescence (TRF), chemiluminescence resonance energy transfer (CRET) and bioluminescence resonance energy transfer (BRET). For miRNA recognition, the fluorescent constituents are coated with (i) organic dyes (Texas Red) fluorophore 6-carboxyfluorescein (6-*FAM*), Cyanine 3 (Cy3) and Cyanine 5 (Cy5), (ii) proteins with fluorescent characteristics (Renilla luciferase), (iii) inorganic NMs such as quantum-dots QDs and (iv) non-fluorescent NPs linked with the fluorescent dyes [217,218].

2.6. Vitamins

Folic acid (FA), also known as Vitamin B9, is a hydrophilic vitamin, B-complex group. FA plays an essential part in carbon metabolism as a cofactor. The insufficiency of FA results in malformation, exacerbation, and neural tube weaknesses during pregnancy. The overdosing of FA can hinder the absorption of zinc and vitamin B12 and cause serious health issues [219].

In a study, the researcher developed a molecular marking ratiometric fluorescence sensor using a simplistic sol-gel technique for fast, specific, and optical recognition of FA. The fabricated FA-treated shell was fixed on the silica NPs core. In this case, FA, 3-aminopropyltriethoxysilane (APTES), cadmium telluride (CdTe) QDs, and tetreaethyloxysilane (TEOS) worked as a model template, functional monomer, analyte-linked fluorescence signal provider, and a cross-linker, respectively. The complex fabrication phase was perceptively omitted, and the imprinting positions endorsed on the surface of the silica matrix increased the sensitivity. The sensor showed two divided emission peaks at 619 nm and 449 nm by a single excitation wavelength (365 nm) fitting to FA-activated red fluorescence and blue fluorescence of CdTe QDs, respectively. When FA was added, the MIPs sensor could rebound FA, and consequently, increased in the blue fluorescence and decreased the red fluorescence followed by diverse colors such as red, pink, purple, and blue. The sensitivity and specificity related to quenching amounts were used to detect FA. At last, the practical use of the designed sensor in six dissimilar real specimens was examined, indicating good practical feasibility, rapidity, simplicity, accuracy, and high selectivity [220].

Vitamin B_{12} (VB_{12}) plays a very significant part in human health. Deficiency of VB_{12} can cause anemia, metabolic abnormalities, neurologic- and psychiatric-illnesses [221]. Excessive amounts of VB_{12} can increase the threat of bone marrow hyperplasia, liver damage, and kidney damage, etc. Currently, a lot of VB_{12} sensors related to CDs have been fabricated. Qiu et al. first designed a unique blue emission and thermally-reduced carbon dots linked to FRET sensor to detect VB_{12}in water-based solutions, which gives a unique idea for fluorescence detecting uses of CDs. Later, numerous techniques were designed to detect VB_{12} related CDs in real models [222,223]. The determination of VB_{12} in biological structures is still a complex process. Wang et al. [224] fabricated extremely fluorescent biomimetic QDs having blue emission for label-free selective, specific, and sensitive recognition of VB_{12} in Hela cells that proved the hidden application of CDs exploited in living cells [225].

In another study, a novel genetically encoded nanosensor was designed for real-time detection of VB_{12} in living cells. VB_{12} and its constituents act as cofactors because it is one of the very rare naturally present organometallic composites used as a coenzyme. It appears to be urgent to detect the fluctuations in the amount of this metabolite in real-time biological cells. A FRET-linked nanosensor has been fabricated for the real-time sensing of vitamin B_{12} at the cellular level [226].

Liu et al. fabricated a fluorescent sensor to quantify VB_{12} levels using glutenin-templated AuNCs [227]. The required vitamin was adsorbed at the surface of glutenin-AuNCs, having a lot of carboxyl and hydroxyl groups, and fluorescence quenching signals were considered for detecting objects with a LOD of 115 nM [228]. Xie et al. fabricated on-off-on fluorescent CDs as a detection tool to sense chromium (VI) and ascorbic acid related to IFE. Chen and coworkers formed an efficient fluorescence detection system to detect 2,4,6-trinitrophenol (TNP) linked to IFE between TNP and graphite carbon nitride (g-C_3N_4) nanosheets. Nevertheless, CDs-based fluorescent inner filter suitable for VB_{12} has never been described until now. Fascinated by these realities, some researchers have designed a unique fluorescent sensing based on CDs for specific and modest determination of VB_{12}. Vitamin B12 reduced the CDs-based fluorescence due to the flawless overlap between the absorption band of VB_{12} and the excitation band of CDs. CDs-related fluorescence declines slowly by adding VB_{12}. The described technique indicates its application in VB_{12} detection as well [223].

A study developed a ratiometric fluorescent nanoprobe for efficient detection of VB_{12}. CDs were fabricated using polyethyleneimine (PEI) and dry carnation petals through a one-step hydrothermal technique. PEI acts as a perfect nitrogen source during the manufacturing procedure as it is a water-soluble macromolecule with many amine groups. It is used to enhance optical characteristics by surface functionalization and to get a positive charge through the electrostatic effect of detection. Thus, fabricated CNDs were a fluorescent detection system to sense $VB_{12}$by the impulsive FRET technique from CNDs to VB_2. The nanoprobe can react with VB_{12} by a novel dual-emission technique that is more required to be used for real specimen detection. Temporarily, CNDs acting as stable and sensitive pH sensors were also recognized by turn-off FL mode at 470 nm. Intracellular pH indicates a beneficial way to control receptor-linked signal transduction, cell growth, ion transport, enzymatic activities, and metabolism apoptosis [229,230].

In a fascinating study, B-doped carbon quantum dots (BCQDs) were manufactured as effective fluorescence probes to detect VB_{12} in the cell system for the first time. CQDs embedded with zwitterion were effectively induced by simply hydrothermal management using cytidine diphosphate choline (CDPC) as an originator that gives outstanding bionic characteristics by affluent —NH_2, —PO_4, —COOH, and —OH ions in its structure. The sensitive fluorescence quenching of BCQDs by metal ions was researched without additional chemical treatment. The results demonstrated that the fluorescence of BCQDs is quenched by VB_{12} only, even at extremely low concentrations. BCQDs, on the other hand, indicated outstanding cell imaging and biocompatibility. Trace amounts of VB_{12} have been detected by using this novel selective and ultrasensitive fluorescence probe [230].

A study was conducted to develop a system for real-time detection of the fluidity of α-tocopherol by a FRET-based genetically encoded nanosensor known as FLIP-α, which acts selectively for sensing α-tocopherol in prokaryotic and eukaryotic cells. The human α-tocopherol transmission protein utilized as the linking protein for α-tocopherol was very effective in causing conformational alterations in the presence of α-tocopherol, which brought the fluorophores nearer to each other, and FRET was produced in the result. FLIP-α nanosensor has the specificity for α-tocopherol, which indicates that it can be used for real-time sensing of α-tocopherol in a complicated pool of mega homologous antioxidants [231].

nIR fluorescent sensors were designed in a study to detect riboflavin (vitamin B2) and vitamin C (Ascorbic acid). Main DNA-coated fluorescent SWCNTs were characterized to recognize ascorbic acid and riboflavin specifically. A hydrogel encapsulation tool was designed using transporting modeling to bound colloidal sensor diffusion. In biological

surroundings, the sensor can be inquired reproducibly and stably. *In-vivo* injections were used to check the overall system. The results indicated the successful intra-peritoneal *in-vivo* statistics and effective removal of experimental noise [232].

2.7. Ions, electrolytes, and complexes

Fluorescent nanosensors can analyze a range of intracellular analytes with molecular markers that were not previously possible. Based on ion selection optode technology, PEBBLE was developed at the nanoscale to measure a set of physiological parameters, including sodium, potassium, and chloride [197]. Fluorescence linked detection commonly uses fluorophore molecule, which is replaced by reaction with an analyte. The fluorescence intensity period and anisotropy are changed depending on the charge and energy transfer technique [233]. Surface-treated NMs like QDs and CDs are mainly used for the detection process. However, some nanoparticle-free techniques, including simplistic benchtop glyceraldehyde 3-phosphate dehydrogenase (GADPH) enzyme-catalyzed fluorescence assay [234] and appealing genetically enhanced green fluorescent proteins (EGFP) [235], could certainly sense As (III) ions in the range of 0–200 and 5–100 ppb, correspondingly. FRET-linked ratiometric sensor between Acriflavine and Rhodamine B could detect As (V) with a LOD of 10 ppb [233].

In 2018, Lu and colleagues developed a fluorescence "on-off–on" nanoprobe to sense Fe(III). They used the hydrothermal process to decompose the silkworm excrement and carbonized it to form CNPs via self-passivation. Under UV light, the synthesized CNPs had excellent stability and showed acceptable blue photoluminescence that could be quenched in the presence of Fe(III) in a sample to produce the N-CNPs/Fe(III) complex. The LOD was found to be 0.20 μM in a linear range (1 to 500 μM) [236] (Fig. 5).

In another study, unique nIR Ru-LPMSN amalgam materials were designed by a self-assembly process. First of all, a coordinating process fabricated an array of Ru1-Ru4 mixtures with 2,2′-dimethypyridine ethylenediamine (DPA) ligand. The compound mixtures indicated red to nIR fluorescence emission characteristics and presented exceptional selectivity for Cu2+ identification as DPA links well with Cu2+ ion. Secondly, Ru4, the most reliable ruthenium composite, considering nIR fluorescence extensively organized piercing, was enchanted into the big mesoporous silica channels (LPMSN) through electrostatic adsorption and hydrogen bonding. The LPMSN absorption ruthenium complex benefits in keeping the surrounding stability and repelling the outer invasion, fluorescence intensity of Ru-LPMSN was highly increased. In the meantime, Cu2+ sensitivity can be enhanced efficiently with the greater surface and extensive tunnel construction of LPMSN for absorption and growth of Cu2+ ions. The designed Ru-LPMSN hybrid compounds indicated sensitive, fast and selective recognition of Cu2+ ion. The *in-vitro* identification limit was 10 nM. Ru-LPMSN hybrid compounds were suitable for application as a nIR Cu2+ recognition mediator both *in-vitro* and *in-vivo*. Ru-LPMSN was demonstrated to show good biocompatibility and reach the cells rapidly to trace intracellular Cu_2+ levels. Further, Ru-LPMSN was applied to determine the dispersion of Cu2+ in zebrafish [237].

In 2019, Wei Huang et al. fabricated fluorescent CDs as selective and sensitive nanoprobes based on the quenched fluorescence signal of CDs to selectively Cu2+ ions. The prepared CDs were carbonized from L-cysteine and poly(vinylpyrrolidone)(PVP). The Cu2+ ions in the sample were attached to the sulfur and nitrogen atoms on the CD's surface. The formation of the absorbed complex resulted in strong quenching of the CD's fluorescence signaling by a prompt metal-to-ligand binding affinity. The fabricated CDs showed a quantum yield of 7.6%, a great photostability, stable fluorescence intensity (in different pH levels from 2 to 12), and a LOD of 0.15 μM in a linear range (0.5 to 7.0 μM) [238](Fig. 6).

Likewise, Zhu and coworkers designated AE-TPEA ([N-(2-aminoethyl)-N, N, N-tris(pyridine-2-ylmethyl) ethane-1,2-diamine]) as a selective Cu2+ receptor and conjugated it with a CdSe@CDs nanohybrid to detect the Cu2+ ions in living cells having a LOD of 1 μM [239].

In another experiment, Ti_3C_2 nanosheets (NSs) were manufactured, and their detection capability for the trace level recognition of Ag+ and Mn2+ by fluorescence quenching procedure. The prepared ultra-small Ti_3C_2 NSs showed excellent optical applications, e.g., excitation-dependent emission spectra, emission peak with high intensity, and quantum yield equivalent to the CDs. The fluorescence of Ti_3C_2 NSs was theatrically quenched by adding Mn2+ and Ag+ ions independently. The fluorine and hydroxyl-ended Ti_3C_2 NSs indicate a novel binding spot to Ag+ and Mn2+ ions. The suggested nanosensor showed unlimited potentiality for the pacific fluorescence detection of Ag+ and Mn2+ ions in the presence of viable metal ions such as As5+, Cd2+, Al3+, Pb2+, Zn2+, As3+, Hg2+, Cu2+, Co2+, Cr3+, and Ni2+ [240].

Semiconductor QDs have been extensively fabricated due to their sensitivity, high fluorescence efficiency, and simple instrumentation. Metal-ion probes have appeared now; however, the fluorescence probes related to pristine CDs undergo low fluorescence output, low sensitivity, and poor specificity [241]. Zhang et al. treated CDs with polyethyleneimine to get extremely bright CDs having a quantum yield of 42.5%. The relative standard deviation (RSD) was less than 3.0% when Fe3+ ions were detected in river water and tap. Qu et al. linked the TPEA (Tris (pyridine-2-ylmethyl) ethane-1,2-diamine) on the surface of CDs to create a CD-related fluorescence probe for accurate sensing of Cu2+ ions in living cells [239].

In a study, the researchers designed a simplistic single-step process to fabricate the polymer dots (PDs) having incredibly green fluorescence through auto-polymerization and self-oxidation by ethylenediamine and hydroquinone as reactors. Thus, manufactured PDs were applied as fluorescent indicators, and MnO_2 nanosheets were useful as GSH detection moieties and fluorescence quenchers to design a PD-MnO_2 nanosensor for turn-on examination of GSH. This PDs-MnO_2 nanosensor has also sensitively detected GSH in human serum samples with acceptable results [242].

A biological nanosensor has been developed to detect K+ that can also be used for PA imaging modalities and fluorescence, i.e., as ISO or ion-selective photo-acoustic optodes (ISPAOs). The potassium ion is the fundamental biological cation that is elaborated to control several physiological processes like pH maintenance, nerve and muscle signal

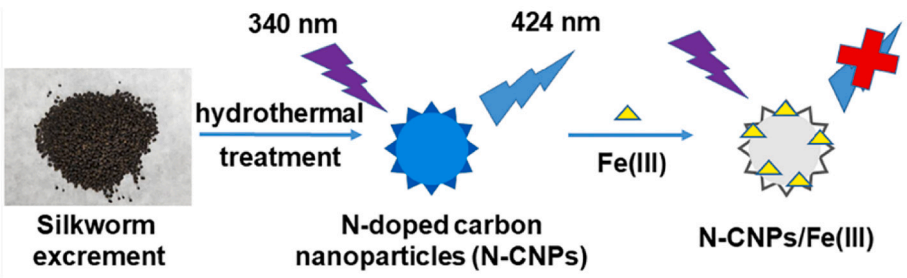

Fig. 5. The preparation of nitrogen-doped CNPs (N-CNPs) from silkworm excrement and the fluorescence sensing of Fe(III) in a sample. Reproduced from ref. [236].

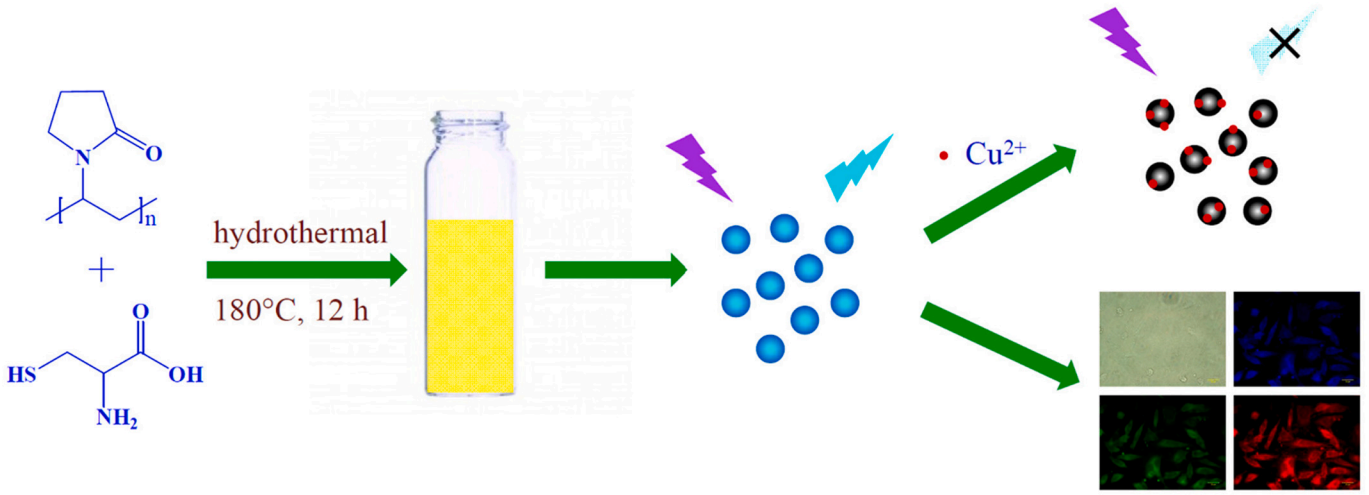

Fig. 6. Illustration of the fabrication process of fluorescent CDs for sensing Cu2+ ions.
Reprinted from ref. [238].

transmission, enzyme activation, and blood pressure regulation [243].

The biological ligands are applied to develop the fluorescent Hg2+ sensors, including DNA, proteins, and antibodies. As the magnitude of Hg2+ is way too small compared to protein and antibody, that is why Hg2+ must get attached to the ligands challenging the other metal ions. DNA has a lot of supreme characteristics to detect Hg2+ ions, for example, easy modification, docile to the combinatorial selection, good stability, cost-effective, and plentiful binding sites [244]. After chelation of Hg2+ ions by impairing thymine nucleotide to develop T-Hg2+-T assembly and T-rich DNA aptamer can be transformed into hairpin conformation organized by Hg2+ [244]. Many Hg2+ sensors were created to sense target ions in biological (i.e., urine, serum) and water samples [245].

In a study, Rox treated T-rich-modified silicon nano-dendrites (SiNDs) for the specific detection of Hg2+ ions. SiNDs were treated with the Rox-labeled (6-carboxy-X-rhodamine) T-rich oligonucleotide using Sulfo-SMCC as a bifunctional linking mediator. Further, this freshly designed sensor has been used to sense Hg2+ in serum or urine samples and for optical detection of Hg2+ in Hela cervical cancer cells [246].

In the study by Han et al. A simple method for fabricating single-scattered carbon dots of N-CDs with fluorescence light with a very bright quantum fluorescence performance of 42.3% by the efficient method of a sterolytic step. Ethylenediamine tetraacetic acid (EDTA) carbonation of ethylene diamine tetraacetic acid and urea was prepared. The obtained N-CDs were evaluated as a label-free fluorescent nanoparticle to detect Fe3þ and apoferritin in an aqueous medium using the on and off fluorescent method with remarkable specificity and sensitivity. The use of this N-CDs-based probe for imaging Fe3þ and apoferritin ions in living cells showed that the system could be measured in biosensing and bioimaging areas. Due to its simple synthesis, excellent biocompatibility, and superior optical properties, a CD-based sensing strategy can promote a potentially suitable method for disease-related molecular purposes [247].

Transcriptional arsenic receptors of the *ars* operon have a solid affinity for As3+. Its ability to attach to arsenic ions renders it an important candidate to fabricate FRET-based nanosensors. In this process, a genetically encoded fluorescent nanosensor was created for the real-time sensing of arsenic in a non-invasive manner. The fluorescent alternatives ECFP (donor) and Venus (acceptor) were attached with the arsenic responsive receptor ArsR at N- and C-terminus to design a recombinant protein. ArsR of *E. coli* is a metalloregulatory protein that detects arsenical forms present in the surroundings. Cloning techniques were used to fabricate the nanosensor inside a bacterial vector plasmid pRSET, developing an ECFP-ArsR-Venus detector built-in pRSET-B. [248].

Komatsu and coworkers designed a single fluorescent probe related to coumarone to determine multi analytes, i.e., Ca2+ and Mg2+, and for optical imaging. Maria J. Ruedas-Rama et al. described the alteration in fluorescence characteristics of an enzyme-based nanosphere sensor to detect creatinine and urea. Similarly, Sugunan et al. studied chitosan-coated AuNPs to detect copper and zinc ions by using chelating quality of chitosan and optical properties of AuNPs. QDs have revolutionized the world of fluorescent nanosensors, and they are used to sense numerous biological and non-biological samples [218,249–255].

Enhanced compartmentalization of compound subcellular and cellular composition of the living things creates a problem in detecting the metabolic pathway of nickel. Therefore, specific monitoring of the vibrant distribution of nickel ions inside a cell is needed to understand the physiology of nickel ions efficiently [215]. Spectroscopic methods like UV–Visible, circular dichrome, infrared, HPLC, liquid chromatography-mass spectroscopy (LC-MS), and traditional dyes-related fluorescence techniques are some diagnostic methodologies used to trace localization and circulation of metabolites and for *in-vivo* imaging [256]. In bulk trials, the identification and quantification of nickel ions were carried out by nuclear magnetic resonance (NMR), inductively coupled plasma mass spectrometry (ICP-MS), atomic absorption spectroscopy (AAS) [257].

Nonetheless, these techniques have a lot of operational and technical complications, such as the requirement of higher amounts for detection and there is no single-cell examination. CL- and bioluminescent-based sensors use organic dyes, but they have a toxic nature, so they are not a good option for nickel ions detection in living cells [258]. Metal sensors are better for determining metal ion balance inside the plants and prokaryotic and eukaryotic systems [259]. In a study, a FRET-based device has been used to identify and quantify nickel ions in the organisms. This nanosensor uses a mutated yellow fluorescence protein (Venus) as an acceptor, and enhanced cyan fluorescent protein (ECFP) acts as a donor. These two work collectively as a FRET pair [260] linked at C- and N-terminus of the ligand sensing domain (NikA). The sensor indicated the ionic flux of nickel inside the living systems following a concentration-dependent fashion, giving us a detailed vision of the nickel ions distribution at sub-cellular and cellular stages inside a living organism at an enhanced spatial and progressive resolution [261].

For the reason of the extensive lead contamination and its toxic nature even at extremely low concentration, the requirement for the fabrication of extremely sensitive methods for its recognition and to avert its toxic effects. Traditionally, the examination of lead was

dependent on laboratory-related refined analytical procedures like atomic emission spectroscopy (AES), atomic absorption spectroscopy (AAS), capillary electrophoresis (CE), inductively coupled plasma atomic emission spectroscopy (ICPAES), inductively coupled plasma-mass spectroscopy (ICP-MS) and X-ray fluorescence spectroscopy (XFS). These methods are mostly confined to the laboratory level despite their accurate lead determination. Nowadays, nanosensors are getting noteworthy consideration in the research area thanks to their small size, surface functionalization and compactness, the desired surface-to-volume ratio, quantum detention effects, improved surface reactivity, great sensitivity, and increased adsorption capacity [262]. Many elements such as QDs, metallic organic frameworks, NPs, nanoclusters, and carbon NMs, e.g., graphene and carbon QDs, have been utilized to fabricate innovative fluorescent sensors. After their fabrication, the NMs can be efficaciously reformed by suitable ligands or biomolecules to detect numerous metal ions simultaneously in a particular approach [67]. The simple technique of fluorescence-linked based sensors has been developed on the actuality that the particular association between detection component (i.e., NMs) and the target sample (lead) cause alterations in the fluorescence characteristics of NM that can be examined in numerous arrangements such as fluorescent enhancement, fluorescent recovery, fluorescence quenching, anisotropy, wavelength shifts, and ratio-metric fluorescence output. Lately, several nanostructures have been utilized in the manufacturing of fluorescent sensors with enhanced selectivity and sensitivity along with the development of NPs and modification with organic linkers [263]. The biomolecules such as DNAzyme, antibody, and aptamer and some ligands and functional groups existing on the surface of NPs help in their particular linkage to the lead ion (Pb+). The NM-Pb+ associations are linked to direct fluorescence quenching or transfer techniques, including PET, nanomaterial surface energy transfer (NSET), and FRET, aiding in analyte detection [264]. Numerous fluorescent NMs such as up-conversion NPs (UCNPs), metallic NPs, gold nanoclusters (AuNCs), semiconductor quantum dots (QDS), silver nanoclusters (AgNCs) and carbon quantum dots (CQDs), polymer dots (PDs), and metal-organic frameworks (MOFs) have been examined for the fabrication of lead ion (Pb+) sensors associated with the sensing methods [67]. An economical, single-phase, green and energy-efficacious method is developed for the solar-running complex of (BiOBr0.75 I0.25 SS) bismuth oxybromideiodied solid solution on rGO sheets by sunlight radioactivity of BiOBr0.75I0.25-graphene oxide (GO) dispersion in ethanol solution. GO was reduced and photocatalized by BiOBr0.75I0.25 and resulted in unbroken fixation of BiOBr0.75I0.25 SS on r GO to get highly pure BiOBr0.75I0.25-rGO heterojunction, i.e., BiOBr0.75I0.25-rGO HJ, in a dispersed colloidal medium. Large-scale formation of rGO related bismuth oxyhalides HJ was performed by this green strategy [265,266]. The Br:I ratio in the manufactured BiOBr0.75I0.25 SS was approximately 0.75:0.25 [267]. The solar-energy caused holes that were used in a redox reaction with ethanol molecules functionalized on the surface of BiOBr0.75I0.25 SS from ethanol medium to obtain ethoxy-(—C_2H_4OH) radicals that could be resulted in further redox reactions finishing at the formation of H_2O and CO_2. The ethanol molecules adsorbed by this method act as hole scavengers (such as electron donors) and increase the life-span of the photo-fabricated electron permitting their growth on the CB of BiOBr0.75I0.25 [268]. In a redox reaction, the electrons react with the oxygen comprising functional groups of GO to develop rGO sheets resulting in synchronic longitudinal fixation of BiOBr0.75I0.25 SS on rGO sheets to obtain BiOBr0.75I0.25-rGO HJ [268–270]. Super-capacitors and catalyst support are three-dimensional (3-D) configurations of graphene that have revolutionized its practical applications. Macroscopic graphene substances are manufactured by self-assembly to impart them numerous valuable properties. In a study, researchers developed a trivial and green system for manufacturing 3D structures of graphene. This procedure relies on the chemical reduction of graphene oxide by using various natural phenolic acids, and the graphene sheets were self-assembled by p-p associations, in-situ. The attained monolithic graphene shows less density, high porosity, outstanding mechanical strength, super-hydrophobicity, and electrical conductivity. These multifunctional yields can act as super-capacitors and as adsorbents to eliminate dyes, oils, and organic solvents from polluted water [271]. Graphene oxide can be highly-distributed in water due to its numerous hydrophilic groups. The GO dispersion continued to be homogenous after the addition of various types of phenolic acid groups. When the dispersion was heated at 95 °C for 0.5 h, it turned black as GO was moderately reduced in the existence of phenolic acids. The phenols were described as efficient, reducing agents for GO [272,273]. A black column was formed after 3 h of heating and moderately hovered to the uppermost part of the vial. After 8 h, the column became more contracted and completely parted, leaving a clear solution at the bottom. This proved that the water-insoluble rGO sheets were assembled into macroscopic 3-D arrangements by p-p associations and lastly, developed the graphene hydrogel [271]. In crude oil, the most plentiful materials are sulfur-containing compounds. The emission of sulfur oxides and sulfate particulate materials is caused by the presence of sulfur in liquid fuel and it is a threat to community property and health. It also has the potential to decrease the life-span of engines and catalysts due to corrosion. A lot of systems having extreme level of accuracy and sensitivity have been fabricated to analyze sulfur in various samples. In a study, the most important and capable techniques and analytical strategies were discussed to remove sulfur from oil [274]. In the refinery, hydro-desulfurization is a dominant sulfur removal technology, but most of the desulfurization techniques such as bio-desulfurization, oxidation, and absorption are evolving. The existing exercise of hydro-desulfurization is a mix of these systems. The study of thiophene hydro-desulfurization is a field of attention for many scientists to obtain the best kinetic design and appropriate catalyst. Another inspiring research areas for the hydro-desulfurization technique is its function in a prime reactor under mild circumstances. The molecular characterization procedures, the upgrading of equipment, the development of technology and the innovation of detection methods have revolutionized our idea about the presence of sulfur compounds in oils, which can screen efficacious fabrication and investigation in upstream and handling out in downstream along with decreasing the environmental threat. Accordingly, these techniques require more research, particularly in the field of designing suitable selective systems [274]. A lot of research is being done on the application of NMs in different fields such as oil processing, construction, food, medicine, water treatment, sensors, building materials and energy storage, etc. Paints, pigments, coatings, cosmetics and catalytic additives are the examples of the yields comprising NMs. Nanotitania is an example of nanomaterial (NM) that is extensively applied in viable industries in two varieties i.e. in photocatalytic procedures such as formation of self-sterilizing surfaces (anatase) and in sunscreen and other stuffs to block ultraviolet (UV) light (rutile). NMs are applied to enhance food properties, safety, and preservation. NMs are used as (i) food extracts such as TiO_2 (E171), Nisin (E234), SiO_2 (E551), and Fe_2O_3 (E172), (ii) as food constituents, for example, gold, AgO, gelatin-related ingredients, nanosilicon, and nano-encapsulation, (iii) as food supplements such as silica-mineral hydride complex and nano-encapsulates and (iv) as pesticides and biocides, for example, nano-formulations and nano-encapsulates with pesticides on a nano-range (carbofuran) [275]. It is needed to calculate the amount of NMs in real and environmental samples. Therefore, consistent quantitative analysis procedures are essential to detect amounts of NMs in numerous matrices [276,277].

As a result of various pollutants, water pollution has become the most serious problem worldwide. There is a requirement for methods and practices to act as strategies for researchers to form and investigate novel adsorbent tools for wastewater management [278]. Numerous water techniques are used to detect pollutants in biological, chemical, and physical processes in treatment procedures. Adsorption is an economical and effective method applied for wastewater refinement by using inexpensive adsorbents. NMs and waste-derived substances are

favorable adsorbents because of their free availability and high sorption capabilities [278]. Sulfite (SO_3^{2-}) and bisulfite (HSO_3^-) are hydrated sulfur oxide (SO_2) have been extensively used in food items, beverages, and pharmaceutical products conservation [279–281] to prevent oxidation and germs growth and to impede the enzymatic reactions. High consumption of SO3 2/HSO3 will result in allergic reactions and tissue injuries in some folks. Hence, the fabrication of small-molecule reactive probes for efficacious, quantitative, and quick identification of SO3 2/HSO3 in many food items have gained collective considerations in recent times. Many response procedures such as keton or aldehyde groups, nucleophilic addition with electron deficit C—C bonds and inhibition of C—N isomerization are applied to design various small-molecule probes for food analysis [282]. Additionally, SO3 2/HSO3 are highly adaptable to the preservative ability [283]. N-terminus of homocysteine (Hcy) and cysteine (Cys) reacts with aldehydes through cyclization reaction to get thiazinane and thiazolidine products have been widely used to generate fluorescent probes for careful Hcy/Cys recognition over GSH [72,75,284]. Guo and group designed an "OFF-ON"fluorescence probe, in 2010, for HSO3 recognition based on coumarin byproducts with associated aldehyde groups [285]. This probe was used to detect HSO3 in two granulated sugar trials.

In 2012, Yu et al. designed fluorescent probe for sesning SO3 2, in which anthacene fluorophore was linked with aldehyde group by secondary amine and hydrophilic amide linker [286]. Du et al. planned and fabricated an OFF-ON fluorescent probe (52) for SO3 2 monitoring [287]. This probe has a spirolactone and is colorless, it remains non-fluorescent during the ring-opening of spirolactone which results in a robust emission and green color. Ring-opening of probe 52 can be attained by the SO3 2-activated breakdown of levulinyl that is a nucleophilic buildup at the 4-position of levulinate tracked by the cut of ester bond in-situ. This particular cleavage reaction permitted the probe to detect SO3 2 particularly in water medium. The results of this test showed the levels of SO3 2 in white wine and it was established by standard iodometry method. The double bond between two carbon atoms is a part of various chemical substances, particularly for the luminophores having great p-conjugation method. For most of the C—C bonds with even dispersal of electrons the group becomes more stable in organic and aqueous solutions. Complexation of C—C bond with electron extracting groups, for example, nitro group (—NO2), cyano group (—CN), and positively charged quinolinium or indolium modifies the electron density of C—C bond [288,289] that gives a particular site for the introduction of nucleophiles such as SO3 2/HSO3 [282,290–292]. Fig. 7 illustrates the biosensing process through fluorescent NPs.

2.8. Blood gases

Photodynamic therapy (PDT) has gained much attention for treating a wide range of solid tumors due to non-piercing quality, outstanding selectivity, and high efficiency. In PDT, photon energy transferred by photosensitizers, got by oxygen molecule, results in ROS production that causes apoptosis, necrosis, and autophagy of cancer cells [294–297]. Oxygen level highly affects the treatment efficiency of PDT. Hence, it is critical to fabricate a non-piercing tool to sense oxygen changes that is crucial for foreseeing PDT treatment reaction and regulating the cure

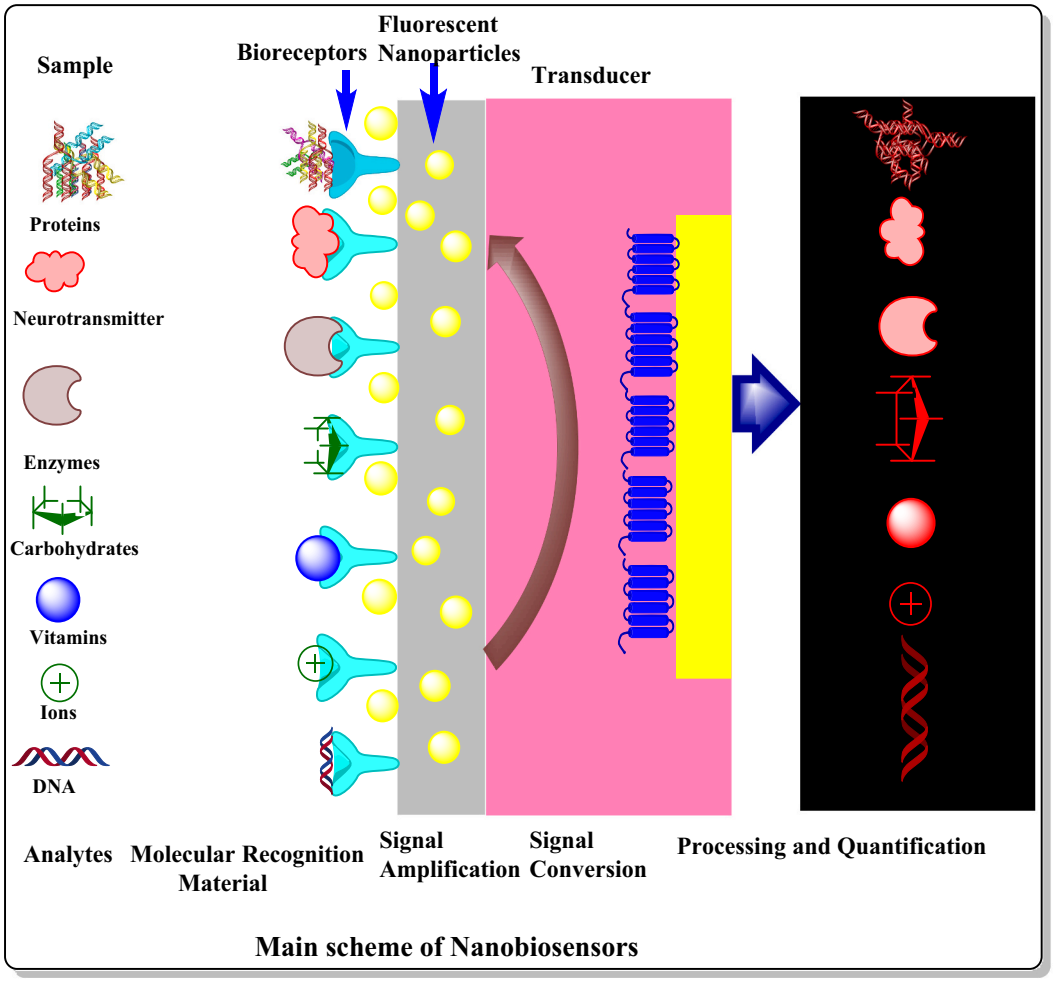

Fig. 7. A schematic representation of the process of sensing different molecules using fluorescent NPs [293].

plan. Fluorescence probes have encouraged remarkable advantages for sensing oxygen because they have high safety and sensitivity [298]. Nanostructures-related oxygen detecting probes for PDT were discovered for *ex-vivo* recognition of oxygen. These probes have not been used *in-vivo* for oxygen detection that is crucial for profound examination and translation. Hollow mesoporous organosilica NPs (HMONs) have extensively been investigated in the biomedical field because of their high surface areas, uniform mesopores, organic-groups hybrid outlines, large hollow cavity, and outstanding biocompatibility [299,300]. In this research, the scientists determine that thioether-bridged deformable HMONS laden with oxygen-sensitive probe $[(Ru(dpp)3]Cl_2$ indicate fabulous oxygen detection efficacy with enhanced cellular uptake and negligible toxicity [301]. Enzyme-related recognition tools for H_2O_2 have been extensively designed because of their high efficacy and selectivity. Nevertheless, enzymes are costly and unstable for long-term usage and storage. Recently, cobalt-related NMs were described as an outstanding catalyst for oxygen evolution and oxygen reduction reactions.

In an investigation, the researchers found that a categorized cobalt or carbon nanotube hybrid nanocomplex (CoCNT) was fabricated using MOFs of ZIF-67 as reactors. It indicates fabulous peroxidase-like characteristics and can quench the fluorescence of scopoletin and alter the non-fluorescent Amplex Red (AR) into its fluorescent constituent with a large fluorescence reaction through oxidation in an H_2O_2 environment. Co-CNT has the inherent catalytic property that permits it to behave as an applicable structural moiety for forming ratiometric fluorescent nanosensors for H_2O_2 [302]. 'Oxygen microscopy' is a term used recently to describe many different hypoxia-related stains, endogenously indicated biosensor structures, phosphorescent oxygen detecting probes, and NPs. On the other hand, there are some equivalent optical procedures for imaging oxygen circulation in cell and tissue microenvironments. They have been extensively used in several experimental methods like 2D and 3D cell cultures, fixed tissues, and cutout slices of live or immobile tissues [303–305].

2.9. Detection of drugs and their toxins

2.9.1. Detection of anti-inflammatory drugs

Liu and coworkers have explored graphene QDs coupled with polypyrrole for fluorescent-based detection of acetaminophen. The fluorescent intensity was reduced on quenching of the oxidation product of the drug by QDs. At the same time, the fluorescence was increased when the oxidation product of paracetamol was reduced by ascorbic acid. The LOD was found to be 0.002 μg/L and 1.05 μg/L for acetaminophen and ascorbic acid, respectively [306].

Li and associates have investigated cadmium tellurium-based fluorescent QDs for quantifying aspirin by quenching method. A linear relationship was observed between the intensity of fluorescence and aspirin concentration [307]. In another study, cadmium tellurium QDs were investigated for sensing ibuprofen in human urine and serum samples. The method was cost-effective, highly selective, and adequately sensitive to detect ibuprofen [308]. Wei and colleagues have investigated cadmium tellurium QDs for fluorescent detection of aspirin using molecularly imprinted polymer. This fluorescent sensor was found to successfully estimate the amount of aspirin in human urine and saliva samples [309].

2.9.2. Detection of antibiotics

Benincasa and associates have demonstrated the fluorescent quenching mechanism to sense florescent labeled Bac $7_{1–35}$ and polymyxin B penetration into the gram-negative bacteria. The system was suitable for intracellular delivery and detection of membrane non-penetrating therapeutic agents [310]. Geng and coworkers have investigated cadmium selenium QDs for fluorescent detection of kanamycin using aptamer conjugated molecularly imprinted polymers for high sensitivity and selectivity [308]. The fluorescent sensor was rapid, selective, and sensitive in determining kanamycin in water, food, and biological samples [308]. Sarmadi and associates have proposed L-cysteine coated. Anand and associates have developed L-cysteine conjugated Cadmium sulfide QDs for selective detection of tetracycline via fluorescence [311]. Niu and associates have also investigated N-doped CDs to sense antibacterial agents [312].

In 2018, Zhou and associates fabricated a MIP-based fluorescent nanobiosensors coated on GQDs for selective sensing of tetracycline. Carboxyl- or -amino-containing GQDs were developed as fluorescent probes using a one-pot green method, while the GQDs-MIPs microspheres were synthesized via applying a sol-gel process. The results demonstrated that the carboxyl group plays a pivotal role in the fluorescence quenching in the presence of tetracycline in a linear concentration (1.0 to 104 μg/L). The LOD was determined to be 1 μg/L [313] (Fig. 8).

2.9.3. Detection of anticancer agents

Jantarat and associates have developed G-quadruplex and thioflavin T containing DNA-based fluorescent sensors to detect cisplatin. The conjugation of DNA with cisplatin caused a decrease in fluorescence intensity. Thus, change in levels of cisplatin can be predicted from changes in fluorescent intensity [314]. Zhang and associates have prepared antibody conjugated L-Cysteine capped CdTe-CdS core-shell type QDs for fluorescent imaging of HeLa cells [315]. Tang and associates have developed fluorescent sensors to detect platinum-based anticancer agents, such as platinum, cisplatin, and nidaplatin in human lung cancer cells [316].

Mitchell and coworkers have investigated a sensing array composed of 6 fluorescent sensors for detecting platinum levels in patients receiving chemotherapy. This fluorescent-based sensing array detected platinum among other related biological components or other heavy metal ions with high accuracy. The sensor successfully detected levels of cisplatin and oxaliplatin in plasma at various stages of platinum therapy [317]. Wang and coworkers have studied fluorescent nanosensors to sense lactate dehydrogenase inhibitors as anticancer agents. The efficacy of drugs was monitored as up-conversion of fluorescence in three types of cancer cells, including A549, HeLa, and human gastric epithelial cell line (Ges-1) [318]. Jiang and coworkers have investigated gold nanoclusters as fluorescence-based switch nanosensors to detect methotrexate and circulating tumor DNA (ctDNA) [319]. Bardajee and associates have also studied CMC-CdTe/zinc sulfide QDs for fluorescence-based epirubicin detection [320].

2.9.4. Detection of miscellaneous agents

Li and Hu have developed CDs from black tea to sense pamidronate disodium and zoledronic acid based on turning off fluorescent signaling [321]. Guan and colleagues have explored cadmium sulfide QDs functionalized by heparin and mercaptopropionic acid for fluorescent-based identification of protamine and hemin. Both molecules were quantified with high sensitivity and selectivity by assessing the fluorescent intensity of a multi-functionalized QDs system [322]. Saini and associates have investigated fluorescent organic nanosensors to sense furosemide in aqueous media [323]. Cai and coworkers have demonstrated CD-based fluorescent sensors for selective and accurate sensing of mercury and glutathione. Conjugation of mercury with CD turned the fluorescence off, while conjugation of mercury with glutathione caused the release of carbon dots and subsequent increase in fluorescence [324]. Peng and associates have explored pyridine-based fluorescent probes for recognizing aluminum ions with a color shift from colorless to aquamarine [325].

Liu and coworkers have demonstrated the use of triple film fluorescent sensors to identify and differentiate commonly abused illicit drugs in the vapor phase [326]. Beatty and coworkers have studied dimeric sensors for rapidly detecting drugs at a very low (micromolar) concentration in aqueous samples and saliva [327]. Kim and colleagues have developed sensors with infra-red dependent fluorescence. The sensor

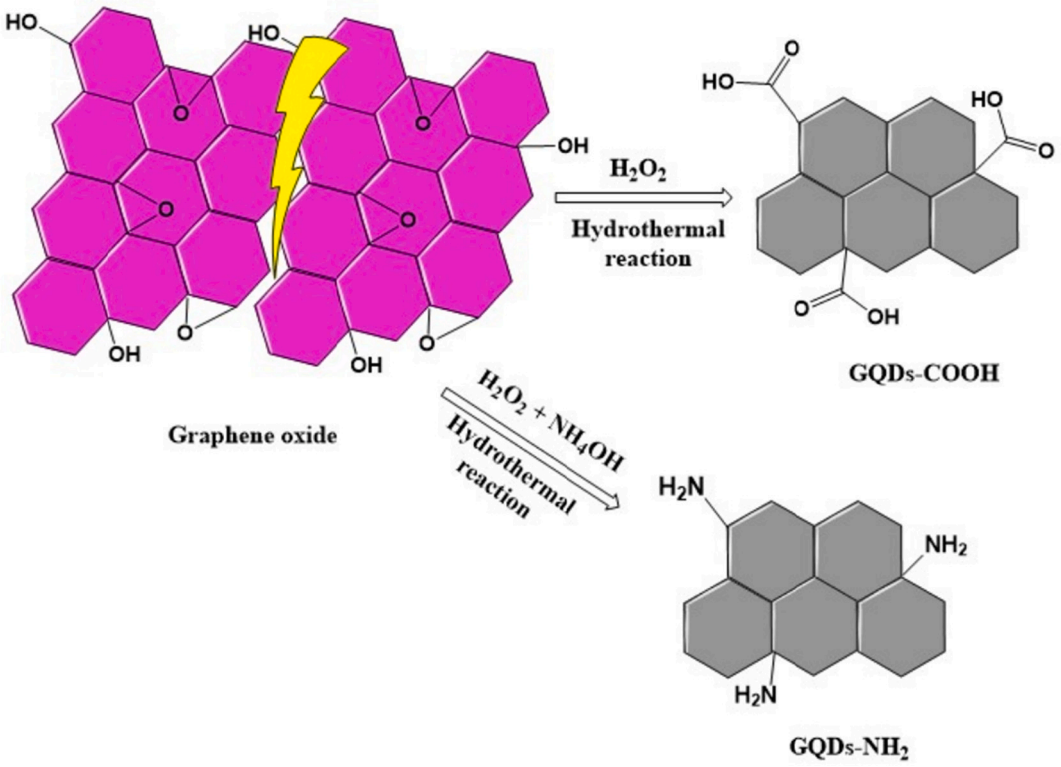

Fig. 8. Schematic illustration of the process of fabricating of GQDs from graphene oxide. Reprinted from ref. [313].

was investigated for recognition of albumin in a human urine specimen with desirable selectivity and sensitivity [328]. Liu and coworkers have fabricated MOFs as fluorescent sensors for discriminating nine different flavonoids. Results indicated successful discrimination of flavonoids along with their quantification [329]. In another study, the amino-BODIPY fluorescent dye was conjugated with a model drug 2-phenyl-3-hydroxy-4(1H)-quinolinone to investigate its release upon cleavage of the conjugate by glutathione. The quantification of the drug was quantified based on ratiometric fluorescence assay using UV–visible spectroscopy [330]. Scarabelli and associates have demonstrated protein conjugated fluorescent biosensors for the investigation of uptake of the drug into cells [331]. Hu and coworkers have explored florescent sensors for cell imaging and drug analysis using coumarin and maleimide conjugate. The sensor successfully distinguished between cysteine and glutathione with a 320 folds increase in the fluorescence emission corresponding to the addition of cysteine [332]. In another study, melamine was detected using fluorescent zirconia-labeled cadmium sulfide QDs by the quenching method [333]. Kulchat and colleagues have developed thioglycolic acid-coated cadmium sulfide QDs to detect dopamine. The fluorescent sensor was sensitive and selective for recognizing dopamine, with the LOD observed to be 0.68 μM [334].

2.9.5. Detection of toxins

NMs have also been investigated to sense various chemical toxins. Ganesan and coworkers have reviewed QDs to detect different types of toxins and drug overdose, drug abuse or misuse, and pesticide toxins [335]. Boron and nitrogen co-doped QDs have been studied for fluorescent detection of mercury and 2,4,6-trinitrophenol with a low LOD [336]. Wang and associates have established a highly sensitive and selective technique for fluorescent-based glyphosate detection utilizing CD-coded antibody and antigen-associated magnetic beads [337]. Nitrogen phosphorous co-doped carbon QDs have also been explored for fluorescent-based carbendazim detection that exhibited strong green fluorescence [115]. In another study, cadmium sulfide fluorescent NPs were studied. These nanosensors selectively detected dicofol, among other pesticides corresponding to a 2.5 times increase in fluorescent intensity [338]. L-Tyrosine functionalized carbon dots have been investigated for fluorescent detection of methyl parathion with high sensitivity and reproducibility [339]. Zhang and associates have developed a fluorescent-based assay to detect morphine using QD labeled anti-morphine antibody [340]. Huang and associates have investigated nitrogen-doped CDs for fluorescent detection of Ach esterase activity and detecting organophosphorus pesticides in food and water [341].

A robust and fast immunological method was designed to detect ochratoxin A (OTA), a mycotoxin mainly formed by Aspergillus. Antigen-modified magnetic NPs were used as immunosensing probes to detect AF B1 and OTA simultaneously in foodstuffs based on the method of competitive fluorescence immunoassay. Similarly, antibody-treated rare-earth-doped NaYF4 (sodium yttrium fluoride) up-conversion NPs acted as multicolor signal probes. The fluorescent intensity was highest in the absence of mycotoxins, but when the amounts of AF B1 and OTA were increased, the fluorescent signals of the nanocomposites decreased slowly [342]. Similarly, organophosphorus pesticides can also be detected by liposome-based nanobiosensor [343]. Here, free substrates and pesticides move into the liposomes by porins implanted into the lipid membrane. This technique is for substrate-linked enzyme activation and the resulting current reaction at the substrate-linked enzyme electrode.

Melamine was also detected similarly by using AuNPs by fluorescence detection method. Li et al. fabricated cadmium telluride (Cd/Te) QDs covered with thioglycolic acid (TGA) and examined their reaction with melamine. It was proved that the fluorescence quenching intensity of TGA-CdTe QDs was directly linked with the concentration of melamine at pH 11.0. This is because the melamine induces quenching of fluorescence emission by QDs [344]. It resulted in the modification of NP's surface by energy transfer, surface absorption, and charge diversion.

2.9.6. Alkaloids

Colchicine belongs to the family of alkaloids, and the potential applications of colchicine have expanded significantly in the fields of oncology, cardiology, immunology, and dermatology [345]. In the study, El-Malla and colleagues designed a fluorescent QD nanosensor to sense colchicine. The sensor was fabricated from uric acid as a carbon/nitrogen source by one-step pyrolysis. The sensor worked based on the internal filter effect (IFE), in which colchicine served as a strong adsorbent and affected the fluorescence excitation of the nanosensor. This overlap led to a slight decrease in the fluorescence of the nanosensor by increasing the concentration of colchicine in the range of 2 to 25 μM. The amount of colchicine was in the range of 1.887 μM QL and 0.623 μM DL [346].

In another study, a FRET nanosensor was fabricated to determine the real-time fluctuation of ajmalicine. Recently, FRET nanosensors have been productively designed to study many analytes *in-vivo*, such as glutamate, ribose, zinc, glycine betaine, lysine, and glucose. A genetically encoded FRET-based nanosensor that was fabricated to detect alkaloid ajmalicine is based on a general framework of sandwiching analyte selective ligand-binding protein between the acceptor fluorescent proteins and the donor, after binding of the target analyte results in the conformational changes that move the non-radiative energy from donor fluorescent protein to the acceptor protein showing an altered emission intensity of fluorophores. Using genetically encoded FRET-related nanosensors, such metabolites can be repeatedly detected in various cell types [347].

2.9.7. Antioxidant

To date, some investigative procedures have been applied to recognize and measure particular biothiols [71,348]. For example, mass spectrometry (MS), capillary electrophoresis, HPLC, and HPLC-MS/MS. Nevertheless, these techniques use expensive equipment and wide-ranging samples [349,350]. Compared to the conventional methods, fluorogenic techniques have attracted great attention because of some particular advantages such as high sensitivity, simple operation, and rapid response time. Multiple biothiols have been designed over the last few years [351–354] for simultaneous detection of homocysteine (Hcy), glutathione (GSH), and/or Cys [355,356]. Nowadays, many nIR or red emission GSH, Cys, or Hcy probes have been fabricated that tag the specific organelle in living cells [357–359]. Recently, a lot of different procedures have been established for GSH recognition, e.g., HPLC and electrochemistry [360], surface-enhanced Raman scattering [361,362], and fluorescence spectroscopy [363,364]. The fluorescent technique has the most benefits, such as high sensitivity, non-destructivity, and simplicity. Many fluorescent probes have been developed to detect GSH, such as BODIPY-based fluorescent sensor, QDs QDs, up-conversion NPs, iridium (III) complex, cyanine-based fluorescent probe, and AuNCs [365–370].

GO has been used to detect multifunctional biomaterials for the past few years due to their outstanding biocompatibility and high cellular uptake. MnO_2 has a very high oxidation ability to reduce to Mn + by GSH, a peptide that modulates redox homeostasis in biological systems [371,372]. In this process, the GO-MnO_2 nanocomposites were first prepared by the reaction between $KMnO_4$ and GO. After that, the fluorescein (FL) was coated on the surface of the nanocomposites by π–π and hydrophobic linkages to develop GO-MnO_2-FL nanocomposite. GO-MnO_2–FL nanocomposite can act as a fluorescent probe for *in-vitro* and *in-vivo* detection of GSH in malignant cells that highly express GSH [373].

Recently, many scientists have proved the quantitative determination of non-enzyme antioxidants such as AA and GSH by using GQDs-ions systems, e.g., Cr_2O_7−, Cu2+, Hg2+, and Fe3+ etc., both turn-on and turn-off fluorescence. In this connection, the fluorescence of GQDs will nearly vanish when there is hypochlorite oxidation, but if the antioxidants are present in the same solution, the quenching will be prevented. Measurements of fluorescence intensity of GQDs-hypochlorite setup permits us to measure the antioxidant present in liquids and cell-fictionalized medium from normal human dermal fibroblasts (NHDF), human keratinocytes (HaCaT), and mesenchymal stem cells (MSCs) after activation of glucose or cytokines [374]. Many CD-based fluorescent Cys probes have been developed, but the disadvantage of this approach is the toxicity caused by the probes when they develop a stable metal-Cys complex with ions such as Ag+ and Hg2+ [375].

Gold nanocrystals are developing NMs having the majority of applications in the biomedical area. AuNCs show unique biocompatibility, large stokes shift, fluorescence properties, high energy levels, and good water solubility [376–378]. These properties make AuNPs a picture-perfect tool for theranostics, imaging, and biosensing at molecular and cellular levels [379,380]. To diagnose hyperthyroid liver damage, thyroid dysfunction is first elucidated, and then the liver function tests are performed [381]. Fast and simple processes have been introduced to simultaneously measure thyroid function and liver injury. GSH plays a significant role in liver damage caused by hyperthyroidism, so the level of liver injury can be measured by detecting GSH levels. Phosphorus metabolism is also linked to thyroid function. UiO-66$(OH)_2$ acted as the core. The shell was fabricated by using Cu-MOFs in the development of core-shell composite metal-organic structure material, which determines the GSH and phosphorus at the same time. The fluorescence signal of UiO-66$(OH)_2$ nanocomposite sensor after a particular action between Zr (IV) and phosphate was used to detect the phosphate. The fluorescence detected GSH based on MOFs framework linked with Cu (II) [382]. A genetically encoded FRET-related nanosensor using fluorescent indicator protein for sialic acid (FLIP-SA) was fabricated to determine NeuAc (N-Acetylneuraminic acid) in living structures non-invasively. This nanosensor is very efficient and can be used to recognize the regulatory phase of the NeuAc biosynthesis pathway and for the metabolic fluctuation detection of NeuAc in its metabolic network. *E. coli* distorted libraries, for diverse manufacturing phases, also use FLIP-SA for high-throughput screening [383].

2.10. Tumor markers

Alpha-fetoprotein (AFP) acts as a highly sensitive prognostic marker for HCC [384]. As an oncofetal glycoprotein, AFP is widely used for the clinical diagnosis of HCC [385]. For the initial prognosis and diagnosis, the increased level of AFP concentration (>20 ng/mL) in adult serum is measured as an early indicator of HCC. ELISA, CLIA [386], surface plasmon resonance imaging (SPRi), and tandem mass spectrometry (HPLC-MS/MS) are employed for systematic biomarker detection. However, there are some limitations, such as severe interferences, slow response, limited sensitivity, and expensive instruments [387–389]. Therefore, it is of extreme importance to manufacture a sensitive, economical and rapid technique to distinguish the trace quantities of AFP for timely and precise diagnosis of HCC.

Chang et al. developed an ultrasensitive fluorescent turn-on biosensor linked to boronic acid functional polymers to detect glycoprotein [390]. There is not very vast research on biomimetic MIPs to sense biological molecules; that is why a biomimetic fluorescent nanobiosensor related to molecularly imprinted polymers was adapted with CDs (CD@MIPs). This sensor was highly sensitive, rapid in action, and capable of detecting AFP in biological samples. The MIPs were used as temperature and pH detection elements in this sensor, and CDs acted as transducer elements. The nanosensor was subjected to characterization such as its stability, binding ability, and selectivity were carefully tested. Furthermore, the CD@MIPs were effectively applied to sense this tumor marker in human specimens. The projected technique can offer a fast and promising opportunity to detect AFP for cancer diagnosis [391].

3. Fluorescent nanosensors to detect urinary metabolites

Several fluorescent nanosensors have been designed to determine urinary metabolites in human serum or urine specimens with promising

outcomes [392].

3.1. Urea

Urea, known as carbamide, is an organic multiple with the chemical formula of CO $(NH_2)_2$. It is mainly synthesized in the liver as a final product of proteins degradation [393]. Blood and urine urea levels could contribute to various diseases, such as nephrotic syndrome, renal failure, gastrointestinal bleeding, liver failure [394,395]; thus, rapid and precise detection of urea and urease is crucial. In the study by Pang et al., pH-sensitive N-CDs, shown in (Fig. 9A), were used as a fluorescent probe for laboratory sensing urea and urease. Based on pH-responsive fluorescent CDs and urea hydrolysis by the urease-catalyzed, they designed a sensing system to determine urea and urease in the range of 0.05 to 3.0 mmol/L and 2.5 to 80 mg/L, respectively. The new raw material used in this study was *m*-phenylenediamine, a pH-sensitive fluorescent CD. The satisfactory linear response of the fluorescence intensity to the pH (in the range of 6.2 to 8.6) and the hydrolysis of urea-catalyzed urease established a new system for sensing these metabolites [396].

Zhang and colleagues designed a fluorescence system to measure pH and detect urea using MoS2 QDs (MQDs) and 2,3-diaminophenazine. MQD was used as a fluorescent reference signal that is not pH sensitive, and DAP was used as a pH-sensitive agent. The increase in pH due to the enzymatic reaction of urea in the presence of urease was used by the above pH assay system to detect urea. The DAP fluorescence intensity increased gradually at 568 nm, but the MQD fluorescence intensity did not change at 420 nm. They observed a linear relationship between urea concentration and fluorescence intensity between 5 and 700 μM and pH reversibility in the range of 3.8–6.0 with a pH interval of 0.2 [397].

In a study by Liu et al., dopamine-functionalized CuInS2 QDs (QDs) were designed as fluorescence probes (Fig. 9B). Urease catalyzes the hydrolysis of urea and releases OH— and changes the pH value. pH-sensitive QDs were used as an effective fluorescence probe to determine urea. The fluorescence intensity of DA-CuInS2 QDs is also associated with enzymatic degradation. The new urea biosensor system effectively quantified urea in the concentration range of 0.2 to 6 mmol/L [398].

In the study by Llopis-Lorente et al., The optical probe includes (i) the enzyme receptor subunit, (ii) the signaling subunit (comprised of a reporter labeled silica), and (iii) the communication mechanism between the two sites created in message generation. Chemical conductors were designed by an enzyme subunit that separates reporter molecules from the silica surface. A urea nanosensor based on the release of oligonucleotides labeled Alexa Fluor 647 from Janus Au-MSNPs with enzymatic function (inter-gold-silica NPs) has been fabricated. Janus Au-MSNP on the silica surface with amino groups attached to oligonucleotides labeled by electrostatic reactions then activated, the gold plate was used to bind the urease enzyme (Fig. 10). This NP can release urea's fluorescent oligonucleotides by enzyme-mediated hydrolysis to further release amino groups on the silica surface. This user-friendly biomedical nanodevice was employed for direct fluorometric determination of urea in human blood samples [399].

3.2. Uric acid

Uric acid (2,6,8-trihydroxypurine, UA) is found in body fluids (i.e., blood serum and urine). Normal UA concentrations vary between 0.12 and 0.46 mM in blood serum and 1.4 and 4.5 mM in urinary excretions. Extremely high levels of UA in the blood (hyperuricemia) can cause several metabolic disorders [400,401], and very high levels of UA can cause multiple sclerosis or oxidative stress. Liu and colleagues

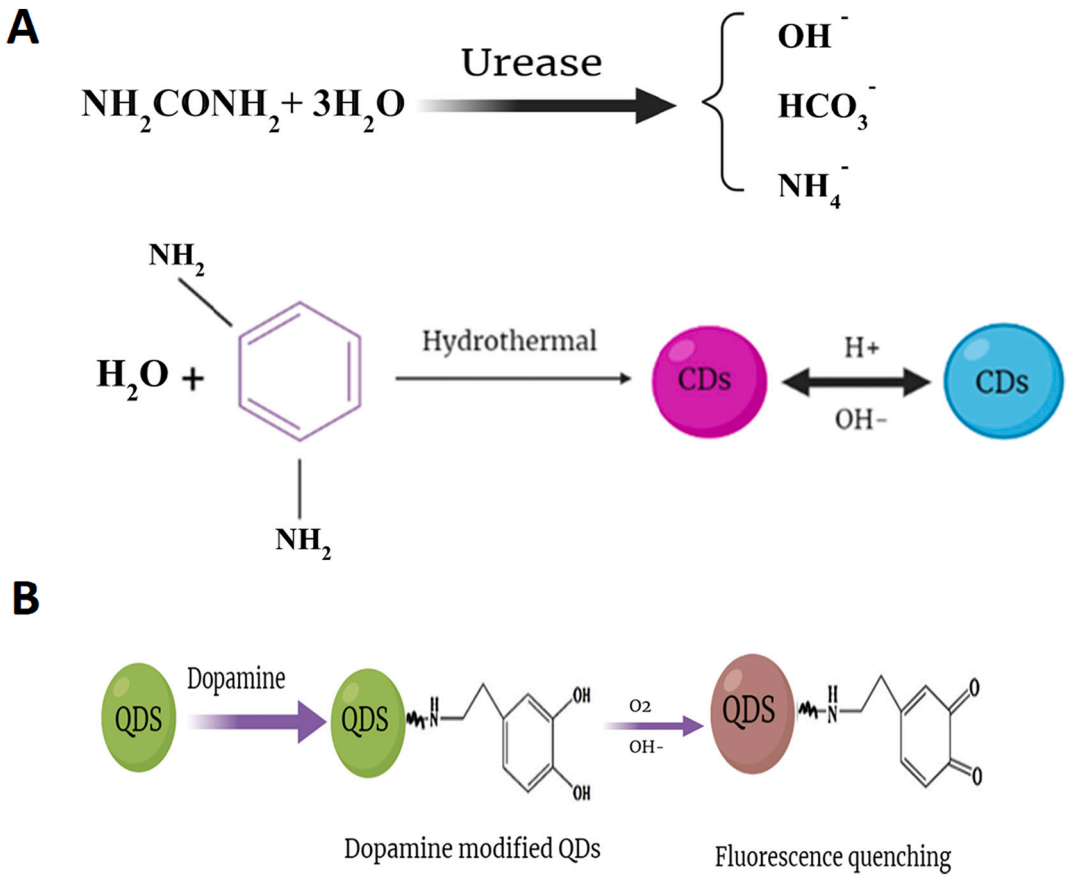

Fig. 9. Fabrication of N-CDs and their application to detect urea or urease (A), synthesis of DA-CuInS2 QDs, and urea detection (B).

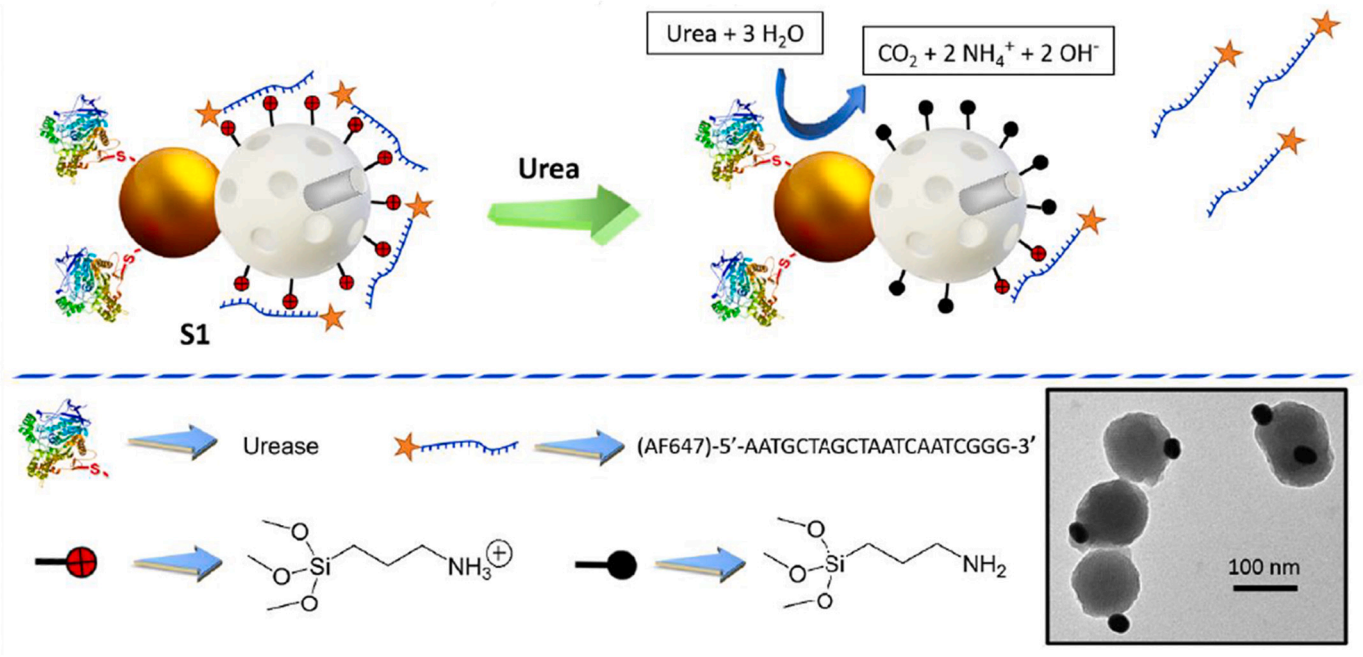

Fig. 10. The sensing performance of the designed nanobiosensor S1 for detection of urea. TEM image of Au-MSNPs. (Reprinted with permission from [399]).

synthesized AuNCs coated with chondroitin sulfate (CS-AuNCs) and poly-(vinylpyrrolidone)-protected AuNPs (PVP-AuNPs) off-fluorescent probes that were able to quantify UA selectively by an internal filter (IFE) (Fig. 11). Uricase-related IFE was used to measure UA at concentrations of 5 to 100 μM (R2 = 0.991) and sensitively detected 1.7 μM (3σ) UA in blood serum specimens [402].

In Hallaj et al.'s study, a two-state colorimetric and fluorometric sensor was designed to determine uric acid by Green emissive N,P co-doped CDs (N,P-CDs), and AuNPs/Ag+. N, P-CDs were prepared from citric acid and urea in a phosphoric acid and formamide mixture to achieve green dots indicating optimal spectral overlap with AuNPs. As a reducing agent in the level of AuNPs, uric acid reduced Ag + to Ag0, resulting in Au @ AgNPs with a more robust surface plasmon resonance peak (SPR). Finally, the results were evaluated by TEM and EDS imaging, and the formation of Au@AgNPs was confirmed. Also, increasing the peak intensity of SPR AuNPs and decreasing the fluorescence of N, P-CD were proportional to the uric acid concentration. Therefore, this sensor could accurately sense UA in human urine samples [403]. Zhao and colleagues, in another experiment, obtained fluorescent carbon spots from pork as a carbon source. These carbon points had strong (17.3%) and stable fluorescent quantum properties. The results showed that fluorescence nanosensors could detect uric acid in the linear range of 0.1–100 μM and 100–500 μM, with a LOD of 0.05 μM (S/N = 3). UA was efficiently detected in human serum and urine samples [392].

In the study by Wang and associates, nitrogen N, sulfur (S) with CDs, Fenton reaction, and UA enzyme reaction were exploited to develop a highly selective fluorescent biosensor to detect uric acid (UA). FL is quenched by hydroxyl radicals induced by the Fenton reaction between H_2O_2 and Fe2+. Under optimal conditions, two linear correlations were observed between the fluorescence attenuation ratio of C points and the UA concentration in the range of 0.08–10 μM and 10–50 μM, respectively. The LOD was reduced to 0.07 μM. The new biosensor also showed successful results in sensing UA in human serum samples [404]. In a study by Wang et al. With two internal filters (IFE) between gold/silver bimetallic nanoclusters (Au/AgNCs) and 2,3-diaminophenazine (DAP) and H_2O_2, a fluorescent probe (RF-probe) was designed to detect uric acid. In this nano-sensor, uric acid was decomposed into allantoin and H_2O_2. By adding horseradish peroxidase (HRP), *o*-phenylenediamine (OPD) is catalytically oxidized to DAP in the presence of H_2O_2. Then, the DAP fluorescence intensity increased to 580 nm by extinguishing the fluorescence of BSA-Au/Ag NCs at 690 nm. This RF probe can detect UA sensitively in the range of 5.0×10^{-6} M to 5.0×10^{-5} M with a LOD of

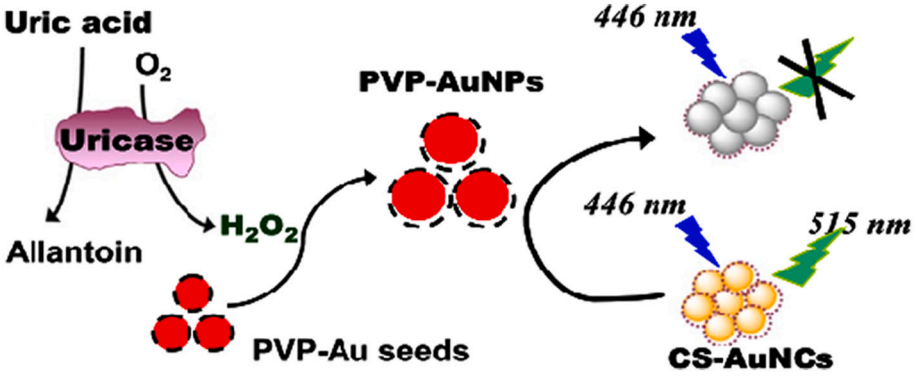

Fig. 11. Detection of H2O2 by IFE-based fluorometric, also UA using the H_2O_2-directed quenching of CS-AuNCs by PVP-AuNPs. (Reprinted with permission from ref. [402]).

5.1×10^{-6} M. The results of the developed probe for determining UA in blood samples were consistent with laboratory measurements at the clinic [405].

In the study by Mathew et al. N—C dot/Cr (VI), nano-exploration was synthesized using one-step pyrolysis using ethanolamine and H_2O_2. Uric acid was synthesized for nanomolar detection. Then its structural properties were evaluated by UV–VIS, FTIR, and XRD. The presence and composition of C, N, O in N-CDs were structurally analyzed and confirmed by SEM-EDX. Detection of Cr (VI) nanomolar values by N-CD by fabricating N-CD/Cr (VI) nanocomposite and switching off in fluorescence function as off-sensor is the lowest detection limit towards Cr (VI) detection of 1.42 nm. The formation of N-CD/Cr (VI) nanocomposites in addition to Cr (VI) in nanocomposites is reduced to non-toxic Cr (III)/Cr (0) in the presence of nanomolar uric acid, which acts as a reducing agent. Cr (VI) to Cr (III)/Cr (0) is observed with the appearance of aqueous fluorescence. Detection of uric acid (UA) is essential in body fluid levels; even a small amount of uric acid in humans leads to Wilson's disease, cardiovascular disorders, and Fanconi syndrome [406].

3.3. Creatinine

Creatinine is produced from the breakdown of creatine by muscles. Creatinine is a waste product that is filtered by the kidneys. Under normal physiological conditions, the amount of creatine in the serum is 35 to 40 μM. Creatine levels in body fluids are measured to check for muscle damage, muscular dystrophy, and kidney failure. Accurate and rapid detection of creatinine can be an important factor in preventing disorders such as kidney, muscle, and thyroid damage. There are several methods for detecting serum creatinine, including spectrophotometers, colorimeters, fluorimetry, etc. [407].

In a study using glutathione-coated copper nanoclusters (CuNCs), Jalili et al. Designed a fluorescent probe to measure creatinine levels accurately. The operation of this fluorescent probe is such that when the Al^{3+} ions and the copper nanoclusters of the probe collide, more fluorescents are emitted. Also, creatinine extinguishes copper nanoclusters, and there is a linear relationship between creatinine concentrations ranging from 2.5 to 34 μg/L and a LOD of 0.63 μg/L. The selectivity of CuNCs was also tested. The results showed that dilution of the samples reduced the level of interference, indicating remarkable selectivity of CuNCs. The probe showed successful results in human serum, although it was not tested in urine [408].

In an experiment performed by Dhara and colleagues, a single-molecule fluorescence fluorescent probe with a naphthalimide probe was designed to quantify creatinine in human serum. Due to the Pd^{2+} quenching effect, the probe slightly emitted fluorescence after coordination with the Pd^{2+} fluorescent ligand. Inhibition of fluorescence behavior is due to the combined effect of the PET process, which operates from fluorophore naphthalimide to Pd^{2+} ion, and the intramolecular charge transfer (ICT) process. The ions Pd^{2+} fluorescence probe reacts with creatinine in the presence of creatinine to produce [Pd $(Cr)_2$ Cl_2] $complex_{56}$ (Cr = creatinine), thereby increasing the fluorescent intensity releasing the fluorescent ligand. The fluorogenic probe measured creatinine as 0.30 μM, being significantly lower than normal in human serum samples [409].

In another study, Du and colleagues designed a fluorescent probe to convert creatinine in an aqueous solution based on the reaction of a palladium catalyst. This group made a water-soluble probe by introducing the hydrophilic ethanol portion of 2-(2-aminoatoxy) with fluorophore naphthalene anhydride. The quenching effect of Pd^{2+} and the effect of photoelectron transfer caused the probe-Pd combination to show poor fluorescence. Nevertheless, in the presence of creatinine, the Pd-probe complex decomposed and regained fluorescence by removing the heavy atom extinguisher and preventing the photoelectron transfer effect. The Pd probe showed an extremely high detection ability of creatinine with a LOD of 0.16 μM. This sensor had high membrane permeability with low cytotoxicity. Therefore, it can potentially be used to detect creatinine in biological samples. In the report by Tajarrod et al., A "turn-on" fluorescence nanobiosensor was fabricated using thioglycolic acid (TGA) ZnS:Mn/ZnS QDs for selective and sensitive determination of creatinine (Crn) in human serum and urine samples. ZnS: Mn/ZnS QDs were fabricated using a simple aqueous sedimentation method. Energy-dispersive X-ray spectroscopy (EDS) showed the emission spectrum of ZGA-functionalized TGA fluorescence: Mn/ZnS QD, increasing the emission intensity in the presence of Crn. The increase in diffusion is due to the inactivation of the surface traps of QDs through the binding of Crn to the QD surface, which results in the formation of recombinant electron-hole radiative centers. The interaction between Crn and QDs was studied exploiting analytical methods, including fluorescence, UV–vis spectroscopy, and DLS assessments. The probe demonstrated an excellent linear relationship between 0.07 and 3.4 EM for Crn with a correlation coefficient (R2) of 0.9963 and a LOD and LOQ of 7.25 nm and 0.0242 EM, respectively. This method was successfully employed to sense Crn content in human urine and blood sample as well. The proposed method has several advantages: high sensitivity, short analysis time, low cost, and ease of operation [410].

4. Fluorescent nanosensors for detecting microorganisms

Various NMs have been studied for fluorescent-based detection of microorganisms with high sensitivity and selectivity. A general scheme to detect microorganisms has been illustrated in Fig. 12. Sutarlie and associates have reviewed various NMs used to detect microbes and their related metabolites concerning the LOD, response time, and dynamic range [411]. Lebegue and associates have reviewed polydiacetylene vesicles for biosensing of various microorganisms and their metabolites because of their ability to show blue to redshift in association with a shift from non-florescent to fluorescent upon exposure to various stimuli [412]. In another study, Alafeef and coworkers have reviewed NPs-based nanosensors for *in-vitro* and *in-vivo* sensing of pathogenic bacteria [413]. Stanisavljevic and coworkers have reviewed the application of QD-nanosensors utilizing the fluorescent resonance energy technique [414]. Jeong and associates have explored supramolecular assembly to detect microorganisms via fluorescent turn on and off mechanism [415].

Jenie and coworkers have demonstrated using rhodamine modified silica NPs for detecting *Escherichia coli* (*E. coli*). The assay was found to be sensitive and selective and exhibited a decreased response time compared to conventional bacterial analysis [416]. Landry and associates have investigated the use of label-free nanosensor array based on estimating a broad range of protein efflux from two microbes, including *E. coli* and *Pichia pastoris* [130]. Li and associates have discussed a calorimetric method to detect microorganisms using AuNPs. The naked eye observed a color shift upon the interaction of AuNPs with microbes [417]. Mehta and associates have investigated fluorescent carbon dots as efficient probes for cellular imaging of *E. coli* and *Saccharomyces cerevisiae* [418]. Kasibabu and coworkers have also demonstrated the use of carbon dots for imaging *Bacillus subtilis* and *Aspergillus aculeatus* cells with green and red emission spectra at different wavelengths [419].

Wang and coworkers have developed a sensitive and rapid method to detect *E. coli*, *Bacillus subtilis*, and *Staphylococcus aureus* in drinking water samples. They have utilized positively charged rhodamine dye to detect negatively charged bacteria by emission of a robust fluorescent peak at 552 nm [420]. Hu and associates have developed a single-step green synthesis of carbon-based QDs for fluorometric detection of *E. coli* in milk [421]. Qiao and associates have investigated gram-negative cell wall-specific NPs via polymyxin B conjugation against *E. coli*. Detection of bacteria was carried out by measuring fluorescent intensity resulting from upconversion of nanocarrier and *E. coli* complexation [422].

Wang and colleagues have developed aptamer-modified nanosensors for detecting *E. coli* using fluorescence resonance transfer. The sensor exhibited a LOD of 17 CFU/mL, demonstrating acceptable sensitivity

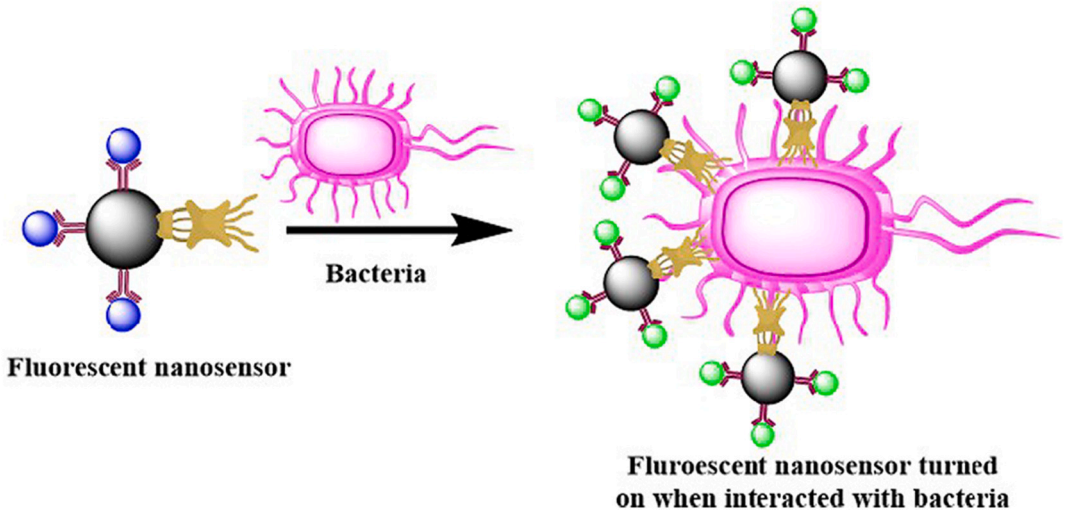

Fig. 12. Illustration of fluorescent nanosensors to detect microorganisms.

and selectivity for detecting *E. coli* [423]. Chen and coworkers have developed an indirect immunofluorescence method using silica NPs to detect *E. coli* O157:H7. The system exhibited stronger fluorescence and improved photostability than the conventional fluorometric dyes [424]. Previous investigations have shown the use of fluorescent nanosensors to detect microorganisms in food and drinking water and other biological samples. These systems appear to be promising to sense a broad range of pathogenic microorganisms in human blood, plasma and urine samples.

AgNPs alleviated with glucose and labeled with a pyrimidine fluorescent conjugated to a monoclonal antibody (IgG) of *Pseudomonas aeruginosa*. When the fluorophore was placed near a metal surface, the fluorescence output was increased due to the specific features of metallic NPs. This nanosystem was used to recognize bacteria in soil, food samples, and water and agriculture samples as well [425].

CdSe/ZnS QDs linked to SiO_2 microspheres form a fluorescent-tagged system to sense *S. typhimurium*. Fluorescent microscopy was used to analyze the conjugation between bacteria and fluorescent NPs. Surface-coatable nIR response fluorescent NPs can be used to detect and kill bacteria in solid and liquid phases. Polydopamine (PdA) is a biological material having binding properties. Carbonized PdA can be treated with polyethyleneimine (PEI) to create fluorescent carbon NPs (FDA: PEI). The anionic bacterial cell wall of Gram-positive and Gram-negative bacteria, e.g., *S. aureus* or *E. coli* gets attached to the cationic surface of NPs by alterations in the fluorescent signal. nIR radioactivity of carbonized NPs generated heat and showed bactericidal effects [426]. The molecular linkages inside the living cells can be studied with increased sensitivity and resolution with this procedure.

FRET is currently used to identify and quantify *Mycobacterium tuberculosis* DNA using fluorometric detection and AuNPs [427]. Immunoassay-related virus recognition procedures have used fluorescent nanostructures as probes [428]. Some researchers have formed a fluorescent diagnostic tool well-matched to a digital camera that transfers its statistics to a central database arrangement and suggests a fascinating POC testing system to detect influenza that could be used as an international real-time investigation system.

Some researchers have improved the process of hepatitis B diagnosis by connecting the fluorescence enzyme-linked immunosorbent assay (FELISA) with metallic NPs. An increase in the LOD of the HBsAg via a traditional assay, i.e., ELISA, has been observed using dually tagged AuNPs [429]. QDs and AuNPs have been exploited for virus detection by FRET as electron donor and acceptor, respectively, in FRET arrays. The fluorophore linked to particular antibodies undergoes a conformational change after attachment to the virus that causes a change distance between fluorescent molecules and a countable shift in the resonance energy transfer. Molecular Beacon hairpin was restrained by using gold or silver nanowires as fluorescence quenchers. QDs have been studied as a fluorophore. They permit the detection and analysis of viral infection by identifying the bioconjugates acquired by antibody affinity and some other linkages. The structural changes in the cytoskeleton can be studied by using different colored QDs. They have proved their capability for influenza virus detection in clinical models and initial stage detection of HIV infections [430]. QDs have also been proposed for detecting the hepatitis B virus (HBV) virus, but their sensitivity is not superior to the already existing methods for this virus detection [431].

Human monoclonal antibodies bind to the viral S protein's primary antigen to stop the host cell entrance and spot the virus for clearance. Each SARS-CoV-2 virion has almost 100 S protein trimers that constitute a significant virus detection target. Seo et al. created a FET-based sensor by treating graphene sheets with SARS-CoV-2 S protein antibodies to accurately sense SARS-CoV-2 with a LOD of 242 copies/mL in nasopharyngeal swabs. Many nanobiosensors for SARS-CoV-2 detection have been developed for both antigen and nucleic acid-based approaches, having sources like QDs and AuNPs. For biological analyte sensing, SWCNTs have proven themselves as an ideal choice. SWCNTs are naturally based on nIR fluorescence, and they can be treated with many other sensing elements to form firm biological sensors having fast fluorescence-shift readouts. Compared to traditional fluorophores, the SWCNTs can be used for a long time without photo-bleaching. Additionally, SWCNTs give simplistic incorporation into transportable factors such as immobilization in hydrogel or paper [432,433] with recognition of nIR SWCNT signal by a charge-coupled device (CCD) camera system similar to a smartphone and Raspberry Pi [434].

5. Challenges in using fluorescent-based nanosensors

Despite substantial achievement in the area of molecular sensing with fluorescent-based nanosensors, there are still technical challenges that limit their application. Identifying reactions that combine a faster rate with high chemoselectivity is considered the main challenge in successfully fabricating a fluorescent probe [435,436]. Overcoming the approaches to incorporating NMs into fluorescent-based nanosensors to detect some metabolites (i.e., glucose) might be controversial. This is because electrochemical sensing of these analytes requires the same sampling procedures and thus, yields no improvement in the patients' quality of life. Moreover, the sensor's lifetime can be another unresolved issue for its application in clinical care [437].

Some NMs, such as MOFs, are insoluble or inadequately dispersive.

Hence, designing practical sensing nanodevices to monitor metabolites in aqueous biological samples is another prominent issue. The lack of selectivity of MOFs has been reported as another challenge for their real-time application in fabricating nanoprobes to sense antibiotics [64]. Because the metal ions often show similar coordination features, fluorescent probes might detect ions interchangeably [436], which is considered a technical barrier.

Some factors, such as essential difficulties in sensor design or inaccessibility of *in-vivo* tissues, have hindered the utilization of fluorescent-based sensors [59]. *In-vivo* sensing and bioimaging demand sensitive instruments which are capable of detecting signals in a living system/organism without perturbing the system/organism being tested. Only a few fluorescent-based nanoprobes have been designed for *in-vivo* imaging of biological molecules. Two examples include AuNP-based nanosensors and QD-based single-molecule fluorescent nanoprobe; both of them use toehold-mediated strand displacement cascade [438]. Before *in-vivo* application of such nanosensors, assessment of biocompatibility, long-time stability, long-term cytotoxicity, metabolic mechanisms, and dynamic behavior of different functional NMs is necessary. The *in-vivo* detection system must also show appropriate spatial and temporal resolution for the interrogated living system [59]. More recently, innovative methods have been introduced to tackle such limitations, and for the first time, allow monitoring of *in-vivo* biology. These strategies were mainly concentrated on enhancing the biocompatibility of the nanosensors of advances in sensing technology. The optimization of physical characterization of NPs [439], coating of biocompatible materials on NP's surface to avoid fast renal clearance [440], utilization of biomimetic hydrogels to reduce foreign body responses [441], miniaturization of electrochemical sensing elements [442], developing wireless power supplies and signal transducers [442], and developing new detection modalities to expand sensing palette [443], are among the most important approaches that have been adopted in the field to address toxicity, biocompatibility, resolution, and multiplexing challenges of developing such *in-vivo* nanobiosensors.

There are marketing issues that limit the application of fluorescent-based biosensors. In this scenario, efforts have been put in making QDs suitable for mass production via different synthetic routes and reaction engineering approaches. Nowadays, home-used glucose nanosensors dominate almost 80% of the world's market of biosensors [444]. Nevertheless, utilizing these nanobiosensors in commercial space is limited because of toxicity, biocompatibility, and stability issues. Compared to their bulk counterparts, the prepared particles could react very differently in physiological conditions, which might be due to their small dimension [445]. The developed sensors must be comparable to the commercially available sensors to justify the additional cost and effort to overcome their manufacturing challenges. One drawback of fluorescent nanoprobes is that they are not widely appropriate for commercial uses because their market pricing is comparatively high, which is not profitable to be used in clinics. In this regard, there is a pressing need to do experiments in order to broaden market prospects and fabricate more reliable and cheaper nanobiosensors. On the other hand, a few detection kits might need fresh preparation of the assay reagents [446], which might limit their commercialization. GO is widely used in establishing sensitive fluorescent nanosensors [447]. So far, the most suitable method for mass production of GO is chemical reduction, forming rGO. However, due to mechanical exfoliation, it is challenging for scientists to complete the task of producing graphene sheets of the same quality in high amounts [448]. In addition to these challenges, fouling, deactivation of the analyte/metabolite, and material degradation might also limit the practical use of these nanosensors [449].

Because of single-molecule fluorescent-based sensors useful application for *in-vitro* or *in-vivo* diagnostics, overcoming current challenges is crucial to facilitate their development for application in biochemistry, biology, biophysics, and pharmacology. Further studies should address such concerns for patients to benefit from fluorescent nanosensing technology.

6. Conclusion and future perspectives

Fluorescent nanosensors have brought revolution nanobiosensing area. These nanoprobes are grouped according to their sensing propensity. They are currently studied for their application in sensing various organic compounds and pharmaceutical agents, microorganisms, and metals at the trace level. This is mainly due to their desirable surface-to-volume ratio, good electronic properties, photostability, tailorability, biocompatibility, high sensitivity, and remarkable selectivity.

The majority of the previously published reports were concerned with applying fluorescent-based nanoprobes in monitoring water pollutants, heavy metals, and ions. In this preliminary review, we comprehensively discussed recent trends in applying fluorescent-based nanoprobes for the analysis of multiple biological molecules and microorganisms. We have also elaborated on structural designing and mechanistic approaches used to develop such nanobiosensors to sense heavy metals, blood gases, amino acids, proteins, enzymes, carbohydrates, urinary metabolites, toxins, antioxidants, drugs, cancer biomarkers, etc. A particular focus is placed on those nanodevices based on CNTs, QDs, CDs, metallic NPs, MOFs, SWCNTs, and nanocrystals. Furthermore, the photophysical processes responsible for monitoring such metabolites, with a low LOD and a wide linear detection range, have been discussed.

As discussed above, fluorescent nanosensors exhibit interesting features for rapid, reliable, and sensitive detection of drug-induced organ damage by estimating elevated or decreased biomarkers levels. The fluorescent bioprode industry will grow rapidly as awareness of early detection and rapid screening for diseases increases. Recently, studies have mainly focused on sensors devoted to monitoring heavy metals or ions or other water pollutants that presented accumulative effects on the human body. Thanks to the functionalizing of NMs, i.e., QDs and aptamers, it is now possible to design nanosensors to analyze a variety of metabolites with remarkable sensitivity, good reversibility, and outstanding specificity.

Various fluorescent-based sensors have been reported so far. Still, most discovered methods are based on blind screening, and the hit rate is not high enough. Some challenges (i.e., toxicity issues) present in utilizing these nanosensors and their commercialization that need to be tackled. This necessitates the dedication of many studies assessing the efficacy of such nanosensors. One strategy to circumvent the insolubility issues of NMs that are used in sensor fabrication is to coat them with layers, films, or fine particles with improved processibility. Combining the powder NMs with other supporting materials might be an alternative strategy to implement such NMs for their practical fluorescent-based sensing uses. Creating structurally robust nano-frameworks via the utilization of organic linkers can feasibly address the collapses observed in post-sensing manipulation of some NMs, such as MOFs. Despite these drawbacks, the small dimension of these nanosensors and their capability for selective, ultrasensitive, label-free, real-time detection could be exploited in array-based screening and *in-vitro* or *in-vivo* diagnostics.

Nanoengineering techniques using fluorescent indicators combined with polymers allow precision control over optical and catalytic features to obtain an ultrasensitive response. These facts, together with the above-mentioned benefits that optic technology provides nowadays, make newly-designed fluorescent biosensors promising nanotools for the analysis of multiple biomolecules in real applications. There is a considerable paucity of knowledge regarding the underlying mechanisms of fluorescence sensing; therefore, more systematic investigations are needed to elucidate the interaction of different NMs with target molecules. For instance, high-throughput biosensing models using fluorescent probes based on computer-aided designs can be developed in future studies to target biological macromolecules, such as carbohydrates. Advancements in terms of the selectivity and fluorescence properties of NMs will pave the way to accurately diagnose and treat various diseases, including human malignancies. From a personal perspective, the research of fluorescent-based nanobiosensors is as hot

not as it has ever been. Altogether, we firmly believe that the current review can foster the wider incorporation of nanomedicine and will be of particular interest to researchers working on fluorescence technology, material chemistry, coordination polymers, and related research areas.

Abbreviations

AIE	Aggregation-induced emission
FRET	Fluorescence resonance energy transfer
AD	Alzheimer's disease
AuNPs	Gold nanoparticles
AuNCs	Gold nanoclusters
AgNPs	Silver nanoparticles
AgNCs	Silver nanoclusters
AFP	Alpha-fetoprotein
CL	Chemiluminescence
CQDs	Carbon QDs
DF-HSI	Dark-field Hyper-spectral Imaging
DFT	Density Function Theory
FITC	Fluorescein isothiocyanate
EDTA	Ethylenediaminetetraacetic acid
AAS	Atomic absorption spectroscopy
IFE	Internal filter effect
E. coli	*Escherichia coli*
N, S-CDs	N, S co-doped carbon dots
NSs	Nanosheets
OGT	O-linked *N*-acetylglucosamine transferase
AAs	Amino acids
QDs	Quantum Dots
CLIA	Chemiluminescence immunoassay
ELISA	Enzyme-linked immunosorbent assay
NPs	Nanoparticles
NMs	Nanomaterials
CDs	Carbon dots
CNPs	Carbon nanoparticles
NCs	Nobel-metal nanocarriers
MOFs	Metal-organic frameworks
GO	Graphene oxide
rGO	Reduced graphene oxide
CSF	Cerebral spinal fluid
LSPR	Localized Surface Plasmon Resonance
SPRi	Surface plasmon resonance imaging
SERS	Surface-enhanced Raman spectroscopy
LOD	Limit of detection
LOQ	Limit of quantification
FTIR	Fourier transform infrared spectroscopy
HPLC	High-performance liquid chromatography
RCA	Rolling circle amplification
HCC	Hepatocellular carcinoma
SWCNTs	Single-walled carbon nanotubes
AFP	Alfa fetoprotein
MIPs	Molecularly imprinted polymers
PKA	Protein kinase A
PBPs	Periplasmic-binding protein superfamily
nIR	near-infrared
DA	Dopamine
NE	Norepinephrine
EP	Epinephrine
Ach	Acetylcholine
FENs	Fluorescent false neurotransmitters
UV	Ultra-violet
HPLC	High performance liquid chromatography
BACE1	β-site amyloid precursor protein cleaving enzyme 1
PET	Photoinduced electron transfer
FET	Field-effect transistor
Gox	Glucose oxidase
GlcNAc	*N*-acetylglucosamine
GSH	Glutathione
Hcy	Homocysteine
MS	Mass spectrometry
MSCs	Mesenchymal stem cells
AuNCs	Gold nanocrystals
GQDs	Graphene quantum dots
PNA	Peptide nucleic acid
GNR	Graphene nanoribbon
FA	Folic acid
VB_{12}	Vitamin B_{12}
PEI	Polyethyleneimine
RSD	Relative standard deviations
SiNDs	Silicon nano-dendrites
PDs	Polymer dots
EDTA	Ethylenediamine tetra acetic acid
ROS	Reactive oxygen species
HRP	Horseradish peroxidase
UA	Uric acid
UCNPs	Upconversion NPs

Funding

None.

Data availability statement

This article's data sharing is not applicable as no new data were created or analyzed in this study.

Ethical approval

Not applicable.

Consent to participate

Not applicable.

Consent for publication

None.

Declaration of competing interest

The authors declare that there is no conflict of interest regarding the publication of this article.

Data availability

No data was used for the research described in the article.

Acknowledgments

None.

References

[1] J.-F. Masson, Consideration of sample matrix effects and "biological" noise in optimizing the limit of detection of biosensors, ACS Publications 5 (11) (2020) 3290–3292.
[2] J.G. Toffaletti, Special topics in diagnostic testing: blood gases and electrolytes, in: AmerAssoc. for Clinical Chemistry, 2001.
[3] L.A. Liotta, E.F. Petricoin, Serum peptidome for cancer detection: spinning biologic trash into diagnostic gold, J. Clin. Invest. 116 (1) (2006) 26–30.
[4] P.L. Wolf, Biochemical diagnosis of liver disease, Indian J. Clin. Biochem. 14 (1) (1999) 59–90.
[5] S. Jain, V. Gautam, S. Naseem, Acute-phase proteins: as diagnostic tool, J. Pharm. Bioallied Sci. 3 (1) (2011) 118.

[6] K.A. Lawton, A. Berger, M. Mitchell, K.E. Milgram, A.M. Evans, L. Guo, R. W. Hanson, S.C. Kalhan, J.A. Ryals, M.V. Milburn, Analysis of the Adult Human Plasma Metabolome, 2008.
[7] S. Li, B. Guo, H. Chen, Z. Shi, Y. Li, Q. Tian, S. Shi, The role of the triglyceride (triacylglycerol) glucose index in the development of cardiovascular events: a retrospective cohort analysis, Sci. Rep. 9 (1) (2019) 1–9.
[8] M. Kowalówka, A.K. Główka, M. Karaźniewicz-Łada, G. Kosewski, Clinical significance of analysis of vitamin D status in various diseases, Nutrients 12 (9) (2020) 2788.
[9] A.C.Y. Laiwah, M.R. Moore, A. Goldberg, Pathogenesis of acute porphyria, QJM 63 (2) (1987) 377–392.
[10] R.L. Wilder, Hormones, pregnancy, and autoimmune diseases, Ann. N. Y. Acad. Sci. 840 (1) (1998) 45–50.
[11] M. Fleischhacker, B. Schmidt, Circulating nucleic acids (CNAs) and cancer—a survey, biochimica et biophysica acta (BBA)-reviews onCancer 1775 (1) (2007) 181–232.
[12] M. Haznadar, C.M. Diehl, A.L. Parker, K.W. Krausz, E.D. Bowman, S. Rabibhadana, M. Forgues, V. Bhudhisawasdi, F.J. Gonzalez, C. Mahidol, Urinary metabolites diagnostic and prognostic of intrahepatic cholangiocarcinoma, Cancer Epidemiol. Biomark. Prev. 28 (10) (2019) 1704–1711.
[13] K.J. Bruemmer, S.W. Crossley, C.J. Chang, Activity-based sensing: a synthetic methods approach for selective molecular imaging and beyond, Angew. Chem. Int. Ed. 59 (33) (2020) 13734–13762.
[14] L. Xue, H. Yamazaki, R. Ren, M. Wanunu, A.P. Ivanov, J.B. Edel, Solid-state nanopore sensors, Nat. Rev. Mater. 5 (12) (2020) 931–951.
[15] M.S. Artiles, C.S. Rout, T.S. Fisher, Graphene-based hybrid materials and devices for biosensing, Adv. Drug Deliv. Rev. 63 (14–15) (2011) 1352–1360.
[16] S. Campuzano, M. Pedrero, G.-P. Nikoleli, J.M. Pingarrón, D.P. Nikolelis, N. Tzamtzis, V.N. Psychoyios, ZnO and graphene microelectrode applications in biosensing, J. Biomed. Nanotechnol. (2014) 1–35.
[17] W. Kim, J.S. Lee, J. Jang, Aptamer-functionalized three-dimensional carbon nanowebs for ultrasensitive and free-standing PDGF biosensor, ACS Appl. Mater. Interfaces 12 (18) (2020) 20882–20890.
[18] J.H. Luong, K.B. Male, J.D. Glennon, Biosensor technology: technology push versus market pull, Biotechnol. Adv. 26 (5) (2008) 492–500.
[19] A. Steinegger, O.S. Wolfbeis, S.M. Borisov, Optical sensing and imaging of pH values: spectroscopies, materials, and applications, Chem. Rev. 120 (22) (2020) 12357–12489.
[20] D. Rajska, A. Brzózka, M. Marciszko-Wiąckowska, M.M. Marzec, D. Chlebda, K. E. Hnida-Gut, G.D. Sulka, Optimization of synthesis conditions of thin Te-doped InSb films and first principles studies of their physicochemical properties, Appl. Surf. Sci. 537 (2021), 147715.
[21] F. Davarpanah, A.K. Yazdi, M. Barani, M. Mirzaei, M. Torkzadeh-Mahani, Magnetic delivery of antitumor carboplatin by using PEGylated-niosomes, DARU J. Pharm. Sci. 26 (1) (2018) 57–64.
[22] A.K. Ebrahimi, M. Barani, I. Sheikhshoaie, Fabrication of a new superparamagnetic metal-organic framework with core-shell nanocomposite structures: characterization, biocompatibility, and drug release study, Mater. Sci. Eng. C 92 (2018) 349–355.
[23] M.R. Hajizadeh, H. Maleki, M. Barani, M.A. Fahmidehkar, M. Mahmoodi, M. Torkzadeh-Mahani, In vitro cytotoxicity assay of D-limonene niosomes: an efficient nano-carrier for enhancing solubility of plant-extracted agents, Res. Pharm. Sci. 14 (5) (2019) 448.
[24] M.R. Hajizadeh, N. Parvaz, M. Barani, A. Khoshdel, M.A. Fahmidehkar, M. Mahmoodi, M. Torkzadeh-Mahani, Diosgenin-loaded niosome as an effective phytochemical nanocarrier: physicochemical characterization, loading efficiency, and cytotoxicity assay, DARU J. Pharm. Sci. 27 (1) (2019) 329–339.
[25] N. Motamedi, M. Barani, A. Lohrasbi-Nejad, M. Mortazavi, A. Riahi-Medvar, R. S. Varma, M. Torkzadeh-Mahani, Enhancement of thermostability of aspergillus flavus urate oxidase by immobilization on the ni-based magnetic metal–organic framework, Nanomaterials 11 (7) (2021) 1759.
[26] M.D. Soltani, H. Meftahizadeh, M. Barani, A. Rahdar, S.M. Hosseinikhah, M. Hatami, M. Ghorbanpour, Guar (Cyamopsis tetragonoloba L.) plant gum: from biological applications to advanced nanomedicine, Int. J. Biol. Macromol. 15 (2021) 1972–1985.
[27] A. Es-Haghi, M.E. Taghavizadeh Yazdi, M. Sharifalhoseini, M. Baghani, E. Yousefi, A. Rahdar, F. Baino, Application of response surface methodology for optimizing the therapeutic activity of ZnO nanoparticles biosynthesized from aspergillus Niger, Biomimetics 6 (2) (2021) 34.
[28] M. Javad Farhangi, A. Es-Haghi, M.E. Taghavizadeh Yazdi, A. Rahdar, F. Baino, MOF-mediated synthesis of CuO/CeO2 composite nanoparticles: characterization and estimation of the cellular toxicity against breast cancer cell line (MCF-7), journal of functionalBiomaterials 12 (4) (2021) 53.
[29] F. Mobaraki, M. Momeni, M.E.T. Yazdi, Z. Meshkat, M.S. Toosi, S.M. Hosseini, Plant-derived synthesis and characterization of gold nanoparticles: investigation of its antioxidant and anticancer activity against human testicular embryonic carcinoma stem cells, Process Biochem. 111 (2021) 167–177.
[30] S.M. Mousavi-Kouhi, A. Beyk-Khormizi, M.S. Amiri, M. Mashreghi, M.E.T. Yazdi, Silver-zinc oxide nanocomposite: from synthesis to antimicrobial and anticancer properties, Ceram. Int. 47 (16) (2021) 21490–21497.
[31] S.M. Mousavi-Kouhi, A. Beyk-Khormizi, V. Mohammadzadeh, M. Ashna, A. Es-haghi, M. Mashreghi, V. Hashemzadeh, H. Mozafarri, M. Nadaf, M.E., Taghavizadeh yazdi, biological synthesis and characterization of gold nanoparticles using Verbascum speciosum schrad. And cytotoxicity properties toward HepG2 cancer cell line, Res. Chem. Intermed. (2021) 1–12.
[32] M.E. Taghavizadeh Yazdi, M. Darroudi, M.S. Amiri, H. Zarrinfar, H.A. Hosseini, M. Mashreghi, H. Mozafarri, A. Ghorbani, S.H. Mousavi, Antimycobacterial, anticancer, antioxidant and photocatalytic activity of biosynthesized silver nanoparticles using berberis integerrima, iranian journal of science and technology, transactions aScience (2021) 1–11.
[33] M.E. Taghavizadeh Yazdi, F. Nourbakhsh, M. Mashreghi, S.H. Mousavi, Ultrasound-based synthesis of ZnO center dot Ag2O3 nanocomposite: characterization and evaluation of its antimicrobial and anticancer properties, Res. Chem. Intermed. 47 (3) (2021) 1285–1296.
[34] M.E.T. Yazdi, M. Darroudi, M.S. Amiri, H.A. Hosseini, F. Nourbakhsh, M. Mashreghi, M. Farjadi, S.M.M. Kouhi, S.H. Mousavi, Anticancer, antimicrobial, and dye degradation activity of biosynthesised silver nanoparticle using Artemisia kopetdaghensis, Micro Nano Lett. 15 (14) (2020) 1046–1050.
[35] A. Shakeri-Zadeh, H. Zareyi, R. Sheervalilou, S. Laurent, H. Ghaznavi, H. Samadian, Gold nanoparticle-mediated bubbles in cancer nanotechnology, J. Control. Release 330 (2021) 49–60.
[36] B. Hashemi, F.-A. Akram, H. Amirazad, M. Dadashpour, M. Sheervalilou, D. Nasrabadi, M. Ahmadi, R. Sheervalilou, M.A.S. Reza, F. Ghazi, Emerging importance of nanotechnology-based approaches to control the COVID-19 pandemic; focus on nanomedicine iterance in diagnosis and treatment of COVID-19 patients, J. Drug Delivery Sci. Technol. 102967 (2021).
[37] Z. Zhou, Y.S. Sohn, R. Nechushtai, I. Willner, DNA tetrahedra modules as versatile optical sensing platforms for multiplexed analysis of miRNAsendonucleases, and aptamer-ligand complexes, ACS nano 14 (7) (2020) 9021–9031.
[38] R. Sheervalilou, O. Shahraki, L. Hasanifard, M. Shirvaliloo, S. Mehranfar, H. Lotfi, Y. Pilehvar-Soltanahmadi, Z. Bahmanpour, S.S. Zadeh, Z. Nazarlou, Electrochemical nano-biosensors as novel approach for the detection of lung cancer-related MicroRNAs, Curr. Mol. Med. 20 (1) (2020) 13–35.
[39] R. Sheervalilou, M. Shirvaliloo, S. Sargazi, H. Ghaznavi, Recent advances in iron oxide nanoparticles for brain cancer theranostics: from in vitro to clinical applications, Expert Opin. Drug Deliv. (2021) 1–29.
[40] H. Jafarizadeh-Malmiri, Z. Sayyar, N. Anarjan, A. Berenjian, Nano-sensors in food nanobiotechnology, in: Nanobiotechnology in Food: Concepts, Applications and Perspectives, Springer, 2019, pp. 81–94.
[41] M. Shamsipur, A. Barati, Z. Nematifar, Fluorescent pH nanosensors: design strategies and applications, J. Photochem. Photobiol. C: Photochem. Rev. 39 (2019) 76–141.
[42] A. Amann, P. Mochalski, V. Ruzsanyi, Y.Y. Broza, H. Haick, Assessment of the exhalation kinetics of volatile cancer biomarkers based on their physicochemical properties, J. Breath Res. 8 (1) (2014), 016003.
[43] S. Dolai, S.K. Bhunia, S. Rajendran, V. UshaVipinachandran, S.C. Ray, P. Kluson, Tunable fluorescent carbon dots: synthesis progress, fluorescence origin, selective and sensitive volatile organic compounds detection, Crit. Rev. Solid State Mater. Sci. 46 (4) (2021) 349–370.
[44] H. Chen, L. Wei, X. Guo, C. Hai, L. Xu, L. Zhang, W. Lan, C. Zhou, Y. She, H. Fu, Determination of l-theanine in tea water using fluorescence-visualized paper-based sensors based on CdTe quantum dots/corn carbon dots and nano-porphyrin with chemometrics, J. Sci. Food Agric. 101 (6) (2021) 2552–2560.
[45] S. Qu, X. Wang, Q. Lu, X. Liu, L. Wang, A biocompatible fluorescent ink based on water-soluble luminescent carbon nanodots, Angew. Chem. Int. Ed. 51 (49) (2012) 12215–12218.
[46] Y. Wu, P. Wei, S. Pengpumkiat, E.A. Schumacher, V.T. Remcho, Development of a carbon dot (C-dot)-linked immunosorbent assay for the detection of human α-fetoprotein, Anal. Chem. 87 (16) (2015) 8510–8516.
[47] Z. Gao, L. Wang, R. Su, R. Huang, W. Qi, Z. He, A carbon dot-based "off–on" fluorescent probe for highly selective and sensitive detection of phytic acid, Biosens. Bioelectron. 70 (2015) 232–238.
[48] P. Wang, M.J. Meziani, Y. Fu, C.E. Bunker, X. Hou, L. Yang, H. Msellek, M. Zaharias, J.P. Darby, Y.-P. Sun, Carbon dots versus nano-carbon/organic hybrids–dramatically different behaviors in fluorescence sensing of metal cations with structural and mechanistic implications, Nanoscale Adv. 3 (8) (2021) 2316–2324.
[49] G. Gao, Y.-W. Jiang, H.-R. Jia, J. Yang, F.-G. Wu, On-off-on fluorescent nanosensor for Fe3+ detection and cancer/normal cell differentiation via silicon-doped carbon quantum dots, Carbon 134 (2018) 232–243.
[50] X. Ren, P. Lu, R. Feng, T. Zhang, Y. Zhang, D. Wu, Q. Wei, An ITO-based point-of-care colorimetric immunosensor for ochratoxin a detection, Talanta 188 (2018) 593–599.
[51] D.U. Yildirim, A. Ghobadi, E. Ozbay, Nanosensors based on localized surface plasmon resonance, in: Plasmonic Sensors and their Applications, 2021, pp. 23–54.
[52] J. Zhou, G. Tian, L. Zeng, X. Song, X.W. Bian, nanoscaled metal-organic frameworks for biosensing, imaging, and cancer therapy, Adv. Healthcare Mater. 7 (10) (2018) 1800022.
[53] M.P. Jewell, M.D. Greer, A.L. Dailey, K.J. Cash, triplet-triplet annihilation upconversion based nanosensors for fluorescence detection of potassium, ACS Sensors 5 (2) (2020) 474–480.
[54] R. Cheng, C. Yu, Z. Zhen, S. Tang, S. Ou, Understanding the selective-sensing mechanism of lysine by fluorescent nanosensors based on graphene quantum dots, Spectrochim. Acta A Mol. Biomol. Spectrosc. 242 (2020), 118732.
[55] X. Luo, Y. Han, X. Chen, W. Tang, T. Yue, Z. Li, Carbon dots derived fluorescent nanosensors as versatile tools for food quality and safety assessment: a review, Trends Food Sci. Technol. 95 (2020) 149–161.
[56] A. Chakraborty, S.P. Ravi, Y. Shamiya, C. Cui, A. Paul, Harnessing the physicochemical properties of DNA as a multifunctional biomaterial for biomedical and other applications, Chem. Soc. Rev. 50 (13) (2021) 7779–7819.

[57] S. Ansari, S. Masoum, Recent advances and future trends on molecularly imprinted polymer-based fluorescence sensors with luminescent carbon dots, Talanta 223 (2021), 121411.
[58] E. Nosheen, A. Shah, F.J. Iftikhar, S. Aftab, N.K. Bakirhan, S.A. Ozkan, Optical nanosensors for pharmaceutical detection, in: New Developments in Nanosensors for Pharmaceutical Analysis, Elsevier, 2019, pp. 119–140.
[59] M.A. Eckert, P.Q. Vu, K. Zhang, D. Kang, M.M. Ali, C. Xu, W. Zhao, Novel molecular and nanosensors for in vivo sensing, Theranostics 3 (8) (2013) 583.
[60] L. Yang, T.J. Webster, Monitoring tissue healing through nanosensors, in: Nanotechnology enabled in situ sensors for monitoring health, 2011, pp. 41–59.
[61] S. Patel, R. Jamunkar, D. Sinha, T.K. Patle, T. Kant, K. Dewangan, K. Shrivas, Recent development in nanomaterials fabricated paper-based colorimetric and fluorescent sensors: a review, Trends Environ. Anal. Chem. 31 (2021), e00136.
[62] Z. Liu, B. Liu, J. Ding, J. Liu, Fluorescent sensors using DNA-functionalized graphene oxide, Anal. Bioanal. Chem. 406 (27) (2014) 6885–6902.
[63] H. Wan, Q. Xu, P. Gu, H. Li, D. Chen, N. Li, J. He, J. Lu, AIE-based fluorescent sensors for low concentration toxic ion detection in water, J. Hazard. Mater. 403 (2021), 123656.
[64] P.R. Lakshmi, P. Nanjan, S. Kannan, S. Shanmugaraju, Recent advances in luminescent metal–organic frameworks (LMOFs) based fluorescent sensors for antibiotics, Coord. Chem. Rev. 435 (2021), 213793.
[65] A. Gupta, N. Kumar, A review of mechanisms for fluorescent "turn-on"probes to detect Al 3+ ions, RSC Adv. 6 (108) (2016) 106413–106434.
[66] R. Balamurugan, J.-H. Liu, B.-T. Liu, A review of recent developments in fluorescent sensors for the selective detection of palladium ions, Coord. Chem. Rev. 376 (2018) 196–224.
[67] H. Singh, A. Bamrah, S.K. Bhardwaj, A. Deep, M. Khatri, K.-H. Kim, N. Bhardwaj, Nanomaterial-based fluorescent sensors for the detection of lead ions, J. Hazard. Mater. 407 (2021), 124379.
[68] M.D. Pluth, E. Tomat, S.J. Lippard, Biochemistry of mobile zinc and nitric oxide revealed by fluorescent sensors, Annu. Rev. Biochem. 80 (2011) 333–355.
[69] L.M. Hyman, K.J. Franz, Probing oxidative stress: small molecule fluorescent sensors of metal ions, reactive oxygen species, and thiols, Coord. Chem. Rev. 256 (19–20) (2012) 2333–2356.
[70] C. Nathan, Specificity of a third kind: reactive oxygen and nitrogen intermediates in cell signaling, J. Clin. Invest. 111 (6) (2003) 769–778.
[71] S.-H. Park, N. Kwon, J.-H. Lee, J. Yoon, I. Shin, Synthetic ratiometric fluorescent probes for detection of ions, Chem. Soc. Rev. 49 (1) (2020) 143–179.
[72] X. Chen, Y. Zhou, X. Peng, J. Yoon, Fluorescent and colorimetric probes for detection of thiols, Chem. Soc. Rev. 39 (6) (2010) 2120–2135.
[73] K. Brieger, S. Schiavone, F.J. Miller, K.-H. Krause, Reactive oxygen species: from health to disease, Swiss Med. Wkly. 142 (2012), w13659.
[74] H. Kobayashi, M.R. Longmire, M. Ogawa, P.L. Choyke, Rational chemical design of the next generation of molecular imaging probes based on physics and biology: mixing modalities, colors and signals, Chem. Soc. Rev. 40 (9) (2011) 4626–4648.
[75] R. Zhang, J. Yong, J. Yuan, Z.P. Xu, Recent advances in the development of responsive probes for selective detection of cysteine, Coord. Chem. Rev. 408 (2020), 213182.
[76] C.J. Chang, T. Gunnlaugsson, T.D. James, Imaging agents, Chem. Soc. Rev. 44 (14) (2015) 4484–4486.
[77] L. Tian, H. Ma, B. Song, Z. Dai, X. Zheng, R. Zhang, K. Chen, J. Yuan, Time-gated luminescence probe for ratiometric and luminescence lifetime detection of hypochorous acid in lysosomes of live cells, Talanta 212 (2020), 120760.
[78] L. Tian, H. Feng, Z. Dai, R. Zhang, Resorufin-based responsive probes for fluorescence and colorimetric analysis, J. Mater. Chem. B 9 (1) (2021) 53–79.
[79] S. Tajik, Z. Dourandish, K. Zhang, H. Beitollahi, Q. Van Le, H.W. Jang, M. Shokouhimehr, Carbon and graphene quantum dots: a review on syntheses, characterization, biological and sensing applications for neurotransmitter determination, RSC Adv. 10 (26) (2020) 15406–15429.
[80] C. Jiang, G. Wang, R. Hein, N. Liu, X. Luo, J.J. Davis, Antifouling strategies for selective in vitro and in vivo sensing, Chem. Rev. 120 (8) (2020) 3852–3889.
[81] J.-M. Liu, Z.-H. Wang, H. Ma, S. Wang, Probing and quantifying the food-borne pathogens and toxins: from in vitro to in vivo, J. Agric. Food Chem. 66 (5) (2018) 1061–1066.
[82] K. Sun, Y. Tang, Q. Li, S. Yin, W. Qin, J. Yu, D.T. Chiu, Y. Liu, Z. Yuan, X. Zhang, In vivo dynamic monitoring of small molecules with implantable polymer-dot transducer, ACS Nano 10 (7) (2016) 6769–6781.
[83] A. Sharma, N. Sharma, A. Kumari, H.-J. Lee, T. Kim, K.M. Tripathi, Nano-carbon based sensors for bacterial detection and discrimination in clinical diagnosis: a junction between material science and biology, Appl. Mater. Today 18 (2020), 100467.
[84] J.A.C. Pérez, J.E. Sosa-Hernández, S.M. Hussain, M. Bilal, R. Parra-Saldivar, H. M. Iqbal, Bioinspired biomaterials and enzyme-based biosensors for point-of-care applications with reference to cancer and bio-imaging, biocatalysis and agricultural, Biotechnology 17 (2019) 168–176.
[85] K.K. Jain, Nanotechnology in clinical laboratory diagnostics, Clin. Chim. Acta 358 (1–2) (2005) 37–54.
[86] O.S. Ahmad, T.S. Bedwell, C. Esen, A. Garcia-Cruz, S.A. Piletsky, Molecularly imprinted polymers in electrochemical and optical sensors, Trends Biotechnol. 37 (3) (2019) 294–309.
[87] N. Mehta, S.P. Sahu, S. Shaik, R. Devireddy, M.R. Gartia, Dark-field hyperspectral imaging for label free detection of nano-bio-materials, Wiley Interdiscip. Rev. Nanomed. Nanobiotechnol. 13 (1) (2021), e1661.
[88] D. Bhatnagar, V. Kumar, A. Kumar, I. Kaur, Graphene quantum dots FRET based sensor for early detection of heart attack in human, Biosens. Bioelectron. 79 (2016) 495–499.
[89] R.E. Wang, L. Tian, Y.-H. Chang, A homogeneous fluorescent sensor for human serum albumin, J. Pharm. Biomed. Anal. 63 (2012) 165–169.
[90] H. Kaspar, K. Dettmer, W. Gronwald, P.J. Oefner, Advances in amino acid analysis, Anal. Bioanal. Chem. 393 (2) (2009) 445–452.
[91] R. Rajamanikandan, A.D. Lakshmi, M. Ilanchelian, Smart phone assisted, rapid, simplistic, straightforward and sensitive biosensing of cysteine over other essential amino acids by β-cyclodextrin functionalized gold nanoparticles as a colorimetric probe, New J. Chem. 44 (28) (2020) 12169–12177.
[92] H. Yao, Y. Zhang, F. Xiao, Z. Xia, J. Rao, Quantum dot/bioluminescence resonance energy transfer based highly sensitive detection of proteases, Angew. Chem. 119 (23) (2007) 4424–4427.
[93] P. Zhou, M. She, P. Liu, S. Zhang, J. Li, Measuring the distribution and concentration of cysteine by fluorescent sensor for the visual study of paracetamol-induced pro-sarcopenic effect, Sensors Actuators B Chem. 318 (2020), 128258.
[94] M. Ioniţă, G.M. Vlăsceanu, A.A. Watzlawek, S.I. Voicu, J.S. Burns, H. Iovu, Graphene and functionalized graphene: extraordinary prospects for nanobiocomposite materials, Compos. Part B 121 (2017) 34–57.
[95] X. Xu, J. Huang, J. Li, J. Yan, J. Qin, Z. Li, A graphene oxide-based AIE biosensor with high selectivity toward bovine serum albumin, Chem. Commun. 47 (45) (2011) 12385–12387.
[96] J. Chen, S.R. Nugen, Detection of protease and engineered phage-infected bacteria using peptide-graphene oxide nanosensors, Anal. Bioanal. Chem. 411 (12) (2019) 2487–2492.
[97] T. Yoshitake, Y. Kiyohara, I. Kato, T. Ohmura, H. Iwamoto, K. Nakayama, S. Ohmori, K. Nomiyama, H. Kawano, K. Ueda, Incidence and risk factors of vascular dementia and Alzheimer's disease in a defined elderly japanese population: the hisayama study, Neurology 45 (6) (1995) 1161–1168.
[98] T. Themelis, R. Gotti, S. Orlandini, R. Gatti, Quantitative amino acids profile of monofloral bee pollens by microwave hydrolysis and fluorimetric high performance liquid chromatography, J. Pharm. Biomed. Anal. 173 (2019) 144–153.
[99] M. Arts, Z. Soons, S.R. Ellis, K.A. Pierzchalski, B. Balluff, G.B. Eijkel, L.J. Dubois, N.G. Lieuwes, S.M. Agten, T.M. Hackeng, Detection of localized hepatocellular amino acid kinetics by using mass spectrometry imaging of stable isotopes, Angew. Chem. Int. Ed. 56 (25) (2017) 7146–7150.
[100] H. Chen, H. Chen, J. Ying, J. Huang, L. Liao, Dispersive liquid–liquid microextraction followed by high-performance liquid chromatography as an efficient and sensitive technique for simultaneous determination of chloramphenicol and thiamphenicol in honey, Anal. Chim. Acta 632 (1) (2009) 80–85.
[101] V. Shapaval, T. Møretrø, H.P. Suso, A.W. Åsli, J. Schmitt, D. Lillehaug, H. Martens, U. Böcker, A. Kohler, A high-throughput microcultivation protocol for FTIR spectroscopic characterization and identification of fungi, J. Biophotonics 3 (8–9) (2010) 512–521.
[102] Z. Zhang, T. Wei, Y. Chen, T. Chen, B. Chi, F. Wang, X. Chen, A polydiacetylenes-based colorimetric and fluorescent probe for L-arginine and L-lysine and its application for logic gate, Sensors Actuators B Chem. 255 (2018) 2211–2217.
[103] R.S. Bhosale, G.V. Shitre, R. Kumar, D.O. Biradar, S.V. Bhosale, R. Narayan, S. V. Bhosale, A 8-hydroxypyrene-1, 3, 6-trisulfonic acid trisodium salt (HPTS) based colorimetric and green turn-on fluorescent sensor for the detection of arginine and lysine in aqueous solution, Sensors Actuators B Chem. 241 (2017) 1270–1275.
[104] A. Han, L. Xiong, S. Hao, Y. Yang, X. Li, G. Fang, J. Liu, Y. Pei, S. Wang, Highly bright self-assembled copper nanoclusters: a novel photoluminescent probe for sensitive detection of histamine, Anal. Chem. 90 (15) (2018) 9060–9067.
[105] H. Ding, B. Li, S. Pu, G. Liu, D. Jia, Y. Zhou, A fluorescent sensor based on a diarylethene-rhodamine derivative for sequentially detecting Cu2+ and arginine and its application in keypad lock, Sensors Actuators B Chem. 247 (2017) 26–35.
[106] M. Wang, L. Guo, D. Cao, Metal-organic framework as luminescence turn-on sensor for selective detection of metal ions: absorbance caused enhancement mechanism, Sensors Actuators B Chem. 256 (2018) 839–845.
[107] M. Xu, S.P. Kelley, T.E. Glass, A multi-component sensor system for detection of amphiphilic compounds, Angew. Chem. Int. Ed. 57 (39) (2018) 12741–12744.
[108] J. Li, Y. Yue, F. Huo, C. Yin, Rational design of cysteine-specific ratiometric probe based on steric hindrance effect and its biological application, Dyes Pigments 164 (2019) 335–340.
[109] J. Luo, Z. Xie, J.W. Lam, L. Cheng, H. Chen, C. Qiu, H.S. Kwok, X. Zhan, Y. Liu, D. Zhu, Aggregation-induced emission of 1-methyl-1, 2, 3, 4, 5-pentaphenylsilole, Chemical communications 18 (2001) 1740–1741.
[110] M. Zhang, M.L. Saha, M. Wang, Z. Zhou, B. Song, C. Lu, X. Yan, X. Li, F. Huang, S. Yin, Multicomponent platinum (II) cages with tunable emission and amino acid sensing, J. Am. Chem. Soc. 139 (14) (2017) 5067–5074.
[111] Y. Yan, R.M. Laine, H. Liu, In Situ Methylation Transforms Aggregation-caused Quenching into Aggregation-induced Emission: Functional Porous Silsesquioxane-based Composites with Enhanced Near-infrared Emission, 2019.
[112] H. Liu, H. Liu, Selective dye adsorption and metal ion detection using multifunctional silsesquioxane-based tetraphenylethene-linked nanoporous polymers, J. Mater. Chem. A 5 (19) (2017) 9156–9162.
[113] H. Fu, O. Hu, Y. Fan, Y. Hu, J. Huang, Z. Wang, Y. She, Rational design of an "on-off-on" fluorescent assay for chiral amino acids based on quantum dots and nanoporphyrin, Sensors Actuators B Chem. 287 (2019) 1–8.
[114] J. Hao, M. Wang, S. Wang, Y. Huang, D. Cao, Dissolution-enhanced emission of 1, 3, 6, 8-tetrakis (p-benzoic acid) pyrene for detecting arginine and lysine amino acids, Dyes Pigments 175 (2020), 108131.

[115] Y. Yang, D. Huo, H. Wu, X. Wang, J. Yang, M. Bian, Y. Ma, C. Hou, N, P-doped carbon quantum dots as a fluorescent sensing platform for carbendazim detection based on fluorescence resonance energy transfer, Sensors Actuators B Chem. 274 (2018) 296–303.
[116] Q. Bao, D. Lin, Y. Gao, L. Wu, J. Fu, K. Galaa, X. Lin, L. Lin, Ultrasensitive off-on-off fluorescent nanosensor for protamine and trypsin detection based on inner-filter effect between NS-CDs and gold nanoparticles, Microchemical Journal 168 (2021), 106409.
[117] J. Hu, Y. Li, Y. Li, B. Tang, C.-Y. Zhang, Single quantum dot-based nanosensor for sensitive detection of O-GlcNAc transferase activity, Anal. Chem. 89 (23) (2017) 12992–12999.
[118] T.A. Saleh, M.M. Al-Shalalfeh, A.T. Onawole, A.A. Al-Saadi, Ultra-trace detection of methimazole by surface-enhanced raman spectroscopy using gold substrate, Vib. Spectrosc. 90 (2017) 96–103.
[119] T.A. Saleh, M.M. Al-Shalalfeh, A.A. Al-Saadi, Silver loaded graphene as a substrate for sensing 2-thiouracil using surface-enhanced raman scattering, Sensors Actuators B Chem. 254 (2018) 1110–1117.
[120] A.A. Al-Saadi, M. Haroon, S.A. Popoola, T.A. Saleh, Sensitive SERS detection and characterization of procaine in aqueous media by reduced gold nanoparticles, Sensors Actuators B Chem. 304 (2020), 127057.
[121] T.A. Saleh, M.M. Al-Shalalfeh, A.A. Al-Saadi, Graphene dendrimer-stabilized silver nanoparticles for detection of methimazole using surface-enhanced Raman scattering with computational assignment, Sci. Rep. 6 (1) (2016) 1–12.
[122] M. Wu, X. Wang, K. Wang, Z. Guo, An ultrasensitive fluorescent nanosensor for trypsin based on upconversion nanoparticles, Talanta 174 (2017) 797–802.
[123] W. Liu, H. Li, Y. Wei, C. Dong, A label-free phosphorescence sensing platform for trypsin based on Mn-ZnS QDs, RSC Adv. 7 (43) (2017) 26930–26934.
[124] D. Zhao, C. Chen, J. Zhao, J. Sun, X. Yang, Label-free fluorescence turn-on strategy for trypsin activity based on thiolate-protected gold nanoclusters with bovine serum albumin as the substrate, Sensors Actuators B Chem. 247 (2017) 392–399.
[125] J. Wang, R.S. Li, H.Z. Zhang, N. Wang, Z. Zhang, C.Z. Huang, Highly fluorescent carbon dots as selective and visual probes for sensing copper ions in living cells via an electron transfer process, Biosens. Bioelectron. 97 (2017) 157–163.
[126] S. Xu, F. Zhang, L. Xu, X. Liu, P. Ma, Y. Sun, X. Wang, D. Song, A fluorescence resonance energy transfer biosensor based on carbon dots and gold nanoparticles for the detection of trypsin, Sensors Actuators B Chem. 273 (2018) 1015–1021.
[127] S. Ghosh, A. Metlushko, S. Chaudhry, M. Dutta, M.A. Stroscio, Detection of c-reactive protein using network-deployable DNA aptamer based optical nanosensor, in: 2019 IEEE EMBS International Conference on Biomedical & Health Informatics (BHI), IEEE, 2019, pp. 1–4.
[128] J.-H. Ahn, J.-H. Kim, N.F. Reuel, P.W. Barone, A.A. Boghossian, J. Zhang, H. Yoon, A.C. Chang, A.J. Hilmer, M.S. Strano, Label-free, single protein detection on a near-infrared fluorescent single-walled carbon nanotube/protein microarray fabricated by cell-free synthesis, Nano Lett. 11 (7) (2011) 2743–2752.
[129] R.M. Williams, C. Lee, D.A. Heller, A fluorescent carbon nanotube sensor detects the metastatic prostate cancer biomarker uPA, ACS Sensors 3 (9) (2018) 1838–1845.
[130] M.P. Landry, H. Ando, A.Y. Chen, J. Cao, V.I. Kottadiel, L. Chio, D. Yang, J. Dong, T.K. Lu, M.S. Strano, Single-molecule detection of protein efflux from microorganisms using fluorescent single-walled carbon nanotube sensor arrays, Nat. Nanotechnol. 12 (4) (2017) 368–377.
[131] K. Lee, J. Lee, B. Ahn, Design of refolding DNA aptamer on single-walled carbon nanotubes for enhanced optical detection of target proteins, Anal. Chem. 91 (20) (2019) 12704–12712.
[132] Y.M. Bar-On, A. Flamholz, R. Phillips, R. Milo, Science forum: SARS-CoV-2 (COVID-19) by the numbers, elife 9 (2020), e57309.
[133] S.Y. Lee, N. Fazlina, G.J. Tye, DNA-templated silver nanocluster for live-intracellular FOXP3 detection, Anal. Biochem. 581 (2019), 113352.
[134] J. Soleymani, V. Shafiei-Irannejad, M.R. Hamblin, M. Hasanzadeh, M.H. Somi, A. Jouyban, Applications of advanced materials in bio-sensing in live cells: methods and applications, Mater. Sci. Eng. C 121 (2021), 111691.
[135] O. Manzoor, N. Soleja, P. Khan, M.I. Hassan, M. Mohsin, Visualization of thiamine in living cells using genetically encoded fluorescent nanosensor, Biochem. Eng. J. 146 (2019) 170–178.
[136] Y. Choi, Y. Cho, M. Kim, R. Grailhe, R. Song, Fluorogenic quantum dot-gold nanoparticle assembly for beta secretase inhibitor screening in live cell, Anal. Chem. 84 (20) (2012) 8595–8601.
[137] B. Thirumalraj, N. Dhenadhayalan, S.-M. Chen, Y.-J. Liu, T.-W. Chen, P.-H. Liang, K.-C. Lin, Highly sensitive fluorogenic sensing of L-cysteine in live cells using gelatin-stabilized gold nanoparticles decorated graphene nanosheets, Sensors Actuators B Chem. 259 (2018) 339–346.
[138] J. Soleymani, V. Shafiei-Irannejad, M.R. Hamblin, M. Hasanzadeh, M.H. Somi, A. Jouyban, Applications of advanced materials in bio-sensing in live cells: methods and applications, Mater. Sci. Eng. C 111691 (2020).
[139] Y. Chen, P. Pei, Z. Lei, X. Zhang, D. Yin, F. Zhang, A promising NIR-II fluorescent sensor for peptide-mediated long-term monitoring of kidney dysfunction, Angew. Chem. Int. Ed. 60 (29) (2021) 15809–15815.
[140] J. Zhang, S. Kruss, A.J. Hilmer, S. Shimizu, Z. Schmois, F. De La Cruz, P. W. Barone, N.F. Reuel, D.A. Heller, M.S. Strano, A rapid, direct, quantitative, and label-free detector of cardiac biomarker troponin T using near-infrared fluorescent single-walled carbon nanotube sensors, Adv. Healthc. Mater. 3 (3) (2014) 412–423.
[141] A. Hendler-Neumark, G. Bisker, Fluorescent single-walled carbon nanotubes for protein detection, Sensors 19 (24) (2019) 5403.
[142] Z. Wang, H. Zheng, C. Zhang, D. Tang, Q. Wu, W. Dessie, Y. Jiang, A red emissive fluorescent turn-on sensor for the rapid detection of selenocysteine and its application in living cells imaging, Sensors 20 (17) (2020) 4768.
[143] H.-B. Wang, Y. Li, G.-L. Dong, T. Gan, Y.-M. Liu, A convenient and label-free colorimetric assay for dopamine detection based on the inhibition of the cu (ii)-catalyzed oxidation of a 3, 3′, 5, 5′-tetramethylbenzidine–H 2 O 2 system, New J. Chem. 41 (23) (2017) 14364–14369.
[144] A. Zhang, J.L. Neumeyer, R.J. Baldessarini, Recent progress in development of dopamine receptor subtype-selective agents: potential therapeutics for neurological and psychiatric disorders, Chem. Rev. 107 (1) (2007) 274–302.
[145] Y. Liu, J. Du, M. Wang, J. Zhang, C. Liu, X. Li, Recent progress in quantitatively monitoring vesicular neurotransmitter release and storage with micro/nanoelectrodes, Front. Chem. 8 (2020).
[146] S. Mignani, M. Bryszewska, M. Zablocka, B. Klajnert-Maculewicz, J. Cladera, D. Shcharbin, J.-P. Majoral, Can dendrimer based nanoparticles fight neurodegenerative diseases?Current situation versus other established approaches, Progress in Polymer Science 64 (2017) 23–51.
[147] A.G. Beyene, K. Delevich, J.T.Del Bonis-O'Donnell, D.J. Piekarski, W.C. Lin, A. W. Thomas, S.J. Yang, P. Kosillo, D. Yang, G.S. Prounis, Imaging striatal dopamine release using a nongenetically encoded near infrared fluorescent catecholamine nanosensor, Sci. Advances 5 (7) (2019), eaaw3108.
[148] C. Wang, C. Pan, Z. Wei, X. Wei, F. Yang, L. Mao, Bionanosensor based on N-doped graphene quantum dots coupled with CoOOH nanosheets and their application for in vivo analysis of ascorbic acid, Anal. Chim. Acta 1100 (2020) 191–199.
[149] C.A. Black, M.L. Bucher, J.M. Bradner, L. Jonas, K. Igarza, G.W. Miller, Assessing vesicular monoamine transport and toxicity using fluorescent false neurotransmitters, Chem. Res. Toxicol. 34 (5) (2020) 1256–1264.
[150] D. Sulzer, D. Sames, Fluorescent false neurotransmitters, compendium of in vivo monitoring in real-time probing brain function, disease and injury with enhanced optical and electrochemical sensors, Mol. Neurosci 3 (2019) 33.
[151] C. Tan, E.M. Robbins, B. Wu, X.T. Cui, Recent advances in in vivo neurochemical monitoring, Micromachines 12 (2) (2021) 208.
[152] D. Diaz-Diestra, B. Thapa, J. Beltran-Huarac, B.R. Weiner, G. Morell, L-cysteine capped ZnS: Mn quantum dots for room-temperature detection of dopamine with high sensitivity and selectivity, Biosens. Bioelectron. 87 (2017) 693–700.
[153] Y. Wang, B. Si, S. Lu, E. Liu, X. Hu, J. Fan, Near-infrared excitation of CdTe quantum dots based on fluorescence resonance energy transfer and their use as fluorescent sensors, Sensors Actuators B Chem. 246 (2017) 127–135.
[154] X. Fu, X. Tan, R. Yuan, S. Chen, A dual-potential electrochemiluminescence ratiometric sensor for sensitive detection of dopamine based on graphene-CdTe quantum dots and self-enhanced Ru (II) complex, Biosens. Bioelectron. 90 (2017) 61–68.
[155] M. Wang, Y. Li, L. Wang, X. Su, A label-free fluorescence nanosensor for the determination of adrenaline based on graphene quantum dots, Anal. Methods 9 (30) (2017) 4434–4438.
[156] K.S. Hettie, X. Liu, K.D. Gillis, T.E. Glass, Selective catecholamine recognition with NeuroSensor 521: a fluorescent sensor for the visualization of norepinephrine in fixed and live cells, ACS Chem. Neurosci. 4 (6) (2013) 918–923.
[157] M. Dunn, A. Henke, S. Clark, Y. Kovalyova, K.A. Kempadoo, R.J. Karpowicz, E. R. Kandel, D. Sulzer, D. Sames, Designing a norepinephrine optical tracer for imaging individual noradrenergic synapses and their activity in vivo, Nat. Commun. 9 (1) (2018) 1–13.
[158] J. Feng, C. Zhang, J.E. Lischinsky, M. Jing, J. Zhou, H. Wang, Y. Zhang, A. Dong, Z. Wu, H. Wu, A genetically encoded fluorescent sensor for rapid and specific in vivo detection of norepinephrine, Neuron 102 (4) (2019) 745–761, e8.
[159] N. Chauhan, S. Soni, P. Agrawal, Y.P.S. Balhara, U. Jain, Recent advancement in nanosensors for neurotransmitters detection: present and future perspective, Process Biochem. 91 (2020) 241–259.
[160] Y. Shi, Y. Pang, N. Huang, C. Sun, Y. Pan, Y. Cheng, Y. Long, H. Zheng, Competitive method for fluorescent dopamine detection in cerebrospinal fluid based on the peroxidase-like activity of ficin, Spectrochim. Acta A Mol. Biomol. Spectrosc. 209 (2019) 8–13.
[161] S. Govindaraju, S.R. Ankireddy, B. Viswanath, J. Kim, K. Yun, Fluorescent gold nanoclusters for selective detection of dopamine in cerebrospinal fluid, Sci. Rep. 7 (1) (2017) 1–12.
[162] J.-L. Chen, X.-P. Yan, K. Meng, S.-F. Wang, Graphene oxide based photoinduced charge transfer label-free near-infrared fluorescent biosensor for dopamine, Anal. Chem. 83 (22) (2011) 8787–8793.
[163] W. Nawrot, K. Drzozga, S. Baluta, J. Cabaj, K. Malecha, A fluorescent biosensors for detection vital body fluids' agents, Sensors 18 (8) (2018) 2357.
[164] J. Liu, C. Duan, W. Zhang, H.T. Ta, J. Yuan, R. Zhang, Z.P. Xu, Responsive nanosensor for ratiometric luminescence detection of hydrogen sulfide in inflammatory cancer cells, Anal. Chim. Acta 1103 (2020) 156–163.
[165] R.M. Williams, S. Chen, R.E. Langenbacher, T.V. Galassi, J.D. Harvey, P.V. Jena, J. Budhathoki-Uprety, M. Luo, D.A. Heller, Harnessing nanotechnology to expand the toolbox of chemical biology, Nat. Chem. Biol. 17 (2) (2021) 129–137.
[166] J. Hu, Z.-Y. Wang, C.-C. Li, C.-Y. Zhang, Advances in single quantum dot-based nanosensors, Chem. Commun. 53 (100) (2017) 13284–13295.
[167] P. Zhang, X.-F. Jiang, X. Nie, Y. Huang, F. Zeng, X. Xia, S. Wu, A two-photon fluorescent sensor revealing drug-induced liver injury via tracking γ-glutamyltranspeptidase (GGT) level in vivo, Biomaterials 80 (2016) 46–56.
[168] J. Chen, D. Huang, M. She, Z. Wang, X. Chen, P. Liu, S. Zhang, J. Li, Recent Progress in fluorescent sensors for drug-induced liver injury assessment, ACS Sensors 6 (3) (2021) 628–640.

[169] J. Ma, X. Cheng, F. Peng, N. Zhang, R. Li, L. Sun, Z.-L. Li, H. Jiang, A polymer dots fluorescent sensor for detection of alkaline phosphatase activity and inhibitor evaluation, J. Mater. Sci. 54 (13) (2019) 10055–10064.
[170] Y. Yue, F. Huo, C. Yin, The chronological evolution of small organic molecular fluorescent probes for thiols, Chem. Sci. 12 (4) (2021) 1220–1226.
[171] S. Needs, The Biochemical Basis of Congenital Disorders of Glycosylation, Open University, United Kingdom, 2018.
[172] J. Liu, Y.-Q. Sun, Y. Huo, H. Zhang, L. Wang, P. Zhang, D. Song, Y. Shi, W. Guo, Simultaneous fluorescence sensing of Cys and GSH from different emission channels, J. Am. Chem. Soc. 136 (2) (2014) 574–577.
[173] S. Qi, W. Liu, P. Zhang, J. Wu, H. Zhang, H. Ren, J. Ge, P. Wang, A colorimetric and ratiometric fluorescent probe for highly selective detection of glutathione in the mitochondria of living cells, Sensors Actuators B Chem. 270 (2018) 459–465.
[174] J. Wang, H. Wang, Y. Hao, S. Yang, H. Tian, B. Sun, Y. Liu, A novel reaction-based fluorescent probe for the detection of cysteine in milk and water samples, Food Chem. 262 (2018) 67–71.
[175] Y. Yue, F. Huo, X. Li, Y. Wen, T. Yi, J. Salamanca, J.O. Escobedo, R.M. Strongin, C. Yin, pH-dependent fluorescent probe that can be tuned for cysteine or homocysteine, Org. Lett. 19 (1) (2017) 82–85.
[176] C. Zhao, H. Cui, J. Duan, S. Zhang, J. Lv, Self-catalyzing chemiluminescence of luminol-diazonium ion and its application for catalyst-free hydrogen peroxide detection and rat arthritis imaging, Anal. Chem. 90 (3) (2018) 2201–2209.
[177] S. Wang, R. Cazelles, W.-C. Liao, M. Vázquez-González, A. Zoabi, R. Abu-Reziq, I. Willner, Mimicking horseradish peroxidase and NADH peroxidase by heterogeneous Cu2+-modified graphene oxide nanoparticles, Nano Lett. 17 (3) (2017) 2043–2048.
[178] R. El Kurdi, D. Patra, Tuning the surface of au nanoparticles using poly (ethylene glycol)-block-poly (propylene glycol)-block-poly (ethylene glycol): enzyme free and label free sugar sensing in serum samples using resonance rayleigh scattering spectroscopy, Phys. Chem. Chem. Phys. 20 (14) (2018) 9616–9629.
[179] D. Yin, X. Bo, J. Liu, L. Guo, A novel enzyme-free glucose and H2O2 sensor based on 3D graphene aerogels decorated with Ni3N nanoparticles, Anal. Chim. Acta 1038 (2018) 11–20.
[180] C.H.D. Nieto, A.M. Granero, J.C. Lopez, G.D. Pierini, G.J. Levin, H. Fernández, M. A. Zon, Development of a third generation biosensor to determine hydrogen peroxide based on a composite of soybean peroxidase/chemically reduced graphene oxide deposited on glassy carbon electrodes, Sensors Actuators B Chem. 263 (2018) 377–386.
[181] D. Jiang, Z. Chu, J. Peng, J. Luo, Y. Mao, P. Yang, W. Jin, One-step synthesis of three-dimensional Co (OH) 2/rGO nano-flowers as enzyme-mimic sensors for glucose detection, Electrochim. Acta 270 (2018) 147–155.
[182] H. Chen, A. Fang, L. He, Y. Zhang, S. Yao, Sensitive fluorescent detection of H2O2 and glucose in human serum based on inner filter effect of squaric acid-iron (III) on the fluorescence of upconversion nanoparticle, Talanta 164 (2017) 580–587.
[183] J. Zhao, W. Dong, X. Zhang, H. Chai, Y. Huang, FeNPs@ Co3O4 hollow nanocages hybrids as effective peroxidase mimics for glucose biosensing, Sensors Actuators B Chem. 263 (2018) 575–584.
[184] Q. Liu, Y. Yang, X. Lv, Y. Ding, Y. Zhang, J. Jing, C. Xu, One-step synthesis of uniform nanoparticles of porphyrin functionalized ceria with promising peroxidase mimetics for H2O2 and glucose colorimetric detection, Sensors Actuators B Chem. 240 (2017) 726–734.
[185] J. Chang, H. Li, T. Hou, W. Duan, F. Li, Based fluorescent sensor via aggregation induced emission fluorogen for facile and sensitive visual detection of hydrogen peroxide and glucose, Biosens. Bioelectron. 104 (2018) 152–157.
[186] T. Wang, X. Hu, X. Zhang, H. Cao, Y. Huang, P. Feng, MoS 2 QDs co-catalytic Fenton reaction for highly sensitive photoluminescence sensing of H 2 O 2 and glucose, Anal. Methods 11 (4) (2019) 415–420.
[187] T. Liu, S. Zhang, W. Liu, S. Zhao, Z. Lu, Y. Wang, G. Wang, P. Zou, X. Wang, Q. Zhao, Smartphone based platform for ratiometric fluorometric and colorimetric determination H2O2 and glucose, Sensors Actuators B Chem. 305 (2020), 127524.
[188] G. Fang, H. Wang, Z. Bian, J. Sun, A. Liu, H. Fang, B. Liu, Q. Yao, Z. Wu, Recent development of boronic acid-based fluorescent sensors, RSC Adv. 8 (51) (2018) 29400–29427.
[189] G. Pandey, R. Chaudhari, B. Joshi, S. Choudhary, J. Kaur, A. Joshi, Fluorescent biocompatible platinum-porphyrin–doped polymeric hybrid particles for oxygen and glucose biosensing, Sci. Rep. 9 (1) (2019) 1–12.
[190] C.-L. Shen, Q. Lou, K.-K. Liu, L. Dong, C.-X. Shan, Chemiluminescent carbon dots: synthesis, properties, and applications, Nano Today 35 (2020), 100954.
[191] C.L. Shen, Q. Lou, J.H. Zang, K.K. Liu, S.N. Qu, L. Dong, C.X. Shan, Near-infrared chemiluminescent carbon nanodots and their application in reactive oxygen species bioimaging, Adv. Sci. 7 (8) (2020) 1903525.
[192] D. Cui, J. Li, X. Zhao, K. Pu, R. Zhang, Semiconducting polymer nanoreporters for near-infrared chemiluminescence imaging of immunoactivation, Adv. Mater. 32 (6) (2020) 1906314.
[193] P. Cheng, Q. Miao, J. Li, J. Huang, C. Xie, K. Pu, Unimolecular chemo-fluoro-luminescent reporter for crosstalk-free duplex imaging of hepatotoxicity, J. Am. Chem. Soc. 141 (27) (2019) 10581–10584.
[194] S. He, C. Xie, Y. Jiang, K. Pu, An organic afterglow protheranostic nanoassembly, Adv. Mater. 31 (32) (2019) 1902672.
[195] J. Huang, Y. Lyu, J. Li, P. Cheng, Y. Jiang, K. Pu, A renal-clearable duplex optical reporter for real-time imaging of contrast-induced acute kidney injury, Angew. Chem. 131 (49) (2019) 17960–17968.
[196] C.L. Shen, Q. Lou, C.F. Lv, J.H. Zang, S.N. Qu, L. Dong, C.X. Shan, Bright and multicolor chemiluminescent carbon nanodots for advanced information encryption, Adv. Sci. 6 (11) (2019) 1802331.
[197] K. Billingsley, M.K. Balaconis, J.M. Dubach, N. Zhang, E. Lim, K.P. Francis, H. A. Clark, Fluorescent nano-optodes for glucose detection, Anal. Chem. 82 (9) (2010) 3707–3713.
[198] M. Fehr, S. Lalonde, I. Lager, M.W. Wolff, W.B. Frommer, In vivo imaging of the dynamics of glucose uptake in the cytosol of COS-7 cells by fluorescent nanosensors, J. Biol. Chem. 278 (21) (2003) 19127–19133.
[199] K. El-Boubbou, X. Huang, Glyco-nanomaterials: translating insights from the "sugar-code" to biomedical applications, Curr. Med. Chem. 18 (14) (2011) 2060–2078.
[200] R.A. Nascimento, R.E. Özel, W.H. Mak, M. Mulato, B. Singaram, N. Pourmand, Single cell "glucose nanosensor" verifies elevated glucose levels in individual cancer cells, Nano Lett. 16 (2) (2016) 1194–1200.
[201] M. Marradi, F. Chiodo, I. García, S. Penadés, Glycoliposomes and metallic glyconanoparticles in glycoscience, in: Synthesis and Biological Applications of Glycoconjugates, 2011, pp. 164–202.
[202] C.-H. Chen, C.-C. Wang, P.-Y. Ko, Y.-L. Chen, Nanomaterial-based adsorbents and optical sensors for illicit drug analysis, J. Food Drug Anal. 28 (4) (2020).
[203] K. Xing, J. Ge, W.-X. Wang, X. Geng, X.-P. Shen, J.-L. Tang, L.-B. Qu, Y.-Q. Sun, Z.-H. Li, A turn-on fluorescent probe for sensitive detection of ascorbic acid based on SiNP–MnO 2 nanocomposites, New J. Chem. 43 (24) (2019) 9466–9471.
[204] J. Ge, R. Cai, L. Yang, L. Zhang, Y. Jiang, Y. Yang, C. Cui, S. Wan, X. Chu, W. Tan, Core–shell HA-AuNPs@ SiNPs nanoprobe for sensitive fluorescence hyaluronidase detection and cell imaging, ACS Sustain. Chem. Eng. 6 (12) (2018) 16555–16562.
[205] M.L. Desai, H. Basu, S. Saha, R.K. Singhal, S.K. Kailasa, Investigation of silicon doping into carbon dots for improved fluorescence properties for selective detection of Fe3+ ion, Opt. Mater. 96 (2019), 109374.
[206] S.H. Baek, T.P. Nguyen, K.Y. Park, S. Ha, R. Rafique, S.K. Kailasa, T.J. Park, Synthesis of fluorescent silicon quantum dots for ultra-rapid and selective sensing of cr (VI) ion and biomonitoring of cancer cells, Mater. Sci. Eng. C 93 (2018) 429–436.
[207] D. Li, N. Li, L. Zhao, S. Xu, Y. Sun, P. Ma, D. Song, X. Wang, Colorimetric and fluorescent dual-mode measurement of blood glucose by organic silicon nanodots, ACS Appl. Nano Mater. 3 (11) (2020) 11600–11607.
[208] M. Rizwan, N.F. Mohd-Naim, M.U. Ahmed, Trends and advances in electrochemiluminescence nanobiosensors, Sensors 18 (1) (2018) 166.
[209] A. Solaimuthu, A.N. Vijayan, P. Murali, P.S. Korrapati, Nano-biosensors and their relevance in tissue engineering, current opinion in biomedical, Engineering 13 (2020) 84–93.
[210] H. Wang, H. Tang, C. Yang, Y. Li, Selective single molecule nanopore sensing of microRNA using PNA functionalized magnetic core–shell Fe3O4–Au nanoparticles, Anal. Chem. 91 (12) (2019) 7965–7970.
[211] T. Kilic, A. Erdem, M. Ozsoz, S. Carrara, microRNA biosensors: opportunities and challenges among conventional and commercially available techniques, Biosens. Bioelectron. 99 (2018) 525–546.
[212] H. Kuang, Y. Zhao, W. Ma, L. Xu, L. Wang, C. Xu, Recent developments in analytical applications of quantum dots, TrAC Trends Anal. Chem. 30 (10) (2011) 1620–1636.
[213] H. Liu, T. Tian, Y. Zhang, L. Ding, J. Yu, M. Yan, Sensitive and rapid detection of microRNAs using hairpin probes-mediated exponential isothermal amplification, Biosens. Bioelectron. 89 (2017) 710–714.
[214] M. Zhang, Y.-Q. Liu, C.-Y. Yu, B.-C. Yin, B.-C. Ye, Multiplexed detection of microRNAs by tuning DNA-scaffolded silver nanoclusters, Analyst 138 (17) (2013) 4812–4817.
[215] Y. Cheng, L. Dong, J. Zhang, Y. Zhao, Z. Li, Recent advances in microRNA detection, Analyst 143 (8) (2018) 1758–1774.
[216] J. Hu, M.-H. Liu, C.-Y. Zhang, Integration of isothermal amplification with quantum dot-based fluorescence resonance energy transfer for simultaneous detection of multiple microRNAs, Chem. Sci. 9 (18) (2018) 4258–4267.
[217] H. Liu, Z. Ye, X. Wang, L. Wei, L. Xiao, Molecular and living cell dynamic assays with optical microscopy imaging techniques, Analyst 144 (3) (2019) 859–871.
[218] M. Norouzi, S. Yasamineh, M. Montazeri, M. Dadashpour, R. Sheervalilou, M. Abasi, Y. Pilehvar-Soltanahmadi, Recent advances on nanomaterials-based fluorimetric approaches for microRNAs detection, Mater. Sci. Eng. C 104 (2019), 110007.
[219] Z. Li, R.-M. Gueant-Rodriguez, D. Quilliot, M.-A. Sirveaux, D. Meyre, J.-L. Gueant, L. Brunaud, Folate and vitamin B12 status is associated with insulin resistance and metabolic syndrome in morbid obesity, Clin. Nutr. 37 (5) (2018) 1700–1706.
[220] C. Li, Q. Yang, X. Wang, M. Arabi, H. Peng, J. Li, H. Xiong, L. Chen, Facile approach to the synthesis of molecularly imprinted ratiometric fluorescence nanosensor for the visual detection of folic acid, Food Chem. 319 (2020), 126575.
[221] C. Lachner, N.I. Steinle, W.T. Regenold, The neuropsychiatry of vitamin B12 deficiency in elderly patients, J. Neuropsychiatry Clin. Neurosci. 24 (1) (2012) 5–15.
[222] G. Kalaiyarasan, J. Joseph, Determination of vitamin B12 via pH-dependent quenching of the fluorescence of nitrogen doped carbon quantum dots, Microchim. Acta 184 (10) (2017) 3883–3891.
[223] L. Ding, H. Yang, S. Ge, J. Yu, Fluorescent carbon dots nanosensor for label-free determination of vitamin B12 based on inner filter effect, Spectrochim. Acta A Mol. Biomol. Spectrosc. 193 (2018) 305–309.
[224] M. Wang, Y. Liu, G. Ren, W. Wang, S. Wu, J. Shen, Bioinspired carbon quantum dots for sensitive fluorescent detection of vitamin B12 in cell system, Anal. Chim. Acta 1032 (2018) 154–162.
[225] Y. Meng, Y. Jiao, Y. Zhang, W. Lu, X. Wang, S. Shuang, C. Dong, Facile synthesis of orange fluorescence multifunctional carbon dots for label-free detection of

vitamin B12 and endogenous/exogenous peroxynitrite, J. Hazard. Mater. 408 (2021), 124422.
[226] M. Ahmad, M. Mohsin, S. Iqrar, O. Manzoor, T.O. Siddiqi, A. Ahmad, Live cell imaging of vitamin B12 dynamics by genetically encoded fluorescent nanosensor, Sensors Actuators B Chem. 257 (2018) 866–874.
[227] J. Liu, L. Gan, X. Yang, Glutenin-directed gold nanoclusters employed for assaying vitamin B 1, New J. Chem. 44 (2) (2020) 487–491.
[228] Y. Bai, T. Shu, L. Su, X. Zhang, Fluorescent gold nanoclusters for biosensor and bioimaging application, Crystals 10 (5) (2020) 357.
[229] W. Song, W. Duan, Y. Liu, Z. Ye, Y. Chen, H. Chen, S. Qi, J. Wu, D. Liu, L. Xiao, Ratiometric detection of intracellular lysine and pH with one-pot synthesized dual emissive carbon dots, Anal. Chem. 89 (24) (2017) 13626–13633.
[230] F. Du, Z. Cheng, G. Wang, M. Li, W. Lu, S. Shuang, C. Dong, Carbon nanodots as a multifunctional fluorescent sensing platform for ratiometric determination of vitamin B2 and "Turn-off" detection of pH, J. Agric. Food Chem. 69 (9) (2021) 2836–2844.
[231] H. Kausar, G. Ambrin, M.K. Okla, S.A. Alamri, W.H. Soufan, E.I. Ibrahim, M. A. Abdel-Maksoud, A. Ahmad, FRET-based genetically encoded nanosensor for real-time monitoring of the flux of α-tocopherol in living cells, ACS Omega 6 (13) (2021) 9020–9027.
[232] N.A. Bakh, X. Gong, M.A. Lee, X. Jin, V.B. Koman, M. Park, F.T. Nguyen, M. S. Strano, Transcutaneous measurement of essential vitamins using near-infrared fluorescent single-walled carbon nanotube sensors, Small 17 (31) (2021) 2100540.
[233] J. Saha, A.D. Roy, D. Dey, J. Nath, D. Bhattacharjee, S.A. Hussain, Development of arsenic (v) sensor based on fluorescence resonance energy transfer, Sensors Actuators B Chem. 241 (2017) 1014–1023.
[234] Y. Liu, C. Yu, Z. Cao, D. Shvarts, W.C. Trogler, A highly sensitive enzymatic catalysis system for trace detection of arsenic in water, Angew. Chem. Weinheim Bergstr. Ger. 23 (43) (2017) 10289.
[235] R.H. Gudlavalleti, S.C. Bose, S.K. Verma, P. Khatri, J. Scaria, S. Dhewa, V. K. Chaubey, A novel fluorometric bio-sensing-based arsenic detection system for groundwater, IEEE Sensors J. 17 (17) (2017) 5391–5398.
[236] X. Lu, C. Liu, Z. Wang, J. Yang, M. Xu, J. Dong, P. Wang, J. Gu, F. Cao, Nitrogen-doped carbon nanoparticles derived from silkworm excrement as on–off–on fluorescent sensors to detect Fe (III) and biothiols, Nanomaterials 8 (6) (2018) 443.
[237] F. Chen, F. Xiao, W. Zhang, C. Lin, Y. Wu, Highly stable and NIR luminescent Ru–LPMSN hybrid materials for sensitive detection of Cu2+ in vivo, ACS Appl. Mater. Interfaces 10 (32) (2018) 26964–26971.
[238] S.-W. Huang, Y.-F. Lin, Y.-X. Li, C.-C. Hu, T.-C. Chiu, Synthesis of fluorescent carbon dots as selective and sensitive probes for cupric ions and cell imaging, Molecules 24 (9) (2019) 1785.
[239] Z. Fu, J. He, F. Jia, M. Wang, F. Cui, Utilizing the interfacial reaction of naphthalenyl thiosemicarbazide-modified carbon dots for the ultrasensitive determination of fe (III) ions, Spectrochim. Acta A Mol. Biomol. Spectrosc. 225 (2020), 117485.
[240] M.L. Desai, H. Basu, R.K. Singhal, S. Saha, S.K. Kailasa, Ultra-small two dimensional MXene nanosheets for selective and sensitive fluorescence detection of Ag+ and Mn2+ ions, Colloids Surf. A Physicochem. Eng. Asp. 565 (2019) 70–77.
[241] X. Xing, D. Wang, Z. Chen, B. Zheng, B. Li, D. Wu, ZnTe quantum dots as fluorescence sensors for the detection of iron ions, J. Mater. Sci. Mater. Electron. 29 (16) (2018) 14192–14199.
[242] L. Han, S.G. Liu, X.F. Zhang, B.X. Tao, N.B. Li, H.Q. Luo, A sensitive polymer dots-manganese dioxide fluorescent nanosensor for "turn-on" detection of glutathione in human serum, Sensors Actuators B Chem. 258 (2018) 25–31.
[243] C. Lee, Utilization of Nanoparticles for Photoacoustic Chemical Imaging, 2018.
[244] W. Zhou, R. Saran, J. Liu, Metal sensing by DNA, Chem. Rev. 117 (12) (2017) 8272–8325.
[245] Z. Wu, H. Shen, J. Hu, Q. Fu, C. Yao, S. Yu, W. Xiao, Y. Tang, Aptamer-based fluorescence-quenching lateral flow strip for rapid detection of mercury (II) ion in water samples, Anal. Bioanal. Chem. 409 (22) (2017) 5209–5216.
[246] Y. Zhang, S. Guo, Z. Jiang, G. Mao, X. Ji, Z. He, Rox-DNA functionalized silicon nanodots for ratiometric detection of mercury ions in live cells, Anal. Chem. 90 (16) (2018) 9796–9804.
[247] C. Han, R. Wang, K. Wang, H. Xu, M. Sui, J. Li, K. Xu, Highly fluorescent carbon dots as selective and sensitive "on-off-on" probes for iron (III) ion and apoferritin detection and imaging in living cells, Biosens. Bioelectron. 83 (2016) 229–236.
[248] N. Soleja, O. Manzoor, P. Khan, M. Mohsin, Engineering genetically encoded FRET-based nanosensors for real time display of arsenic (As 3+) dynamics in living cells, Sci. Rep. 9 (1) (2019) 1–14.
[249] W. Zhang, D. Lin, H. Wang, J. Li, G.U. Nienhaus, Z. Su, G. Wei, L. Shang, Supramolecular self-assembly bioinspired synthesis of luminescent gold nanocluster-embedded peptide nanofibers for temperature sensing and cellular imaging, Bioconjug. Chem. 28 (9) (2017) 2224–2229.
[250] L. Nair, R. Nair, S. Shenoy, A. Thekkuveettil, R. Jayasree, Blood brain barrier permeable gold nanocluster for targeted brain imaging and therapy: an in vitro and in vivo study, J. Mater. Chem. B 5 (42) (2017) 8314–8321.
[251] R.V. Nair, H. Santhakumar, R.S. Jayasree, Gold nanorods decorated with a cancer drug for multimodal imaging and therapy, Faraday Discuss. 207 (2018) 423–435.
[252] H. Santhakumar, R.V. Nair, D.S. Philips, S.J. Shenoy, A. Thekkuveettil, A. Ajayaghosh, R.S. Jayasree, Real time imaging and dynamics of hippocampal zn 2+ under epileptic condition using a ratiometric fluorescent probe, Sci. Rep. 8 (1) (2018) 1–11.
[253] W. Wei, X. Zhang, S. Zhang, G. Wei, Z. Su, Biomedical and bioactive engineered nanomaterials for targeted tumor photothermal therapy: a review, Mater. Sci. Eng. C 104 (2019), 109891.
[254] R. Eivazzadeh-Keihan, K.K. Chenab, R. Taheri-Ledari, J. Mosafer, S.M. Hashemi, A. Mokhtarzadeh, A. Maleki, M.R. Hamblin, Recent advances in the application of mesoporous silica-based nanomaterials for bone tissue engineering, Mater. Sci. Eng. C 107 (2020), 110267.
[255] R.V. Nair, P.R.P. Suma, R.S. Jayasree, A dual signal on-off fluorescent nanosensor for the simultaneous detection of copper and creatinine, Mater. Sci. Eng. C 109 (2020), 110569.
[256] M. Mohsin, A. Ahmad, M. Iqbal, FRET-based genetically-encoded sensors for quantitative monitoring of metabolites, Biotechnol. Lett. 37 (10) (2015) 1919–1928.
[257] K.P. Carter, A.M. Young, A.E. Palmer, Fluorescent sensors for measuring metal ions in living systems, Chem. Rev. 114 (8) (2014) 4564–4601.
[258] M. Atsushii, L. Juan, H. Roger, Fluorescent indicators for Ca2+ based on green fluorescent proteins and calmodulin, Nature 388 (28) (1997) 882–887.
[259] S.C. Dodani, Q. He, C.J. Chang, A turn-on fluorescent sensor for detecting nickel in living cells, J. Am. Chem. Soc. 131 (50) (2009) 18020–18021.
[260] W.C. Claycomb, N.A. Lanson, B.S. Stallworth, D.B. Egeland, J.B. Delcarpio, A. Bahinski, N.J. Izzo, HL-1 cells: a cardiac muscle cell line that contracts and retains phenotypic characteristics of the adult cardiomyocyte, Proc. Natl. Acad. Sci. 95 (6) (1998) 2979–2984.
[261] N. Soleja, M. Mohsin, Real time quantification of intracellular nickel using genetically encoded FRET-based nanosensor, Int. J. Biol. Macromol. 138 (2019) 648–657.
[262] Y. Ding, S. Wang, J. Li, L. Chen, Nanomaterial-based optical sensors for mercury ions, TrAC Trends Anal. Chem. 82 (2016) 175–190.
[263] N. Bhardwaj, S.K. Bhardwaj, M.K. Nayak, J. Mehta, K.-H. Kim, A. Deep, Fluorescent nanobiosensors for the targeted detection of foodborne bacteria, TrAC Trends Anal. Chem. 97 (2017) 120–135.
[264] T. Rasheed, M. Bilal, F. Nabeel, H.M. Iqbal, C. Li, Y. Zhou, Fluorescent sensor based models for the detection of environmentally-related toxic heavy metals, Sci. Total Environ. 615 (2018) 476–485.
[265] F. Shen, L. Zhou, J. Shi, M. Xing, J. Zhang, Preparation and characterization of SiO 2/BiOX (X= cl, br, I) films with high visible-light activity, RSC Adv. 5 (7) (2015) 4918–4925.
[266] C. Zeng, Y. Hu, H. Huang, BiOBr0. 75I0. 25/BiOIO3 as a novel heterojunctional photocatalyst with superior visible-light-driven photocatalytic activity in removing diverse industrial pollutants, Acs Sustainable Chemistry & Engineering 5 (5) (2017) 3897–3905.
[267] H. Zhao, X. Liu, Y. Dong, Y. Xia, H. Wang, A special synthesis of BiOCl photocatalyst for efficient pollutants removal: new insight into the band structure regulation and molecular oxygen activation, Appl. Catal. B Environ. 256 (2019), 117872.
[268] G. Williams, B. Seger, P.V. Kamat, TiO2-graphene nanocompositesUV-assisted photocatalytic reduction of graphene oxide, ACS nano 2 (7) (2008) 1487–1491.
[269] Y. Wang, W. Wang, H. Mao, Y. Lu, J. Lu, J. Huang, Z. Ye, B. Lu, Electrostatic self-assembly of BiVO4–reduced graphene oxide nanocomposites for highly efficient visible light photocatalytic activities, ACS Appl. Mater. Interfaces 6 (15) (2014) 12698–12706.
[270] A.M. Alansi, T.F. Qahtan, T.A. Saleh, Solar-driven fixation of bismuth oxyhalides on reduced graphene oxide for efficient sunlight-responsive immobilized photocatalytic systems, Adv. Mater. Interfaces 8 (3) (2021) 2001463.
[271] J. Wang, Z. Shi, J. Fan, Y. Ge, J. Yin, G. Hu, Self-assembly of graphene into three-dimensional structures promoted by natural phenolic acids, J. Mater. Chem. 22 (42) (2012) 22459–22466.
[272] Y. Wang, Z. Shi, J. Yin, Facile synthesis of soluble graphene via a green reduction of graphene oxide in tea solution and its biocomposites, ACS Appl. Mater. Interfaces 3 (4) (2011) 1127–1133.
[273] R. Liao, Z. Tang, Y. Lei, B. Guo, Polyphenol-reduced graphene oxide: mechanism and derivatization, J. Phys. Chem. C 115 (42) (2011) 20740–20746.
[274] T.A. Saleh, Characterization, determination and elimination technologies for sulfur from petroleum: toward cleaner fuel and a safe environment, Trends Environ. Anal. Chem. 25 (2020), e00080.
[275] Y. Picó, Challenges in the determination of engineered nanomaterials in foods, TrAC Trends Anal. Chem. 84 (2016) 149–159.
[276] C. Blasco, Y. Pico, Determining nanomaterials in food, TrAC Trends Anal. Chem. 30 (1) (2011) 84–99.
[277] T.A. Saleh, Trends in the sample preparation and analysis of nanomaterials as environmental contaminants, trends in environmentalAnal. Chem. 28 (2020) e00101.
[278] T.A. Saleh, Protocols for synthesis of nanomaterials, polymers, and green materials as adsorbents for water treatment technologies, Environ. Technol. Innov. 24 (2021), 101821.
[279] N. Okamoto, T. Bito, N. Hiura, A. Yamamoto, M. Iida, Y. Baba, T. Fujita, A. Ishihara, Y. Yabuta, F. Watanabe, Food additives (Hypochlorous acid water, sodium metabisulfite, and sodium Sulfite) strongly affect the chemical and biological properties of vitamin B12 in aqueous solution, ACS Omega 5 (11) (2020) 6207–6214.
[280] R. Franco, G. Navarro, E. Martínez-Pinilla, Antioxidants versus food antioxidant additives and food preservatives, Antioxidants 8 (11) (2019) 542.
[281] P. Hou, S. Chen, K. Voitchovsky, X. Song, A colorimetric and ratiometric fluorescent probe for sulfite based on an intramolecular cleavage mechanism, Luminescence 29 (7) (2014) 749–753.

[282] H. Feng, J. Liu, A. Qaitoon, Q. Meng, Y. Sultanbawa, Z. Zhang, Z.P. Xu, R. Zhang, Responsive small-molecule luminescence probes for sulfite/bisulfite detection in food samples, TrAC Trends Anal. Chem. 116199 (2021).
[283] S.L. Taylor, N.A. Higley, R.K. Bush, Sulfites in foods: uses, analytical methods, residues, fate, exposure assessment, metabolism, toxicity, and hypersensitivity, Adv. Food Res. 30 (1986) 1–76.
[284] L.-Y. Niu, Y.-Z. Chen, H.-R. Zheng, L.-Z. Wu, C.-H. Tung, Q.-Z. Yang, Design strategies of fluorescent probes for selective detection among biothiols, Chem. Soc. Rev. 44 (17) (2015) 6143–6160.
[285] K. Chen, Y. Guo, Z. Lu, B. Yang, Z. Shi, Novel coumarin-based fluorescent probe for selective detection of bisulfite anion in water, Chin. J. Chem. 28 (1) (2010) 55–60.
[286] C. Yu, M. Luo, F. Zeng, S. Wu, A fast-responding fluorescent turn-on sensor for sensitive and selective detection of sulfite anions, Anal. Methods 4 (9) (2012) 2638–2640.
[287] X. Ma, C. Liu, Q. Shan, G. Wei, D. Wei, Y. Du, A fluorescein-based probe with high selectivity and sensitivity for sulfite detection in aqueous solution, Sensors Actuators B Chem. 188 (2013) 1196–1200.
[288] H. Singh, K. Tiwari, R. Tiwari, S.K. Pramanik, A. Das, Small molecule as fluorescent probes for monitoring intracellular enzymatic transformations, Chem. Rev. 119 (22) (2019) 11718–11760.
[289] J.V. Jun, D.M. Chenoweth, E.J. Petersson, Rational design of small molecule fluorescent probes for biological applications, Org. Biomol. Chem. 18 (30) (2020) 5747–5763.
[290] U. Tamima, M. Santra, C.W. Song, Y.J. Reo, K.H. Ahn, A benzopyronin-based two-photon fluorescent probe for ratiometric imaging of lysosomal bisulfite with complete spectral separation, Anal. Chem. 91 (16) (2019) 10779–10785.
[291] W. Wang, X.-J. Han, J.-T. Liu, J.-Y. Miao, B.-X. Zhao, A novel lipid droplets-targeted ratiometric fluorescence probe for HSO3−/SO32− in living cells, Dyes Pigments 173 (2020), 107892.
[292] M. Li, P. Cui, K. Li, J. Feng, M. Zou, X. Yu, Dual-site fluorescent probe for highly selective and sensitive detection of sulfite and biothiols, Chin. Chem. Lett. 29 (6) (2018) 992–994.
[293] K. Girigoswami, N. Akhtar, Nanobiosensors and fluorescence based biosensors: an overview, Int. J. Nano Dimens. 10 (1) (2019) 1–17.
[294] P. Wang, X. Li, C. Yao, W. Wang, M. Zhao, A.M. El-Toni, F. Zhang, Orthogonal near-infrared upconversion co-regulated site-specific O2 delivery and photodynamic therapy for hypoxia tumor by using red blood cell microcarriers, Biomaterials 125 (2017) 90–100.
[295] H.-R. Jia, Y.-W. Jiang, Y.-X. Zhu, Y.-H. Li, H.-Y. Wang, X. Han, Z.-W. Yu, N. Gu, P. Liu, Z. Chen, Plasma membrane activatable polymeric nanotheranostics with self-enhanced light-triggered photosensitizer cellular influx for photodynamic cancer therapy, J. Control. Release 255 (2017) 231–241.
[296] M. Abbas, Q. Zou, S. Li, X. Yan, Self-assembled peptide-and protein-based nanomaterials for antitumor photodynamic and photothermal therapy, Adv. Mater. 29 (12) (2017) 1605021.
[297] S. Li, Q. Zou, Y. Li, C. Yuan, R. Xing, X. Yan, Smart peptide-based supramolecular photodynamic metallo-nanodrugs designed by multicomponent coordination self-assembly, J. Am. Chem. Soc. 140 (34) (2018) 10794–10802.
[298] C. Wang, Z. Wang, T. Zhao, Y. Li, G. Huang, B.D. Sumer, J. Gao, Optical molecular imaging for tumor detection and image-guided surgery, Biomaterials 157 (2018) 62–75.
[299] Z. Teng, C. Wang, Y. Tang, W. Li, L. Bao, X. Zhang, X. Su, F. Zhang, J. Zhang, S. Wang, Deformable hollow periodic mesoporous organosilica nanocapsules for significantly improved cellular uptake, J. Am. Chem. Soc. 140 (4) (2018) 1385–1393.
[300] Z. Teng, W. Li, Y. Tang, A. Elzatahry, G. Lu, D. Zhao, Organosilica: mesoporous organosilica hollow nanoparticles: synthesis and applications (Adv. Mater. 38/2019), Advanced Materials 31 (38) (2019), 1970273.
[301] Z. Yang, J. Wen, Q. Wang, Y. Li, Y. Zhao, Y. Tian, X. Wang, X. Cao, Y. Zhang, G. Lu, Sensitive, real-time, and in-vivo oxygen monitoring for photodynamic therapy by multifunctional mesoporous nanosensors, ACS Appl. Mater. Interfaces 11 (1) (2018) 187–194.
[302] P. Qian, Y. Qin, Y. Lyu, Y. Li, L. Wang, S. Wang, Y. Liu, A hierarchical cobalt/carbon nanotube hybrid nanocomplex-based ratiometric fluorescent nanosensor for ultrasensitive detection of hydrogen peroxide and glucose in human serum, Anal. Bioanal. Chem. 411 (8) (2019) 1517–1524.
[303] J.-N. Liu, W. Bu, J. Shi, Chemical design and synthesis of functionalized probes for imaging and treating tumor hypoxia, Chem. Rev. 117 (9) (2017) 6160–6224.
[304] T. Yoshihara, Y. Hirakawa, M. Hosaka, M. Nangaku, S. Tobita, Oxygen imaging of living cells and tissues using luminescent molecular probes, J. Photochem. Photobiol. C: Photochem. Rev. 30 (2017) 71–95.
[305] D.B. Papkovsky, R.I. Dmitriev, Imaging of oxygen and hypoxia in cell and tissue samples, Cell. Mol. Life Sci. 75 (16) (2018) 2963–2980.
[306] X. Liu, W. Na, H. Liu, X. Su, Fluorescence turn-off-on probe based on polypyrrole/graphene quantum composites for selective and sensitive detection of paracetamol and ascorbic acid, Biosens. Bioelectron. 98 (2017) 222–226.
[307] H. Li, X. Wei, Y. Xu, T. Hao, J. Dai, J. Wang, L.H. Gao, Y. Yan, Determination of aspirin using functionalized cadmium-tellurium quantum dots as a fluorescence probe, Anal. Lett. 48 (2015) 1117–1127.
[308] S.M. Tawfik, B.T. Huy, M. Sharipov, A. Abd-Elaal, Y.-I. Lee, Enhanced fluorescence of CdTe quantum dots capped with a novel nonionic alginate for selective optosensing of ibuprofen, Sensors Actuators B Chem. 256 (2018) 243–250.
[309] X. Wei, Z. Zhou, T. Hao, Y. Xu, H. Li, K. Lu, J. Dai, X. Zheng, L. Gao, J. Wang, Specific recognition and fluorescent determination of aspirin by using core-shell CdTe quantum dot-imprinted polymers, Microchim. Acta 182 (7–8) (2015) 1527–1534.
[310] M. Benincasa, S. Pacor, R. Gennaro, M. Scocchi, Rapid and reliable detection of antimicrobial peptide penetration into gram-negative bacteria based on fluorescence quenching, Antimicrob. Agents Chemother. 53 (8) (2009) 3501–3504.
[311] S.K. Anand, U. Sivasankaran, A.R. Jose, K.G. Kumar, Interaction of tetracycline with l-cysteine functionalized CdS quantum dots - fundamentals and sensing application, Spectrochim. Acta A Mol. Biomol. Spectrosc. 213 (2019) 410–415.
[312] J. Niu, H. Gao, Synthesis and drug detection performance of nitrogen-doped carbon dots, J. Lumin. 149 (2014) 159–162.
[313] T. Zhou, A. Halder, Y. Sun, Fluorescent nanosensor based on molecularly imprinted polymers coated on graphene quantum dots for fast detection of antibiotics, Biosensors 8 (3) (2018) 82.
[314] T. Jantarat, S. Chuaychob, C. Thammakhet-Buranachai, P. Thavarungkul, P. Kanatharana, W. Srisintorn, C. Buranachai, A label-free DNA-based fluorescent sensor for cisplatin detection, Sensors Actuators B Chem. 326 (2021), 128764.
[315] H. Zhang, P. Sun, C. Liu, H. Gao, L. Xu, J. Fang, M. Wang, J. Liu, S. Xu, L-cysteine capped CdTe–CdS core–shell quantum dots: preparation, characterization and immuno-labeling of HeLa cells, Luminescence 26 (2) (2011) 86–92.
[316] F.-K. Tang, J. Zhu, F.K.-W. Kong, M. Ng, Q. Bian, V.W.-W. Yam, A.K.-W. Tse, Y.-C. Tse, K.C.-F. Leung, A BODIPY-based fluorescent sensor for the detection of Pt2 + and pt drugs, Chem. Commun. 56 (18) (2020) 2695–2698.
[317] L. Mitchell, C. Shen, H.C. Timmins, S.B. Park, E.J. New, A versatile fluorescent sensor array for platinum anticancer drug detection in biological fluids, ACS Sensors 6 (3) (2021) 1261–1269.
[318] Z. Wang, X. Qiu, W. Xi, M. Tang, J. Liu, H. Jiang, L. Sun, Tailored upconversion nanomaterial: a hybrid nano fluorescent sensor for evaluating efficacy of lactate dehydrogenase inhibitors as anticancer drugs, Sensors Actuators B Chem. 345 (2021), 130417.
[319] X. Jiang, D.-Q. Feng, G. Liu, D. Fan, W. Wang, A fluorescent switch sensor for detection of anticancer drug and ctDNA based on the glutathione stabilized gold nanoclusters, Sensors Actuators B Chem. 232 (2016) 276–282.
[320] G.R. Bardajee, M. Sharifi, H. Mahmoodian, Novel CMC-CdTe / ZnS QDs nanosensor for the detection of anticancer drug epirubicin, J. Fluoresc. 31 (3) (2021) 651–658.
[321] P. Li, Y. Hu, "Turn-off" fluorescent sensor for pamidronate disodium and zoledronic acid based on newly synthesized carbon dots from black tea, J. Anal. Methods Chem. 2018 (2018) 3631249.
[322] G. Guan, J. Sha, D. Zhu, Heparin-MPA dual modified CdS quantum dots used as a simple and rapid label-free fluorescent sensor for protamine and hemin detection, Microchem. J. 133 (2017) 391–397.
[323] A. Saini, N. Kaur, N. Singh, A highly fluorescent sensor based on hybrid nanoparticles for selective determination of furosemide in aqueous medium, Sensors Actuators B Chem. 228 (2016) 221–230.
[324] L. Cai, Z. Fu, F. Cui, Synthesis of carbon dots and their application as turn off–on fluorescent sensor for mercury (II) and glutathione, J. Fluoresc. 30 (2020) 11–20.
[325] H. Peng, Y. Han, N. Lin, H. Liu, Two pyridine-derived schiff-bases as turn-on fluorescent sensor for detection of aluminium ion, Opt. Mater. 95 (2019), 109210.
[326] K. Liu, C. Shang, Z. Wang, Y. Qi, R. Miao, K. Liu, T. Liu, Y. Fang, Non-contact identification and differentiation of illicit drugs using fluorescent films, Nat. Commun. 9 (1) (2018) 1695.
[327] M.A. Beatty, A.J. Selinger, Y. Li, F. Hof, Parallel synthesis and screening of supramolecular chemosensors that achieve fluorescent turn-on detection of drugs in saliva, J. Am. Chem. Soc. 141 (42) (2019) 16763–16771.
[328] Y. Kim, E. Shin, W. Jung, M.K. Kim, Y. Chong, A near-infrared turn-on fluorescent sensor for sensitive and specific detection of albumin from urine samples, Sensors 20 (4) (2020) 1232.
[329] Q. Liu, J. Gao, Z. Zheng, D. Ning, Q. Wang, X.-M. Du, B. Zhao, W.-J. Ruan, Y. Li, Metal-organic frameworks based fluorescent sensor array for discrimination of flavonoids, Talanta 203 (2019) 248–254.
[330] M. Porubský, S. Gurská, J. Stanková, M. Hajdúch, P. Džubák, J. Hlaváč, Amino-BODIPY as the ratiometric fluorescent sensor for monitoring drug release or "power supply" selector for molecular electronics, RSC Adv. 9 (43) (2019) 25075–25083.
[331] S. Scarabelli, K.T. Tan, R. Griss, R. Hovius, P.L. D'Alessandro, T. Vorherr, K. Johnsson, Evaluating cellular drug uptake with fluorescent sensor proteins, ACS Sensors 2 (8) (2017) 1191–1197.
[332] L. Hu, T. Zheng, Y. Song, J. Fan, H. Li, R. Zhang, Y. Sun, Ultrasensitive and selective fluorescent sensor for cysteine and application to drug analysis and bioimaging, Anal. Biochem. 620 (2021), 114138.
[333] K. Swarnalatha, A. Muthuvinothini, Fluorescence sensing of melamine based on zirconia-coated CdS quantum dots, J. Mater. Sci. 50 (5) (2015) 2318–2326.
[334] S. Kulchat, W. Boonta, A. Todee, P. Sianglam, W. Ngeontae, A fluorescent sensor based on thioglycolic acid capped cadmium sulfide quantum dots for the determination of dopamine, Spectrochim. Acta A Mol. Biomol. Spectrosc. 196 (2018) 7–15.
[335] M. Ganesan, P. Nagaraaj, Quantum dots as nanosensors for detection of toxics: a literature review, Anal. Methods 12 (35) (2020) 4254–4275.
[336] Q. Ye, F. Yan, D. Shi, T. Zheng, Y. Wang, X. Zhou, L. Chen, N, B-doped carbon dots as a sensitive fluorescence probe for Hg2+ ions and 2,4,6-trinitrophenol detection for bioimaging, J. Photochem. Photobiol. B Biol. 162 (2016) 1–13.
[337] D. Wang, B. Lin, Y. Cao, M. Guo, Y. Yu, A highly selective and sensitive fluorescence detection method of glyphosate based on an immune reaction strategy of carbon dot labeled antibody and antigen magnetic beads, J. Agric. Food Chem. 64 (30) (2016) 6042–6050.

[338] S. Walia, A. Acharya, Fluorescent cadmium sulfide nanoparticles for selective and sensitive detection of toxic pesticides in aqueous medium, J. Nanopart. Res. 16 (12) (2014) 2778.
[339] J. Hou, J. Dong, H. Zhu, X. Teng, S. Ai, M.J.B. Mang, A simple and sensitive fluorescent sensor for methyl parathion based on L-tyrosine methyl ester functionalized carbon dots, Biosens. Bioelectron. 68 (2015) 20–26.
[340] C. Zhang, Y. Han, L. Lin, N. Deng, B. Chen, Y. Liu, Development of quantum dots-labeled antibody fluorescence immunoassays for the detection of morphine, J. Agric. Food Chem. 65 (6) (2017) 1290–1295.
[341] S. Huang, J. Yao, X. Chu, Y. Liu, Q. Xiao, Y. Zhang, One-step facile synthesis of nitrogen-doped carbon dots: a ratiometric fluorescent probe for evaluation of acetylcholinesterase activity and detection of organophosphorus pesticides in tap water and food, J. Agric. Food Chem. 67 (40) (2019) 11244–11255.
[342] B. Kuswandi, D. Futra, L. Heng, Nanosensors for the detection of food contaminants, in: Nanotechnology Applications in Food, Elsevier, 2017, pp. 307–333.
[343] V. Vamvakaki, N.A. Chaniotakis, Pesticide detection with a liposome-based nano-biosensor, Biosens. Bioelectron. 22 (12) (2007) 2848–2853.
[344] X. Li, J. Li, H. Kuang, L. Feng, S. Yi, X. Xia, H. Huang, Y. Chen, C. Tang, Y. Zeng, An ultrasensitive method for the determination of melamine using cadmium telluride quantum dots as fluorescence probes, Anal. Chim. Acta 802 (2013) 82–88.
[345] I.A. Gracheva, E.S. Shchegravina, H.-G. Schmalz, I.P. Beletskaya, A.Y. Fedorov, Colchicine alkaloids and synthetic analogues: current progress and perspectives, J. Med. Chem. 63 (19) (2020) 10618–10651.
[346] S.F. El-Malla, E.A. Elshenawy, S.F. Hammad, F.R. Mansour, N-doped carbon dots as a fluorescent nanosensor for determination of colchicine based on inner filter effect, J. Fluoresc. 31 (3) (2021) 675–684.
[347] G. Ambrin, M. Ahmad, A.A. Alqarawi, A. Hashem, A. Ahmad, E.F. Abd-Allah, Conversion of cytochrome P450 2D6 of human into a FRET-based tool for real-time monitoring of Ajmalicine in living cells, Frontiers in bioengineering and biotechnology 7 (2019) 375.
[348] C.S. Park, T.H. Ha, S.-A. Choi, D.N. Nguyen, S. Noh, O.S. Kwon, C.-S. Lee, H. Yoon, A near-infrared "turn-on" fluorescent probe with a self-immolative linker for the in vivo quantitative detection and imaging of hydrogen sulfide, Biosens. Bioelectron. 89 (2017) 919–926.
[349] M. Ren, K. Zhou, L. He, W. Lin, Mitochondria and lysosome-targetable fluorescent probes for HOCl: recent advances and perspectives, J. Mater. Chem. B 6 (12) (2018) 1716–1733.
[350] W.J. Shi, D.K. Ng, S. Zhao, P.C. Lo, A phthalocyanine-based glutathione-activated photosensitizer with a ferrocenyl boron dipyrromethene dark quencher for photodynamic therapy, ChemPhotoChem 3 (10) (2019) 970.
[351] L. Tang, F. Yu, B. Tang, Z. Yang, W. Fan, M. Zhang, Z. Wang, O. Jacobson, Z. Zhou, L. Li, Tumor microenvironment-activated ultrasensitive nanoprobes for specific detection of intratumoral glutathione by ratiometric photoacoustic imaging, ACS Appl. Mater. Interfaces 11 (31) (2019) 27558–27567.
[352] S. Wang, Y. Fan, D. Li, C. Sun, Z. Lei, L. Lu, T. Wang, F. Zhang, Anti-quenching NIR-II molecular fluorophores for in vivo high-contrast imaging and pH sensing, Nat. Commun. 10 (1) (2019) 1–11.
[353] Y. Wen, F. Huo, C. Yin, Organelle targetable fluorescent probes for hydrogen peroxide, Chin. Chem. Lett. 30 (10) (2019) 1834–1842.
[354] D. Wu, L. Chen, Q. Xu, X. Chen, J. Yoon, Design principles, sensing mechanisms, and applications of highly specific fluorescent probes for HOCl/OCl–, Acc. Chem. Res. 52 (8) (2019) 2158–2168.
[355] D. Wu, Y. Shen, J. Chen, G. Liu, H. Chen, J. Yin, Naphthalimide-modified near-infrared cyanine dye with a large stokes shift and its application in bioimaging, Chin. Chem. Lett. 28 (10) (2017) 1979–1982.
[356] Z. Xu, T. Qin, X. Zhou, L. Wang, B. Liu, Fluorescent probes with multiple channels for simultaneous detection of cys, hcy, GSH, and H2S, TrAC Trends Anal. Chem. 121 (2019), 115672.
[357] C.X. Yin, K.M. Xiong, F.J. Huo, J.C. Salamanca, R.M. Strongin, Fluorescent probes with multiple binding sites for the discrimination of cysHcy, and GSH, Angewandte Chemie International Edition 56 (43) (2017) 13188–13198.
[358] C. Zhan, G. Zhang, D. Zhang, Zincke's salt-substituted tetraphenylethylenes for fluorometric turn-on detection of glutathione and fluorescence imaging of cancer cells, ACS Appl. Mater. Interfaces 10 (15) (2017) 12141–12149.
[359] H.Y. Zou, Q. Wang, T. Yang, P.F. Gao, C.M. Li, Y.F. Li, C.Z. Huang, Modulation of inner filter effect between plasmonic Cu2− xSySe1− y and rhodamine 6G for detection of biothiols, Sensors Actuators B Chem. 262 (2018) 966–973.
[360] K. Ngamchuea, C. Lin, C. Batchelor-McAuley, R.G. Compton, Supported microwires for electroanalysis: sensitive amperometric detection of reduced glutathione, Anal. Chem. 89 (6) (2017) 3780–3786.
[361] S. Chinnakkannu Vijayakumar, K. Venkatakrishnan, B. Tan, SERS active nanobiosensor functionalized by self-assembled 3D nickel nanonetworks for glutathione detection, ACS applied materials & interfaces 9 (6) (2017) 5077–5091.
[362] K. Ngamchuea, C. Batchelor-McAuley, R.G. Compton, Rapid method for the quantification of reduced and oxidized glutathione in human plasma and saliva, Anal. Chem. 89 (5) (2017) 2901–2908.
[363] X. Chen, Y. Wang, R. Chai, Y. Xu, H. Li, B. Liu, Luminescent lanthanide-based organic/inorganic hybrid materials for discrimination of glutathione in solution and within hydrogels, ACS Appl. Mater. Interfaces 9 (15) (2017) 13554–13563.
[364] Q. Li, A. Sun, Y. Si, M. Chen, L. Wu, One-pot synthesis of polysaccharide–diphenylalanine ensemble with gold nanoparticles and dye for highly efficient detection of glutathione, Chem. Mater. 29 (16) (2017) 6758–6765.
[365] J. Zhang, X. Bao, J. Zhou, F. Peng, H. Ren, X. Dong, W. Zhao, A mitochondria-targeted turn-on fluorescent probe for the detection of glutathione in living cells, Biosens. Bioelectron. 85 (2016) 164–170.
[366] H. Lu, D. Zhang, C. Fan, Y. Guo, X. Xia, S. Pu, Iridium (III) complex-based fluorescent probe for detection of thiophenols and its application in water samples, Dyes Pigments 163 (2019) 138–144.
[367] Z.-Z. Dong, L. Lu, C.-N. Ko, C. Yang, S. Li, M.-Y. Lee, C.-H. Leung, D.-L. Ma, A MnO 2 nanosheet-assisted GSH detection platform using an iridium (III) complex as a switch-on luminescent probe, Nanoscale 9 (14) (2017) 4677–4682.
[368] Z. Bai, F. Yan, J. Xu, J. Zhang, J. Wei, Y. Luo, L. Chen, Dual-channel fluorescence detection of mercuric (II) and glutathione by down-and up-conversion fluorescence carbon dots, Spectrochim. Acta A Mol. Biomol. Spectrosc. 205 (2018) 29–39.
[369] X. Zhang, F.G. Wu, P. Liu, N. Gu, Z. Chen, Enhanced fluorescence of gold nanoclusters composed of HAuCl4 and histidine by glutathione: glutathione detection and selective cancer cell imaging, Small 10 (24) (2014) 5170–5177.
[370] J. Yin, Y. Kwon, D. Kim, D. Lee, G. Kim, Y. Hu, J.-H. Ryu, J. Yoon, Cyanine-based fluorescent probe for highly selective detection of glutathione in cell cultures and live mouse tissues, J. Am. Chem. Soc. 136 (14) (2014) 5351–5358.
[371] C. Chu, H. Lin, H. Liu, X. Wang, J. Wang, P. Zhang, H. Gao, C. Huang, Y. Zeng, Y. Tan, Tumor microenvironment-triggered supramolecular system as an in situ nanotheranostic generator for cancer phototherapy, Adv. Mater. 29 (23) (2017) 1605928.
[372] H. Zhang, W. Li, X. Guo, F. Kong, Z. Wang, C. Zhu, L. Luo, Q. Li, J. Yang, Y. Du, Specifically increased paclitaxel release in tumor and synergetic therapy by a hyaluronic acid–tocopherol nanomicelle, ACS Appl. Mater. Interfaces 9 (24) (2017) 20385–20398.
[373] X. Zhang, X. Chen, Y.-W. Jiang, N. Ma, L.-Y. Xia, X. Cheng, H.-R. Jia, P. Liu, N. Gu, Z. Chen, Glutathione-depleting gold nanoclusters for enhanced cancer radiotherapy through synergistic external and internal regulations, ACS Appl. Mater. Interfaces 10 (13) (2018) 10601–10606.
[374] M. Wang, J. Chen, C. Liu, J. Qiu, X. Wang, P. Chen, C. Xu, A graphene quantum dots–hypochlorite hybrid system for the quantitative fluorescent determination of total antioxidant capacity, Small 13 (30) (2017) 1700709.
[375] H. Wang, P. Zhang, Y. Tian, Y. Zhang, H. Yang, S. Chen, R. Zeng, Y. Long, J. Chen, Real-time monitoring of endogenous cysteine levels in living cells using a CD-based ratiometric fluorescent nanoprobe, Anal. Bioanal. Chem. 410 (18) (2018) 4379–4386.
[376] H. Li, H. Li, A. Wan, Luminescent gold nanoclusters for in vivo tumor imaging, Analyst 145 (2) (2020) 348–363.
[377] J.R. Bhamore, S. Jha, R.K. Singhal, Z. Murthy, S.K. Kailasa, Amylase protected gold nanoclusters as chemo-and bio-sensor for nanomolar detection of deltamethrin and glutathione, Sensors Actuators B Chem. 281 (2019) 812–820.
[378] Y. Su, T. Xue, Y. Liu, J. Qi, R. Jin, Z. Lin, Luminescent metal nanoclusters for biomedical applications, Nano Res. 12 (6) (2019) 1251–1265.
[379] J. Wang, X. Lin, L. Su, J. Yin, T. Shu, X. Zhang, Chemical etching of pH-sensitive aggregation-induced emission-active gold nanoclusters for ultra-sensitive detection of cysteine, Nanoscale 11 (1) (2019) 294–300.
[380] X.Y. Wong, A. Sena-Torralba, R. Alvarez-Diduk, K. Muthoosamy, A. Merkoçi, Nanomaterials for nanotheranostics: tuning their properties according to disease needs, ACS Nano 14 (3) (2020) 2585–2627.
[381] Y.-W. Tan, L. Sun, K. Zhang, L. Zhu, Therapeutic plasma exchange and a double plasma molecular absorption system in the treatment of thyroid storm with severe liver injury: a case report, World J. Clin. Cases 7 (10) (2019) 1184.
[382] W. Zhang, X. Wang, P. Li, W. Zhang, H. Wang, B. Tang, Evaluating hyperthyroidism-induced liver injury based on in situ fluorescence imaging of glutathione and phosphate via Nano-MOFs sensor, Anal. Chem. 92 (13) (2020) 8952–8958.
[383] R. Naz, M.K. Okla, U. Fatima, M. Mohsin, W.H. Soufan, I.A. Alaraidh, M.A. Abdel-Maksoud, A. Ahmad, Designing and development of FRET-based nanosensor for real time analysis of N-Acetyl-5-neuraminic acid in living cells, Front. Nutr. 8 (2021).
[384] P.R. Galle, F. Foerster, M. Kudo, S.L. Chan, J.M. Llovet, S. Qin, W.R. Schelman, S. Chintharlapalli, P.B. Abada, M. Sherman, Biology and significance of alpha-fetoprotein in hepatocellular carcinoma, Liver Int. 39 (12) (2019) 2214–2229.
[385] X. Ren, H. Ma, T. Zhang, Y. Zhang, T. Yan, B. Du, Q. Wei, Sulfur-doped graphene-based immunological biosensing platform for multianalysis of cancer biomarkers, ACS Appl. Mater. Interfaces 9 (43) (2017) 37637–37644.
[386] J. Liu, J. Zhao, S. Li, L. Zhang, Y. Huang, S. Zhao, A novel microchip electrophoresis-based chemiluminescence immunoassay for the detection of alpha-fetoprotein in human serum, Talanta 165 (2017) 107–111.
[387] X. Zhou, X. Gao, F. Song, C. Wang, F. Chu, S. Wu, A sensing approach for dopamine determination by boronic acid-functionalized molecularly imprinted graphene quantum dots composite, Appl. Surf. Sci. 423 (2017) 810–816.
[388] J.-R. Wei, H.-Y. Chen, W. Zhang, J.-X. Pan, F.-Q. Dang, Z.-Q. Zhang, J. Zhang, Ratiometric fluorescence for sensitive and selective detection of mitoxantrone using a MIP@ rQDs@ SiO2 fluorescence probe, Sensors Actuators B Chem. 244 (2017) 31–37.
[389] T. Zhang, N. Ma, A. Ali, Q. Wei, D. Wu, X. Ren, Electrochemical ultrasensitive detection of cardiac troponin I using covalent organic frameworks for signal amplification, Biosens. Bioelectron. 119 (2018) 176–181.
[390] L. Chang, H. Wu, X. He, L. Chen, Y. Zhang, A highly sensitive fluorescent turn-on biosensor for glycoproteins based on boronic acid functional polymer capped mn-doped ZnS quantum dots, Anal. Chim. Acta 995 (2017) 91–98.
[391] C. Sun, L. Pan, L. Zhang, J. Huang, D. Yao, C.-Z. Wang, Y. Zhang, N. Jiang, L. Chen, C.-S. Yuan, A biomimetic fluorescent nanosensor based on imprinted

polymers modified with carbon dots for sensitive detection of alpha-fetoprotein in clinical samples, Analyst 144 (22) (2019) 6760–6772.
[392] C. Zhao, Y. Jiao, F. Hu, Y. Yang, Green synthesis of carbon dots from pork and application as nanosensors for uric acid detection, Spectrochim. Acta A Mol. Biomol. Spectrosc. 190 (2018) 360–367.
[393] A. Soni, R.K. Surana, S.K. Jha, Smartphone based optical biosensor for the detection of urea in saliva, Sensors Actuators B Chem. 269 (2018) 346–353.
[394] R. Sha, K. Komori, S. Badhulika, Graphene-polyaniline composite based ultra-sensitive electrochemical sensor for non-enzymatic detection of urea, Electrochim. Acta 233 (2017) 44–51.
[395] S. Mondal, M. Sangaranarayanan, A novel non-enzymatic sensor for urea using a polypyrrole-coated platinum electrode, Sensors Actuators B Chem. 177 (2013) 478–486.
[396] S. Pang, A pH sensitive fluorescent carbon dots for urea and urease detection, Fullerenes, Nanotubes, Carbon Nanostruct. 28 (9) (2020) 752–760.
[397] F. Zhang, M. Wang, L. Zhang, X. Su, Ratiometric fluorescence system for pH sensing and urea detection based on MoS2 quantum dots and 2, 3-diaminophenazine, Anal. Chim. Acta 1077 (2019) 200–207.
[398] S. Liu, F. Shi, L. Chen, X. Su, Dopamine functionalized CuInS2 quantum dots as a fluorescence probe for urea, Sensors Actuators B Chem. 191 (2014) 246–251.
[399] A. Llopis-Lorente, R. Villalonga, M.D. Marcos Martínez, R. Martínez-Máñez, F. Sancenón Galarza, A versatile new paradigm for the design of optical nanosensors based on enzyme-mediated detachment of labeled reporters: the example of urea detection, chemistry-aEuropean Journal 25 (14) (2019) 3575–3581.
[400] D. Daoussis, G.D. Kitas, Uric Acid and Cardiovascular Risk in Rheumatoid Arthritis, Oxford University Press, 2011.
[401] F. Martinon, V. Pétrilli, A. Mayor, A. Tardivel, J. Tschopp, Gout-associated uric acid crystals activate the NALP3 inflammasome, Nature 440 (7081) (2006) 237–241.
[402] Y. Liu, H. Li, B. Guo, L. Wei, B. Chen, Y. Zhang, Gold nanoclusters as switch-off fluorescent probe for detection of uric acid based on the inner filter effect of hydrogen peroxide-mediated enlargement of gold nanoparticles, Biosens. Bioelectron. 91 (2017) 734–740.
[403] T. Hallaj, N. Azizi, M. Amjadi, A dual-mode colorimetric and fluorometric nanosensor for detection of uric acid based on N, P co-doped carbon dots and in-situ formation of Au/Ag core-shell nanoparticles, Microchem. J. 162 (2021), 105865.
[404] H. Wang, Q. Lu, Y. Hou, Y. Liu, Y. Zhang, High fluorescence S, N co-doped carbon dots as an ultra-sensitive fluorescent probe for the determination of uric acid, Talanta 155 (2016) 62–69.
[405] X.-Y. Wang, G.-B. Zhu, Z.-J. Liu, C.-G. Pan, W.-J. Hu, W.-Y. Zhao, J.-F. Sun, A novel ratiometric fluorescent probe for the detection of uric acid in human blood based on H2O2-mediated fluorescence quenching of gold/silver nanoclusters, Talanta 191 (2019) 46–53.
[406] A. Mathew, T.M. Vergheese, N-C dot/Cr (VI) nanoprobe: a fluorescent uric acid sensor, Chem. Pap. (2021) 1–11.
[407] K. Sarkar, A review on the development of spectroscopic sensors for the detection of creatinine in human blood serum, Int. J. Life Sci. Pharma Res 11 (1) (2021) L91–L101.
[408] X. Zhang, B. Yao, Q. Hu, Y. Hong, A. Wallace, K. Reynolds, C. Ramsey, A. Maeder, R. Reed, Y. Tang, Detection of biomarkers in body fluids using bioprobes based on aggregation-induced emission fluorogens, Mater. Chem. Front. 4 (9) (2020) 2548–2570.
[409] S. Kumar, R. Singh, Recent optical sensing technologies for the detection of various biomolecules, Opt. Laser Technol. 134 (2021), 106620.
[410] N. Tajarrod, M.K. Rofouei, M. Masteri-Farahani, R. Zadmard, A quantum dot-based fluorescence sensor for sensitive and enzymeless detection of creatinine, Anal. Methods 8 (30) (2016) 5911–5920.
[411] L. Sutarlie, S.Y. Ow, X. Su, Nanomaterials-based biosensors for detection of microorganisms and microbial toxins, Biotechnol. J. 12 (4) (2017).
[412] E. Lebègue, C. Farre, C. Jose, J. Saulnier, F. Lagarde, Y. Chevalier, C. Chaix, N. Jaffrezic-Renault, Responsive polydiacetylene vesicles for biosensing microorganisms, Sensors 18 (2) (2018) 599.
[413] M. Alafeef, P. Moitra, D. Pan, Nano-enabled sensing approaches for pathogenic bacterial detection, Biosens. Bioelectron. 165 (2020), 112276.
[414] M. Stanisavljevic, S. Krizkova, M. Vaculovicova, R. Kizek, V. Adam, Quantum dots-fluorescence resonance energy transfer-based nanosensors and their application, Biosens. Bioelectron. 74 (2015) 562–574.
[415] W.-J. Jeong, S.-H. Choi, H.-S. Lee, Y.-B. Lim, A fluorescent supramolecular biosensor for bacterial detection via binding-induced changes in coiled-coil molecular assembly, Sensors Actuators B Chem. 290 (2019) 93–99.
[416] S.N.A. Jenie, Y. Kusumastuti, F.S.H. Krismastuti, Y.M. Untoro, R.T. Dewi, L. Z. Udin, N. Artanti, Rapid fluorescence quenching detection of Escherichia coli using natural silica-based nanoparticles, Sensors 21 (3) (2021) 881.
[417] B. Li, X. Li, Y. Dong, B. Wang, D. Li, Y. Shi, Y. Wu, Colorimetric sensor Array based on gold nanoparticles with diverse surface charges for microorganisms identification, Anal. Chem. 89 (20) (2017) 10639–10643.
[418] V.N. Mehta, S. Jha, S.K. Kailasa, One-pot green synthesis of carbon dots by using Saccharum officinarum juice for fluorescent imaging of bacteria (Escherichia coli) and yeast (Saccharomyces cerevisiae) cells, Mater. Sci. Eng. C 38 (2014) 20–27.
[419] B.S.B. Kasibabu, S.L. D'souza, S. Jha, S.K. Kailasa, Imaging of bacterial and fungal cells using fluorescent carbon dots prepared from Carica papaya juice, J. Fluoresc. 25 (4) (2015) 803–810.
[420] Y. Wang, C. Jiang, G. Wen, X. Zhang, Y. Luo, A. Qin, A. Liang, Z. Jiang, A sensitive fluorescence method for detection of E. coli using rhodamine 6G dyeing, Luminescence 31 (4) (2016) 972–977.
[421] X. Hu, Y. Li, Y. Xu, Z. Gan, X. Zou, J. Shi, X. Huang, Z. Li, Y. Li, Green one-step synthesis of carbon quantum dots from orange peel for fluorescent detection of Escherichia coli in milk, Food Chem. 339 (2021), 127775.
[422] Y. Qiao, H. Geng, N. Jiang, X. Zhu, C. Li, Q. Cai, Polymyxin B–modified upconversion nanoparticles for selective detection of gram-negative bacteria such as Escherichia coli, J. Chem. Res. 44 (11–12) (2020) 756–761.
[423] P. Wang, A. Wang, M.M. Hassan, Q. Ouyang, H. Li, Q. Chen, A highly sensitive upconversion nanoparticles-WS2 nanosheet sensing platform for Escherichia coli detection, Sensors Actuators B Chem. 320 (2020), 128434.
[424] Z.-Z. Chen, L. Cai, M.-Y. Chen, Y. Lin, D.-W. Pang, H.-W. Tang, Indirect immunofluorescence detection of E. coli O157:H7 with fluorescent silica nanoparticles, Biosens. Bioelectron. 66 (2015) 95–102.
[425] S. Ellairaja, N. Krithiga, S. Ponmariappan, V.S. Vasantha, Novel pyrimidine tagged silver nanoparticle based fluorescent immunoassay for the detection of Pseudomonas aeruginosa, J. Agric. Food Chem. 65 (8) (2017) 1802–1812.
[426] Z.A.I. Mazrad, C.A. Choi, Y.M. Kwon, I. In, K.D. Lee, S.Y. Park, Design of surface-coatable NIR-responsive fluorescent nanoparticles with PEI passivation for bacterial detection and killing, ACS Appl. Mater. Interfaces 9 (38) (2017) 33317–33326.
[427] A. Mansour, S. Tammam, A. Althani, H.M. Azzazy, A single tube system for the detection of mycobacterium tuberculosis DNA using gold nanoparticles based FRET assay, J. Microbiol. Methods 139 (2017) 165–167.
[428] R.L. Pinals, F. Ledesma, D. Yang, N. Navarro, S. Jeong, J.E. Pak, L. Kuo, Y.-C. Chuang, Y.-W. Cheng, H.-Y. Sun, Rapid SARS-CoV-2 detection by carbon nanotube-based near-infrared nanosensors, Medrxiv 21 (5) (2020) 2272–2280.
[429] Y. Wu, W. Guo, W. Peng, Q. Zhao, J. Piao, B. Zhang, X. Wu, H. Wang, X. Gong, J. Chang, Enhanced fluorescence ELISA based on HAT triggering fluorescence "turn-on" with enzyme–antibody dual labeled AuNP probes for ultrasensitive detection of AFP and HBsAg, ACS Appl. Mater. Interfaces 9 (11) (2017) 9369–9377.
[430] A.A.S. Samson, J.M. Song, in: Hypermulticolor Detector for Quantum-antibody Based Concurrent Detection of Intracellular Markers for HIV Diagnosis, Biosensors and Biodetection, Springer, 2017, pp. 221–232.
[431] C.I. Colino, C.G. Millán, J.M. Lanao, Nanoparticles for signaling in biodiagnosis and treatment of infectious diseases, Int. J. Mol. Sci. 19 (6) (2018) 1627.
[432] D.P. Salem, X. Gong, A.T. Liu, K. Akombi, M.S. Strano, Immobilization and function of nIR-fluorescent carbon nanotube sensors on paper substrates for fluidic manipulation, Anal. Chem. 92 (1) (2019) 916–923.
[433] D. Kozawa, S.-Y. Cho, X. Gong, F.T. Nguyen, X. Jin, M.A. Lee, H. Lee, A. Zeng, G. Xue, J. Schacherl, A fiber optic interface coupled to nanosensors: applications to protein aggregation and organic molecule quantification, ACS Nano 14 (8) (2020) 10141–10152.
[434] M.H. Wong, J.P. Giraldo, S.-Y. Kwak, V.B. Koman, R. Sinclair, T.T.S. Lew, G. Bisker, P. Liu, M.S. Strano, Nitroaromatic detection and infrared communication from wild-type plants using plant nanobionics, Nat. Mater. 16 (2) (2017) 264–272.
[435] F.C.-M. Leung, S.Y.-L. Leung, C.Y.-S. Chung, V.W.-W. Yam, Metal–metal and π–π interactions directed end-to-end assembly of gold nanorods, J. Am. Chem. Soc. 138 (9) (2016) 2989–2992.
[436] X. Li, X. Gao, W. Shi, H. Ma, Design strategies for water-soluble small molecular chromogenic and fluorogenic probes, Chem. Rev. 114 (1) (2014) 590–659.
[437] K.J. Cash, H.A. Clark, Nanosensors and nanomaterials for monitoring glucose in diabetes, Trends Mol. Med. 16 (12) (2010) 584–593.
[438] M. Liu, J.G. Qiu, F. Ma, C.Y. Zhang, Advances in single-molecule fluorescent nanosensors, Wiley Interdisciplinary Reviews: Nanomedicine and Nanobiotechnology 13 (5) (2021) e1716.
[439] T.H. Kim, M. Kim, H.S. Park, U.S. Shin, M.S. Gong, H.W. Kim, Size-dependent cellular toxicity of silver nanoparticles, J. Biomed. Mater. Res. A 100 (4) (2012) 1033–1043.
[440] S.-D. Li, L. Huang, Nanoparticles evading the reticuloendothelial system: role of the supported bilayer, Biochim. Biophys. Acta Biomembr. 1788 (10) (2009) 2259–2266.
[441] Y. Wang, F. Papadimitrakopoulos, D.J. Burgess, Polymeric "smart" coatings to prevent foreign body response to implantable biosensors, J. Control. Release 169 (3) (2013) 341–347.
[442] T.-I. Kim, J.G. McCall, Y.H. Jung, X. Huang, E.R. Siuda, Y. Li, J. Song, Y.M. Song, H.A. Pao, R.-H. Kim, Injectable, cellular-scale optoelectronics with applications for wireless optogenetics, Science 340 (6129) (2013) 211–216.
[443] J. Kottmann, U. Grob, J.M. Rey, M.W. Sigrist, Mid-infrared fiber-coupled photoacoustic sensor for biomedical applications, Sensors 13 (1) (2013) 535–549.
[444] A.G. Aggidis, J.D. Newman, G.A. Aggidis, Investigating pipeline and state of the art blood glucose biosensors to formulate next steps, Biosens. Bioelectron. 74 (2015) 243–262.
[445] B. Bhattacharya, S. Singha, S. Basu, Fluorescent nanosensors: rapid tool for detection of food contaminants, in: Nanobiosensors, Elsevier, 2017, pp. 841–874.
[446] A.V. Alex, A. Mukherjee, Review of recent developments (2018–2020) on acetylcholinesterase inhibition based biosensors for organophosphorus pesticides detection, Microchem. J. 161 (2021), 105779.

[447] J. Wang, X. Qu, Recent progress in nanosensors for sensitive detection of biomolecules, Nanoscale 5 (9) (2013) 3589–3600.
[448] S.C. Ray, Application and uses of graphene oxide and reduced graphene oxide, in: Applications of graphene and graphene-oxide based nanomaterials 1, 2015.
[449] M.J. McShane, Potential for glucose monitoring with nanoengineered fluorescent biosensors, Diabetes Technol. Ther. 4 (4) (2002) 533–538.